**Supporting Information**

# Bisindole-based small molecules as transmembrane anion transporters and potential anticancer agents

Swati Bansi Salunke,[a] Shreyada N. Save,[b] Naveen J. Roy,[a] Ronedy Naorem,[a] Shilpy Sharma[b] and Pinaki Talukdar* [a]

[a] Department of Chemistry, Indian Institute of Science Education and Research Pune, Dr. Homi Bhabha Road, Pashan, Pune 411008, Maharashtra, India.

[b] Department of Biotechnology, Savitribai Phule Pune University (Formerly University of Pune), Pune 411007, Maharashtra, India.

**Table of contents**

## I. General Methods

All chemical reactions were performed under a nitrogen atmosphere. All reagents and solvents for synthesis were purchased from commercial sources (Sigma-Aldrich, Spectrochem, Avra) and used further without purification. The column chromatography was carried out using Rankem silica gel (100-200 mesh size). The thin layer chromatography was performed on Merck 60-F254 silica gel plates. Egg yolk phosphatidylcholine (EYPC) as a solution in chloroform (25 mg/mL), 1,2-dipalmitoyl-*sn*-glycero-3-phosphocholine (DPPC), mini extruder set, polycarbonate membranes of 100 nm and 200 nm pore size, and filter supports were purchased from Avanti Polar Lipids (Merck). HEPES, HPTS, lucigenin, NaOH, Triton X-100, FCCP, valinomycin, Sephadex-G50, and all inorganic salts were of molecular biology grade from Sigma-Aldrich (Merck). All buffer solutions were prepared using autoclaved Milli-Q water. All stock solutions were prepared in HPLC grade DMSO (Rankem) or acetonitrile (NICE).

## II. Physical Measurements

The $^{1}H$ (400 MHz) and $^{13}C$ (101 MHz) NMR spectra were recorded on Bruker Avance III HD 400 MHz and JEOL JNM-ECS 400 MHz NMR spectrometers. The residual solvent signals were considered as an internal reference $\delta H$ = 7.26 ppm for $CDCl_3$, $\delta H$ = 2.50 for DMSO-$d_6$, $\delta H$ = 2.05 for $(CD_3)_2CO$, and $\delta H$ = 1.94 for $CD_3CN$ to calibrate spectra. The chemical shifts were reported in ppm. The following abbreviations were used to indicate multiplicity patterns m: multiplet, s: singlet, d: doublet, t: triplet, q: quartet, p: pentet, sx: sextet, dd: doublet of doublets, td: triplet of doublets. Coupling constants were measured in Hz. Infra-red (IR) spectra were measured in $cm^{-1}$ using a Bruker ALPHA II FT-IR spectrometer. High-resolution mass spectra (HRMS) were recorded on a Waters SYNAPT G2 mass spectrometer equipped with a Waters Z-Spray™ electrospray ionization (ESI) source. Single crystal X-ray diffraction (SCXRD) measurements were done on Bruker D8 VENTURE diffractometer. Fluorescence measurements were recorded on HORIBA Jobin Yvon Fluoromax-4 or Fluoromax+ spectrofluorometers equipped with injector port and magnetic stirrer in quartz fluorescence cuvettes. Adjustment of the pH of buffer solutions was performed using a Hanna Instruments (HI98108 pHep+) pocket-size pH meter. Data from fluorescence studies was plotted using OriginPro 8.5 software. Compound lipophilicity (log*P*) and p$K_a$ values were calculated using calculator plugins of MarvinSketch software (v5.8.0). ChemDraw 22.2.0 was used for drawing

chemical structures and processing figures. 3D structure images were generated using Avogadro 1.2.0 and BIOVIA Discovery Studio 2021. Molecular structure conformations were predicted using CONFLEX 8 software package. DFT calculations were performed using Gaussian 09 program suite on the PARAM Brahma supercomputer (IISER Pune).

## III. Synthesis

**General procedure for synthesizing 7-nitro indole ester derivatives (3a-3d):**

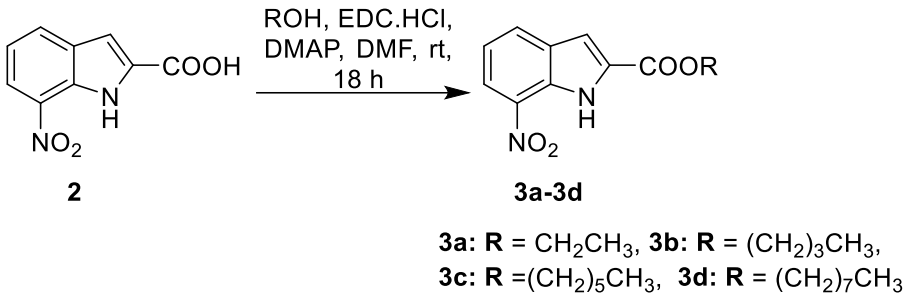


**Scheme S1.** Synthetic scheme for the compounds **3a-3d**.

In a 10 mL round bottom flask, 7-nitro-1H-indole-2-carboxylic acid (**2**) (100 mg, 0.49 mmol) was dissolved in dry DMF (4 mL). To this solution, EDC·HCl (112 mg, 0.58 mmol), corresponding alcohol derivative (0.53 mmol) and DMAP (cat.) were added. The resulting reaction mixture was stirred at room temperature for 18 h. After completion of product formation, DMF was evaporated. The crude mixture was dissolved in EtOAc (3 mL) and washed with Sat. $NaHCO_3$ solution (2 mL). The product was extracted with EtOAc (3 × 3 mL), and the organic phase was washed with brine (2 × 3 mL) and then dried over $Na_2SO_4$, filtered, and the solvent removed under reduced pressure. The crude product was purified by silica gel column chromatography to give pure compound **3a-3d**.

**Ethyl 7-nitro-1*H*-indole-2-carboxylate (3a):**

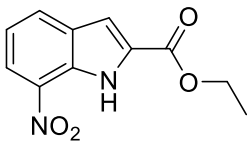


**Eluent for column chromatography**: 4% ethyl acetate in petroleum ether. **Physical appearance**: yellow solid. **Yield**: 85%. **$^1$H NMR (400 MHz, $CDCl_3$)**: δ 10.32 (s, 1H), 8.28 (d, *J* = 7.9 Hz, 1H), 8.03 (d, *J* = 7.9 Hz, 1H), 7.34 (d, *J* = 2.3 Hz, 1H), 7.26 (t, *J* = 7.9 Hz, 1H), 4.45 (q, *J* = 7.3 Hz, 2H), 1.43 (t, *J* = 7.9 Hz, 3H). **$^{13}$C NMR (101 MHz, $CDCl_3$):** δ 160.9, 131.1, 130.9 (2C), 130.3, 129.8, 122.3, 120.2, 109.4, 61.7, 14.5. **IR (ṽ $cm^{-1}$):** 3276.96, 2928.27, 1711.15, 1633.02, 1536.12, 1327.90, 1290.52, 1243.80,

1192.57, 1109.10, 1020.25, 730.88. **HRMS (ESI):** Calc. for $C_{11}H_{11}N_2O_4$ $[M+H]^+$: 235.0719; Observed: 235.0716.

**Butyl 7-nitro-1*H*-indole-2-carboxylate (3b):**

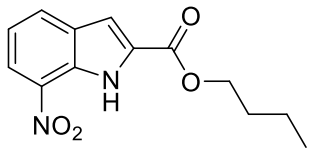

**Eluent for column chromatography**: 3% ethyl acetate in petroleum ether. **Physical appearance**: yellow solid. **Yield**: 92%. **$^1$H NMR (400 MHz, $CDCl_3$)**: δ 10.31 (s, 1H), 8.26 (d, *J* = 8.1 Hz, 1H), 8.01 (d, *J* = 7.8 Hz, 1H), 7.32 (d, *J* = 2.3 Hz, 1H), 7.23 (d, *J* = 6.9 Hz, 1H), 4.37 (t, *J* = 6.7 Hz, 2H), 1.80 (p, *J* = 6.8, 2H), 1.46 (sx, *J* = 7.4 Hz, 2H), 0.97 (t, *J* = 7.4 Hz, 3H). **$^{13}$C NMR (101 MHz, $CDCl_3$)**: δ 161.0, 133.6, 131.1, 130.9, 130.4, 129.9, 122.4, 120.3, 109.4, 65.6, 30.9, 19.3, 13.9. **IR (ṽ cm$^{-1}$):** 3460.69, 3332.51, 2960.47, 2875.44, 1711.19, 1547.47, 1292.15, 1234.10, 832.11, 766.63, 733.95. **HRMS (ESI):** Calc. for $C_{13}H_{15}N_2O_4$ $[M+H]^+$: 263.1032; Observed: 263.1032.

**Hexyl 7-nitro-1*H*-indole-2-carboxylate (3c):**

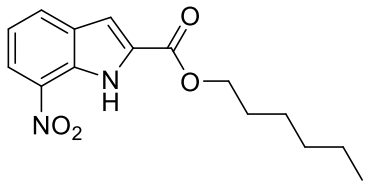

**Eluent for column chromatography**: 3% ethyl acetate in petroleum ether. **Physical appearance**: yellow solid. **Yield**: 85%.**$^1$H NMR (400 MHz, $CDCl_3$)**: δ 10.35 (s, 1H), 8.30 (d, *J* = 8.0 Hz, 1H), 8.05 (d, *J* = 7.9 Hz, 1H), 7.36 (d, *J* = 2.2 Hz, 1H), 7.29 (d, *J* = 8.0 Hz, 1H), 4.40 (t, *J* = 6.8 Hz, 2H), 1.80 (p, *J* = 7.0 Hz, 2H), 1.46 (p, *J* = 7.0 Hz, 2H), 1.36 (m, 4H), 0.92 (t, *J* = 7.0 Hz, 3H). **$^{13}$C NMR (101 MHz, $CDCl_3$)**: δ 161.0, 133.6, 131.2, 130.9, 130.4, 129.9, 122.4, 120.3, 109.4, 65.9, 31.6, 28.8, 25.8, 22.7, 14.1. **IR (ṽ cm$^{-1}$):** 3455.15, 2924.69, 1713.34, 1546.92, 1337.54, 1318.65, 1291.69, 1232.58, 730.61. **HRMS (ESI):** Calc. for $C_{15}H_{19}N_2O_4$ $[M+H]^+$: 291.1345; Observed: 291.1375.

**Octyl 7-nitro-1*H*-indole-2-carboxylate (3d):**

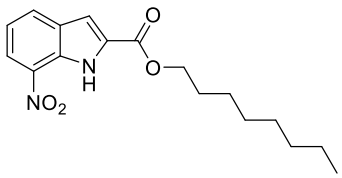

**Eluent for column chromatography**: 2% ethyl acetate in petroleum ether. **Physical appearance**: light yellow solid. **Yield**: 88%. **$^1$H NMR (400 MHz, $CDCl_3$)**: δ 10.33 (s, 1H), 8.28 (d, *J* = 8.0 Hz, 1H), 8.03 (d, *J* = 7.8 Hz, 1H), 7.34 (d, *J* = 2.1 Hz, 1H), 7.26 (t, *J* = 8.0 Hz, 1H), 4.38 (t, *J* = 6.8 Hz, 2H), 1.8 (p, *J* = 6.8 Hz, 2H), 1.44 (p, *J* = 6.8 Hz, 2H), 1.39 – 1.23 (m, 8H), 0.87 (t, *J* = 6.7 Hz, 3H). **$^{13}$C NMR (101 MHz, $CDCl_3$)**: δ 161.0, 133.6, 131.1, 130.9, 130.4, 129.9, 122.4, 120.3, 109.4, 65.9, 31.9, 29.4, 29.3, 28.8, 26.1, 22.8, 14.2.

**General procedure for synthesizing 7- amine indole ester derivatives (4a-4d):**

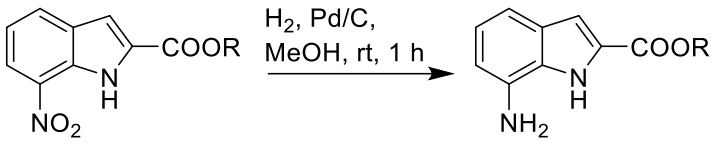


**Scheme S2.** Synthetic scheme for the compounds **4a-4d**.

In stirring solution of compound **3a-3d** (100 mg) in ethyl acetate (8 mL) was added Pd/C (15 mg). The solution was completely degassed three times under vacuum/$N_2$. The reaction mixture was reacted with $H_2$ (1 atm) for 2 h. After completion of the reduction process, the reaction mixture was filtered through a celite pad. The celite bed was washed with EtOAc (3×5 mL) and the filtrate was concentrated under reduced pressure to obtain a crude product. The crude product was purified by silica gel column chromatography to give pure compound **4a-4d**.

**Ethyl 7-amino-1*H*-indole-2-carboxylate (4a):**

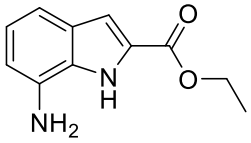

**Eluent for column chromatography**: 15% ethyl acetate in petroleum ether. **Physical appearance**: white solid. **Yield**: 92%. **$^1$H NMR (400 MHz, $CDCl_3$):** δ 10.02 (s, 1H), 7.23 (d, J = 2.1 Hz, 1H), 7.18 (d, J = 8.1 Hz, 1H), 6.99 (t, J = 8.0, 1H), 6.66 (dd, J = 7.4, 0.8 Hz, 1H), 4.43 (q, J = 7.1 Hz, 2H), 4.36 - 4.00 (br s, 2H), 1.44 (t, J = 7.1 Hz, 3H). **$^{13}$C NMR (101 MHz, $CDCl_3$):** δ 163.4, 132.3, 128.6, 128.6, 127.0, 121.8, 113.4, 110.0, 109.9, 61.45, 14.48. **IR (ṽ cm$^{-1}$):** 3335.07, 1680.30, 1253.98, 1214.95, 1025.94, 828.94, 735.70, 645.5. **HRMS (ESI):** Calc. for $C_{11}H_{13}N_2O_2$ $[M+H]^+$: 205.0977; Observed: 205.0979.

**Butyl 7-amino-1*H*-indole-2-carboxylate (4b):**

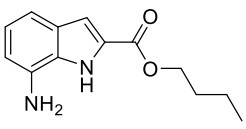

**Eluent for column chromatography**: 20% ethyl acetate in petroleum ether. **Physical appearance**: white solid. **Yield**: 95%. **$^1$H NMR (400 MHz, $CDCl_3$):** δ 9.63 (s, 1H), 7.22 (t, *J* = 2 Hz, 1H), 7.19 (d, *J* = 8 Hz, 1H), 6.99 (t, *J* = 8 Hz, 1H), 6.67 (d, *J* = 7.4 Hz, 1H), 4.37 (t, *J* = 6.8 Hz, 2H), 1.79 (q, *J* = 6.8 Hz, 2H), 1.50 (sx, *J* = 7.6 Hz, 2H), 1.0 (t, *J* = 7.6 Hz, 3H). **$^{13}$C NMR (101 MHz, $CDCl_3$)**: δ 163.0, 132.0, 128.6, 128.6, 127.2, 121.8, 113.8, 110.4, 109.7, 65.2, 30.9, 19.4, 13.9. **IR (ṽ cm$^{-1}$):** 3366.77, 3336.15,

2959.33, 1678.44, 1285.89, 1248.37, 1209.98, 826.39, 781.61, 732.70. **HRMS (ESI):** Calc. for $C_{13}H_{17}N_2O_2$ $[M+H]^+$: 233.1290; Observed: 233.1288.

**Hexyl 7-amino-1*H*-indole-2-carboxylate (4c):**

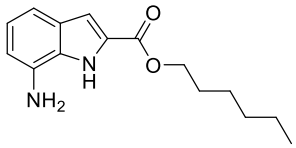

**Eluent for column chromatography**: 18% ethyl acetate in petroleum ether. **Physical appearance**: white solid. **Yield**: 89%. **$^1$H NMR (400 MHz, $CDCl_3$)**: δ 9.64 (s, 1H), 7.21 (d, *J* = 1.8 Hz, 1H), 7.18 (d, *J* = 8.1 Hz, 1H), 6.99 (t, *J* = 7.8 Hz, 1H), 6.66 (d, *J* = 7.4 Hz, 1H), 4.36 (t, *J* = 6.7 Hz, 2H), 4.02 (s, 2H), 1.79 (p, *J* = 6.7 Hz, 2H), 1.46 (p, *J* = 7.2 Hz, 2H), 1.36 (m, 4H), 0.91 (t, *J* = 7.0 Hz, 3H). **$^{13}$C NMR (101 MHz, $CDCl_3$)**: δ 163.1, 132.1, 128.6, 128.6, 127.2, 121.8, 113.7, 110.3, 109.7, 65.5, 31.6, 28.8, 25.8, 22.7, 14.2. **IR (ṽ cm$^{-1}$):** 3364.06, 3328.22, 2956.93, 2927.31, 2858.55, 1682.35, 1248.18, 1215.06, 750.19, 731.53. **HRMS (ESI):** Calc. for $C_{15}H_{21}N_2O_2$ $[M+H]^+$: 261.1603; Observed: 261.1605.

**Octyl 7-amino-1*H*-indole-2-carboxylate (4d):**

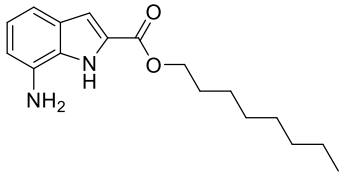

**Eluent for column chromatography**: 18% ethyl acetate in petroleum ether. **Physical appearance**: white solid. **Yield**: 90%. **$^1$H NMR (400 MHz, $CDCl_3$)**: δ 9.88 (s, 1H), 7.22 (d, *J* = 2.1 Hz, 1H), 7.18 (d, *J* = 8.1 Hz, 1H), 6.99 (t, *J* = 7.0 Hz, 1H), 6.66 (dd, *J* = 7.3, 0.7 Hz, 1H), 4.36 (t, *J* = 6.7 Hz, 2H), 4.11 (s, 2H), 1.8 (p, *J* = 6.9 Hz, 2H), 1.46 (p, *J* = 7.0 Hz, 2H), 1.41 – 1.24 (m, 8H), 0.89 (t, *J* = 6.9 Hz, 3H). **$^{13}$C NMR (101 MHz, $CDCl_3$)**: δ 163.4, 132.2, 128.6, 127.1, 121.8, 113.5, 110.1, 110.0, 109.8, 65.6, 31.9, 29.4, 29.3, 28.8, 26.2, 22.8, 14.2. **IR (ṽ cm$^{-1}$):** 3442.57, 3330.35, 2922.56, 2855.10, 1687.35, 1289.18, 1245.74, 1215.99, 825.82, 780.14, 731.19. **HRMS (ESI):** Calc. for $C_{17}H_{25}N_2O_2$ $[M+H,]^+$: 289.1916; Observed: 289.1918.

**General procedure for synthesizing bis-indole-based transporter (1a-1d):**

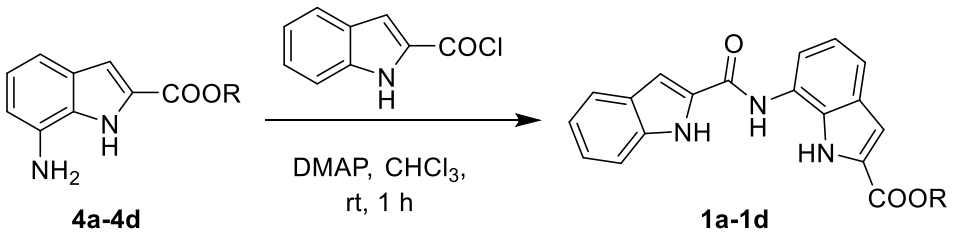


**Scheme S3.** Synthetic scheme for the compounds **1a-1d**.

To a solution of indole-2-carboxylic acid (200 mg, 1.24 mmol) in $CH_2Cl_2$ (2 mL), thionyl chloride (0.36 mL, 4.96 mmol) and 2 drops of DMF were added. The reaction mixture was stirred for 1 h at room temperature. Then, the solvent was evaporated to dryness in *vacuo* to give indole-2-carbonyl chloride. The residue was dissolved in $CHCl_3$ (3 mL). This solution was added dropwise to the mixture of **4a-4d** (0.68 mmol) and DMAP (0.68 mmol) in $CHCl_3$ (3 mL). The reaction mixture was stirred for 1 h and quenched with water. Following extraction with $CH_2Cl_2$ (3 × 5 mL), the organic phase was washed with brine (2 × 4 mL) and then dried over $Na_2SO_4$, filtered, and the solvent removed under reduced pressure. The crude product was purified by silica gel column chromatography to give pure compound **1a-1d**.

**Ethyl 7-(1*H*-indole-2-carboxamido)-1*H*-indole-2-carboxylate (1a):**

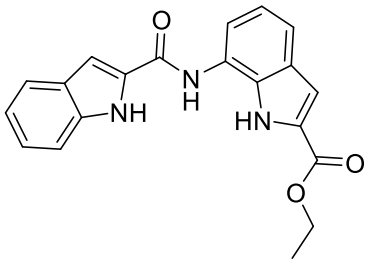

**Eluent for column chromatography**: 15% ethyl acetate in petroleum ether. **Physical appearance**: white solid. **Yield**: 30%. **$^1$H NMR (400 MHz, DMSO-$d_6$)**: δ 11.99 (s, 1H), 11.81 (s, 1H), 10.06 (s, 1H), 7.99 – 7.91 (m, 1H), 7.73 (d, J = 8.0 Hz, 1H), 7.52 – 7.48 (m, 3H), 7.28 – 7.21 (m, 2H), 7.18 – 7.06 (m, 2H), 4.38 (q, J = 7.1 Hz, 2H), 1.36 (t, J = 7.1 Hz, 3H). **$^{13}$C NMR (101 MHz, DMSO-$d_6$):** δ 161.3, 160.1, 136.9, 131.4, 129.6, 128.4, 127.4, 127.0, 124.1, 123.8, 121.7, 120.5, 120.0, 118.3, 116.9, 112.4, 108.4, 104.4, 60.6, 14.3. **IR (ṽ cm$^{-1}$):** 3325.26, 3255.64, 2926.01, 1692.96, 1628.27, 1535.13, 1418.37, 1374.84, 1309.20, 1242.92, 1202.05, 1119.38, 1020.28, 738.01. **HRMS (ESI):** Calc. for $C_{20}H_{18}N_3O_3$ $[M+H]^+$: 348.1348; Observed: 348.1352.

**Butyl 7-(1*H*-indole-2-carboxamido)-1*H*-indole-2-carboxylate (1b):**

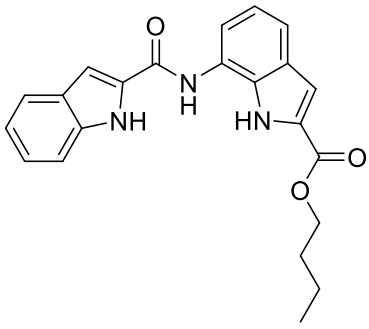

**Eluent for column chromatography**: 10% ethyl acetate in petroleum ether. **Physical appearance**: white solid. **Yield**: 37%. **$^1$H NMR (400 MHz, Acetone- $d_6$):** δ 11.00 (s, 2H), 9.80 (s, 1H), 7.70 (d, *J* = 8.0 Hz, 1H), 7.61 (d, *J* = 8.3 Hz, 1H), 7.57 (dd, *J* = 7.8, 3.5 Hz, 2H), 7.45 (s, 1H), 7.29 (t, *J* = 7.6 Hz, 1H), 7.24 (d, *J* = 1.9 Hz, 1H), 7.13 (td, *J* = 7.6, 4.8 Hz, 2H), 4.35 (t, *J* = 6.6 Hz, 2H), 1.76 (q, *J* = 6.8 Hz, 2H), 1.49 (sx, *J* = 7.6 Hz, 2H), 0.98 (t, *J* = 7.4 Hz, 3H). **$^{13}$C NMR (101 MHz, Acetone- $d_6$):** δ 162.4, 161.1, 138.2, 132.1, 131.1, 130.6, 129.0, 128.8, 125.3, 125.0, 122.9, 121.5, 121.3, 120.2, 118.4, 113.3, 109.2, 105.2, 65.2, 31.7, 19.9, 14.1. **IR (ṽ cm$^{-1}$):** 3305.42,

2959.83, 1693.99, 1643.28, 1537.13, 1417.39, 1309.48, 1243.79, 1202.49, 739.32. **HRMS (ESI):** Calc. for $C_{22}H_{22}N_3O_3$ $[M+H]^+$: 376.1661; Observed: 376.1655.

**Hexyl 7-(1*H*-indole-2-carboxamido)-1*H*-indole-2-carboxylate (1c):**

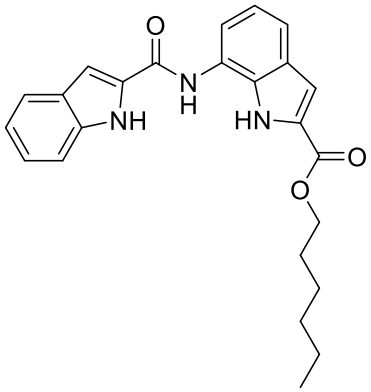

**Eluent for column chromatography**: 10% ethyl acetate in petroleum ether. **Physical appearance**: white solid. **Yield**: 30%. **$^1$H NMR (400 MHz, DMSO-$d_6$)**: δ 11.99 (s, 1H), 11.81 (s, 1H), 10.06 (s, 1H), 7.95 (d, *J* = 7.7 Hz, 1H), 7.72 (d, *J* = 8.0 Hz, 1H), 7.50 (t, *J* = 5.6 Hz, 3H), 7.25 (d, *J* = 7.3 Hz, 1H), 7.22 (s, 1H), 7.16 – 7.06 (m, 2H), 4.33 (t, *J* = 6.5 Hz, 2H), 1.73 (p, *J* = 6.4, 2H), 1.41 (p, *J* = 7.2 Hz, 2H), 1.32 (m, 4H), 0.88 (t, *J* = 6.3 Hz, 3H). **$^{13}$C NMR (101 MHz, DMSO-$d_6$)**: δ 161.4, 160.1, 136.9, 131.4, 129.7, 128.4, 127.3, 127.0, 124.1, 124.0, 121.7, 120.5, 120.0, 118.4, 116.9, 112.4, 108.3, 104.4, 64.6, 30.9, 28.3, 25.1, 22.0, 13.9. **IR (ṽ cm$^{-1}$):** 3333.85, 3301.67, 3248.29, 1690.49, 1627.04, 1535.74, 1265.53, 738.07. **HRMS (ESI):** Calc. for $C_{24}H_{25}N_3NaO_3$ $[M+Na]^+$: 426.1794; Observed: 426.1794.

**Octyl 7-(1*H*-indole-2-carboxamido)-1*H*-indole-2-carboxylate (1d):**

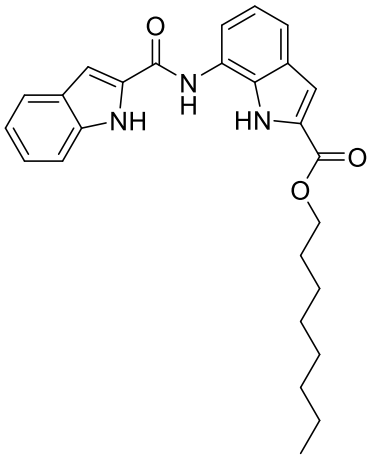

**Eluent for column chromatography**: 8% ethyl acetate in petroleum ether. **Physical appearance**: white solid. **Yield**: 40%. **$^1$H NMR (400 MHz, DMSO-$d_6$)**: δ 11.98 (s, 1H), 11.80 (s, 1H), 10.06 (s, 1H), 7.94 (d, *J* = 7.6 Hz, 1H), 7.72 (d, *J* = 7.9 Hz, 1H), 7.56 – 7.45 (m, 3H), 7.29 – 7.20 (m, 1H), 7.18 – 7.03 (m, 2H), 4.32 (t, *J* = 6.5 Hz, 2H), 1.78 – 1.67 (m, 2H), 1.41 – 1.24 (m, 10H), 0.85 (t, *J* = 5.9 Hz, 3H). **$^{13}$C NMR (101 MHz, DMSO-$d_6$)**: δ 161.5, 160.2, 136.9, 131.4, 129.7, 128.5, 127.4, 127.0, 124.11, 123.9, 121.8, 120.6, 120.0, 118.4, 117.0, 112.5, 108.4, 104.5, 64.6, 31.2, 28.7, 28.6, 28.3, 25.5, 22.1, 14.0. **IR (ṽ cm$^{-1}$):** 3333.76, 2921.59, 1693.78, 1625.21, 1532.96, 1260.42, 740.50. **HRMS (ESI):** Calc. for $C_{26}H_{30}N_3O_3$ $[M+H]^+$: 432.2287; Observed: 432.2284.

## IV. Ion Transport Studies

**Ion transport activity studies across EYPC-LUVs⊃HPTS:**

**Preparation of HEPES buffer and stock solutions:** The HEPES buffer (pH = 7.0) was prepared by the addition of a calculated amount of HEPES (10 mM) and NaCl (100 mM) in autoclaved

Milli-Q water. The adjustment of pH 7.0 was done by the addition of aliquots of 0.5 M NaOH. The stock solution of all transporters was prepared in HPLC grade DMSO.

**Preparation of EYPC-LUVs⊃HPTS in NaCl:** The thin transparent film of egg yolk phosphatidylcholine (EYPC) was prepared by the slow evaporation of 1 mL chloroform solution of EYPC (25 mg/mL in chloroform) under nitrogen gas. The thin transparent film was kept on high vacuum for 4-5 h to remove all traces of chloroform. After that, the thin transparent film was hydrated with 1 mL HEPES buffer (10 mM HEPES, 100 mM NaCl, 1 mM HPTS) by giving vertex at 10 min intervals for 1 h. The resulting suspension was subjected to 15 cycles of freeze-thaw (liquid nitrogen, 55 °C) followed by extrusion through a 100 nm polycarbonate membrane 21 times to access vesicles of average 100 nm diameter. The extravesicular HPTS dye was removed by the size exclusion chromatography using Sephadex-G50 (stationary phase) with HEPES buffer (10 mM HEPES, 100 mM NaCl, pH = 7.0) as the mobile phase. Finally, vesicles were diluted to 6 mL to get EYPC-LUVs⊃HPTS. *Final conditions*: ~ 5 mM EYPC, Inside: 1 mM HPTS, 10 mM HEPES, 100 mM NaCl, pH = 7.0, Outside: 10 mM HEPES, 100 mM NaCl, pH = 7.0.

**Ion transport activity by HPTS assay:** In clean and dry fluorescence cuvette, 1975 mL HEPES buffer (10 mM HEPES, 100 mM NaCl, pH = 7.0) and 25 µL EYPC-LUVs⊃HPTS vesicles were taken. The cuvette was placed in fluorescence instrument furnishes with slow stirring conditions ($t$ = 0). After 20 s, a NaOH pulse (0.5 M, 20 µL) was given to create a pH gradient ($pH_{in}$ = 7.0, $pH_{out}$ = 7.8) across intra and extravesicular system. The time-dependent fluorescence intensity of HPTS at $\lambda_{em}$ = 510 nm ($\lambda_{ex}$ = 450 nm) was monitored after the addition of transporter molecule (DMSO solution) at t = 100 s. Finally, vesicles were lysed upon the addition of 10% Triton X-100 (20 µL) at t = 300 s for the complete dissipation of the pH gradient.

The time-dependent data were normalized to percent change in fluorescence intensity using Equation S1:

$$I_F = [(I_t - I_0) / (I_\infty - I_0)] \times 100 \qquad \text{Equation S1}$$

Where $I_0$ is the initial intensity, $I_t$ is the intensity at time $t$, and $I_\infty$ is the final intensity after the addition of 10% Triton X-100.

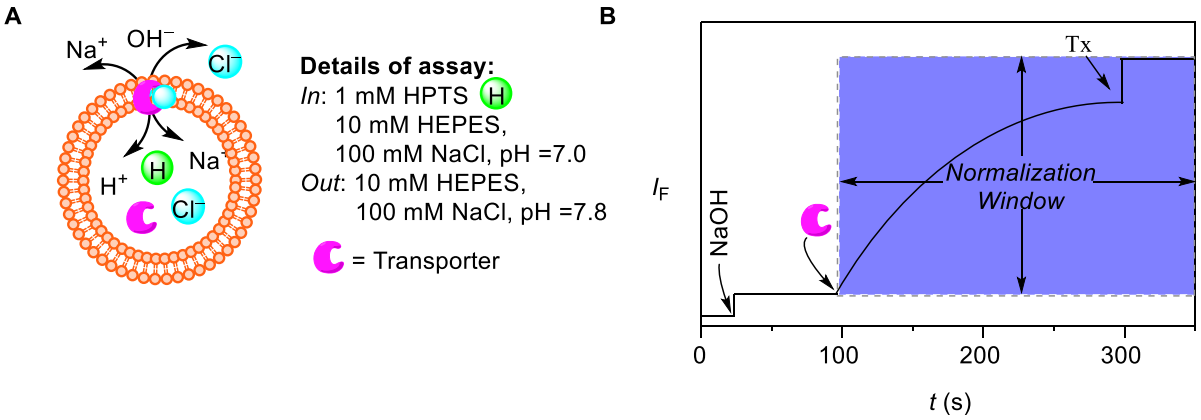


**Fig. S1** Schematic representations of fluorescence-based ion transport activity assay using EYPC-LUVs⊃HPTS (**A**), and illustration of ion transport kinetics showing normalization window (**B**).

**Dose-response activity:** The transport activity of transporters at different concentrations was examined by monitoring the fluorescence kinetics of HPTS over the course of time. The dose-responsive data provide $EC_{50}$ (i.e., effective concentration to achieve 50% transport activity) and Hill coefficient $n$ (number of molecules involved in the ion transport) using the Hill equation.

$$Y = Y_\infty + (Y_0 - Y_\infty) / [1 + (c/EC_{50})^n] \qquad \text{Equation S2}$$

where, $Y_0$ = fluorescence intensity just before the transporter addition (at $t$ = 0 s), $Y_\infty$ = fluorescence intensity with excess transporter concentration, $c$ = concentration of transporter compound, and $n$ = Hill coefficient (i.e. indicative for the number of monomers needed to form an active supramolecule).

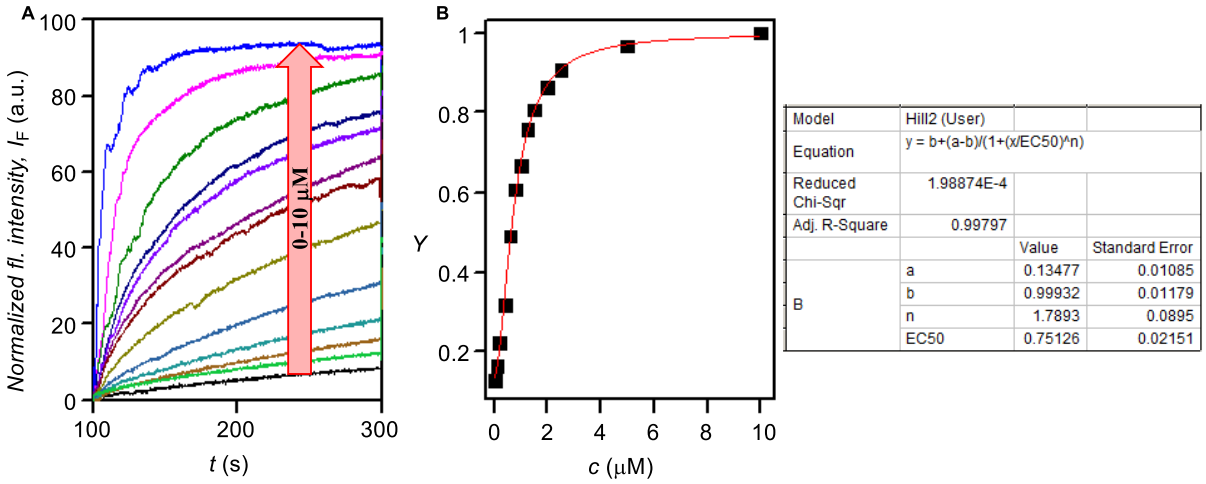


**Fig. S2** Dose-dependent activity of compound **1a** across EYPC-LUVs⊃HPTS (**A**). Hill plot analysis of compound **1a** at $t$ = 290 s.

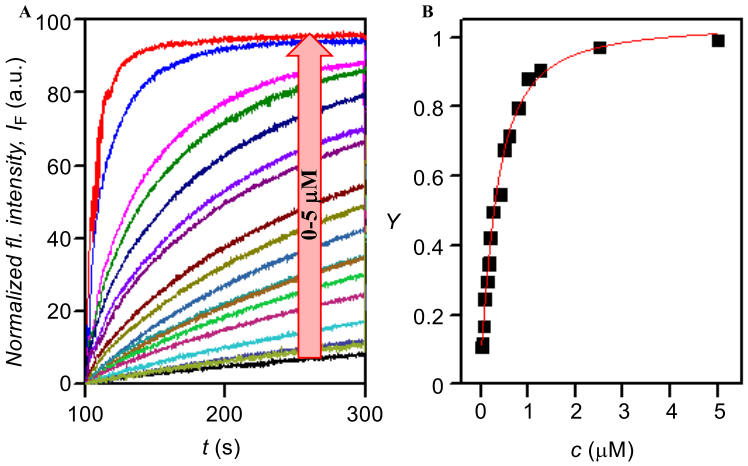


| Model | Hill2 (User) | | |
|---|---|---|---|
| Equation | y = b+(a-b)/(1+(x/EC50)^n) | | |
| Reduced Chi-Sqr | 6.95046E-4 | | |
| Adj. R-Square | 0.99255 | | |
| | | Value | Standard Error |
| B | a | 0.08961 | 0.024 |
| | b | 1.03908 | 0.02889 |
| | n | 1.30102 | 0.11316 |
| | EC50 | 0.34752 | 0.02402 |

**Fig. S3** Dose-dependent activity of compound **1b** across EYPC-LUVs⊃HPTS (**A**). Hill plot analysis of compound **1b** at *t* = 290 s.

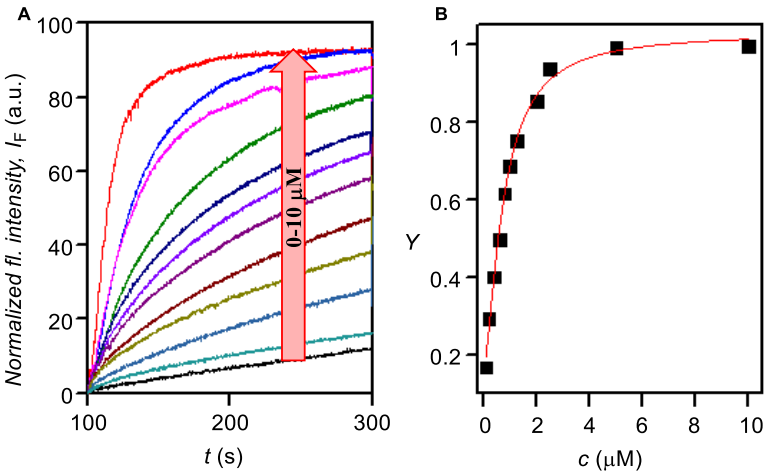


| Model | Hill2 (User) | | |
|---|---|---|---|
| Equation | y = b+(a-b)/(1+(x/EC50)^n) | | |
| Reduced Chi-Sqr | 5.3085E-4 | | |
| Adj. R-Square | 0.99351 | | |
| | | Value | Standard Error |
| B | a | 0.15273 | 0.03296 |
| | b | 1.03071 | 0.02421 |
| | n | 1.50957 | 0.16881 |
| | EC50 | 0.748 | 0.05051 |

**Fig. S4** Dose-dependent activity of compound **1c** across EYPC-LUVs⊃HPTS (**A**). Hill plot analysis of compound **1c** at *t* = 290 s.

**Anion selectivity studies across EYPC-LUVs⊃HPTS:**

**Preparation of EYPC-LUVs⊃HPTS:** The vesicles were prepared by following the protocol as stated above.

**Preparation of buffer and stock solution:** The HEPES buffers of 10 mM HEPES and 100 mM inorganic salts were prepared by dissolution of the required amount of solid HEPES and inorganic salts (NaBr, NaCl, NaI, $NaNO_3$, $NaClO_4$, and NaOAc) in autoclaved Milli-Q water. The pH of all buffers was adjusted to 7.0 by the addition of aliquots of 0.5 M NaOH. The stock solution of the most active transporter **1b** was prepared in HPLC grade DMSO.

**Anion selectivity assay:** In clean and dry fluorescence cuvette, 1975 mL HEPES buffer (10 mM HEPES, 100 mM NaX, pH = 7.0, where X = $Cl^-$, $Br^-$, $I^-$, $NO_3^-$, $OAc^-$ and $ClO_4^-$) and 25 µL vesicles

were taken. The cuvette was placed in fluorescence instrument furnishes with slow stirring conditions ($t$ = 0). After 20 s, a NaOH pulse (0.5 M, 20 µL) was given to create a pH gradient ($pH_{in}$ = 7.0, $pH_{out}$ = 7.8). The change in fluorescence intensity of HPTS at $\lambda_{em}$ = 510 nm ($\lambda_{ex}$ = 450 nm) was monitored after the addition of transporter molecule (500 nM DMSO solution) at t = 100 s. Finally, vesicles were lysed at $t$ = 300 s upon the addition of 20 µL 10% Triton X-100 for the complete dissipation of the pH gradient. The time-dependent data were normalized to percent change in intensity using Equation S1.

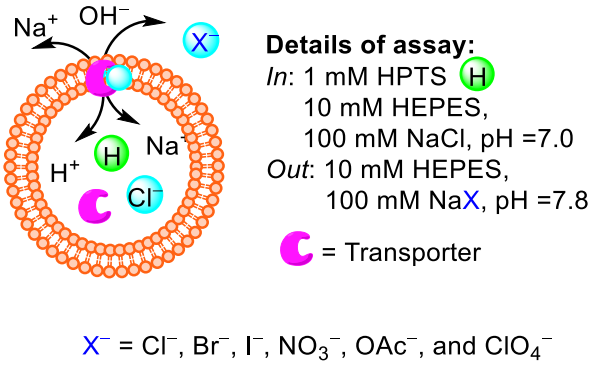


**Fig. S5** Schematic representation of fluorescence-based anion selectivity assay by the variation of extravesicular anions across EYPC-LUVs⊃HPTS.

**Ion transport studies across EYPC-LUVs⊃lucigenin:**

**Preparation of EYPC-LUVs⊃lucigenin:** The thin transparent film of egg yolk phosphatidylcholine (EYPC) was prepared by the slow evaporation of 1 mL chloroform solution of EYPC (25 mg/mL in chloroform) under nitrogen gas. The thin transparent film was kept on a high vacuum for 4-5 h to remove all traces of chloroform. After that, a thin transparent film was hydrated with 1 mL aqueous $NaNO_3$ solution (200 mM, 1 mM lucigenin) by vortexing at 10 min intervals for 1 h. The resulting suspension was subjected to 15 cycles of freeze-thaw (liquid nitrogen, 55 °C) followed by extrusion through a 200 nm polycarbonate membrane 21 times, to access vesicles of average 200 nm diameter. The extravesicular HPTS dye was removed by size exclusion chromatography using Sephadex G-50 (stationary phase) with eluting aqueous $NaNO_3$ (200 mM). Finally, vesicles were diluted to 4 mL to get EYPC-LUVs⊃lucigenin. *Final conditions*: ~7.5 mM EYPC, Inside: 1 mM lucigenin, 200 mM $NaNO_3$, Outside: 200 mM $NaNO_3$.

**Ion transport activity by lucigenin assay:** In a clean and dry fluorescence cuvette, 1975 µL aqueous $NaNO_3$ (200 mM) and 25 µL EYPC-LUVs⊃lucigenin vesicles were taken. The cuvette was placed in fluorescence instrument furnishes with slow stirring conditions ($t$ = 0). After 20 s, a NaCl pulse (2 M, 33.3 µL) was given to create a chloride gradient across vesicular membranes. The time-dependent quenching of fluorescence intensity of lucigenin at $\lambda_{em}$ = 535 nm ($\lambda_{ex}$ = 455 nm) was monitored after the addition of transporter molecule at $t$ = 100 s. Finally, vesicles were lysed upon the addition of 10% Triton X-100 (20 µL) at $t$ = 300 s for the complete dissipation of the chloride gradient.

The time-dependent data were normalized to percent change in fluorescence intensity using Equation S3:

$$I_F = [(I_t - I_0) / (I_\infty - I_0)] \times (-100) \qquad \text{Equation S3}$$

where, $I_0$ is the initial intensity, $I_t$ is the intensity at time $t$, $I_\infty$ is the final intensity after addition of Triton X-100.

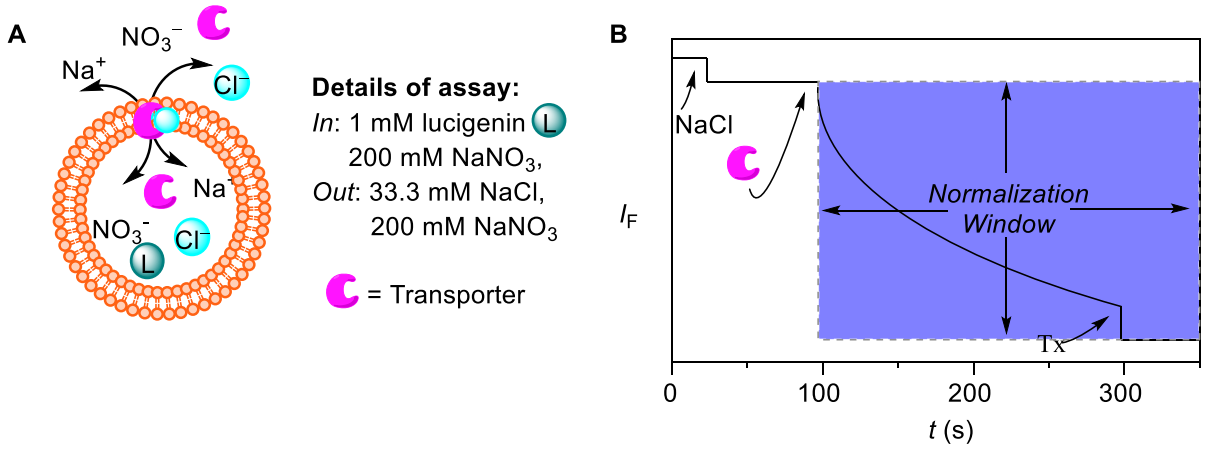


**Fig. S6** Schematic representation of fluorescence-based ion transport activity assay using EYPC-LUVs⊃lucigenin (**A**), and illustration of ion transport kinetics showing normalization window (**B**).

**Dose-response activity:** The activity of transporters at different concentrations was examined by monitoring the fluorescence kinetics of lucigenin over the course of time. The dose-response data provided $EC_{50}$ and Hill coefficient ($n$) by fitting to the Hill equation (Equation S2).

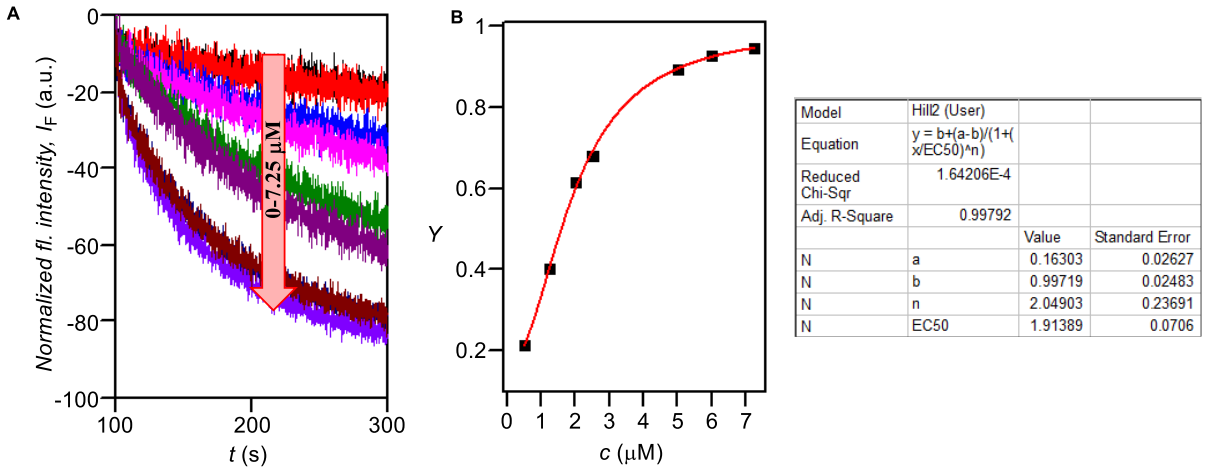


| Model | Hill2 (User) | | |
|---|---|---|---|
| Equation | y = b+(a-b)/(1+(x/EC50)^n) | | |
| Reduced Chi-Sqr | 1.64206E-4 | | |
| Adj. R-Square | 0.99792 | | |
| | | Value | Standard Error |
| N | a | 0.16303 | 0.02627 |
| N | b | 0.99719 | 0.02483 |
| N | n | 2.04903 | 0.23691 |
| N | EC50 | 1.91389 | 0.0706 |

**Fig. S7** Dose-dependent activity of compound **1a** across EYPC-LUVs⊃lucigenin (**A**). Hill plot analysis of compound **1a** at *t* = 290 s.

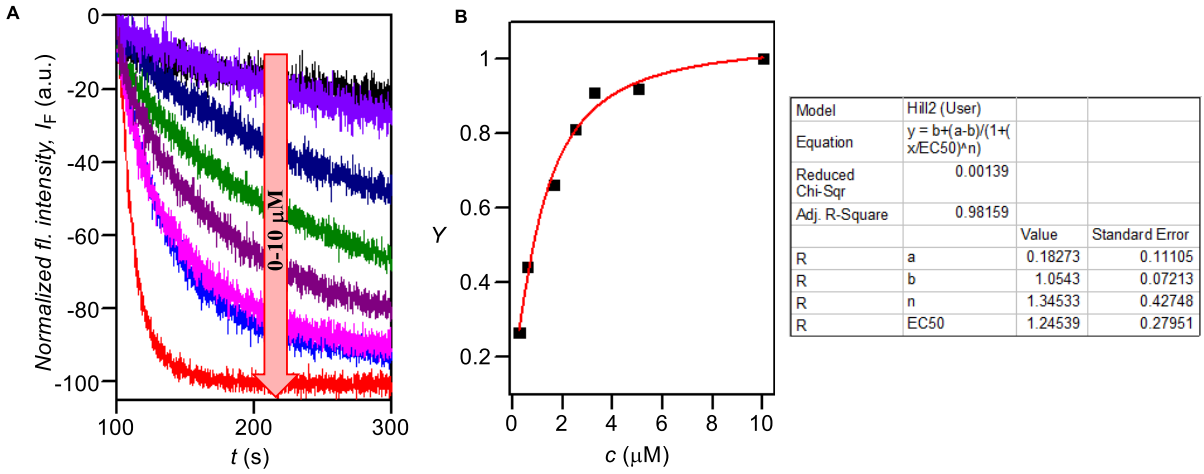


| Model | Hill2 (User) | | |
|---|---|---|---|
| Equation | y = b+(a-b)/(1+(x/EC50)^n) | | |
| Reduced Chi-Sqr | 0.00139 | | |
| Adj. R-Square | 0.98159 | | |
| | | Value | Standard Error |
| R | a | 0.18273 | 0.11105 |
| R | b | 1.0543 | 0.07213 |
| R | n | 1.34533 | 0.42748 |
| R | EC50 | 1.24539 | 0.27951 |

**Fig. S8** Dose-dependent activity of compound **1b** across EYPC-LUVs⊃lucigenin (**A**). Hill plot analysis of compound **1b** at *t* = 290 s.

**Cation selectivity assay across EYPC-LUVs⊃lucigenin:** The vesicles were prepared by following the same protocol as stated above. In a clean and dry fluorescence cuvette, 1975 µL aqueous $NaNO_3$ (200 mM) and 25 µL EYPC-LUVs⊃lucigenin vesicles were taken. The cuvette was placed in fluorescence instrument furnishes with slow stirring conditions (*t* = 0). After 20 s, chloride salts of different cations, MCl (where $M^+$ = $Li^+$, $Na^+$, $K^+$, $Rb^+$, and $Cs^+$) pulse (2 M, 33.3 µL) was given to create a chloride gradient across intra and extravesicular system. The time-dependent quenching of fluorescence intensity of lucigenin at $\lambda_{em}$ = 535 nm ($\lambda_{ex}$ = 455 nm) was monitored after the addition of transporter molecule at *t* = 100 s. Finally, vesicles were lysed upon the addition of 10% Triton X-100 (20 µL) at *t* = 300 s for the complete

dissipation of the chloride gradient. The time-dependent data were normalized to percent change in fluorescence intensity using Equation S3.

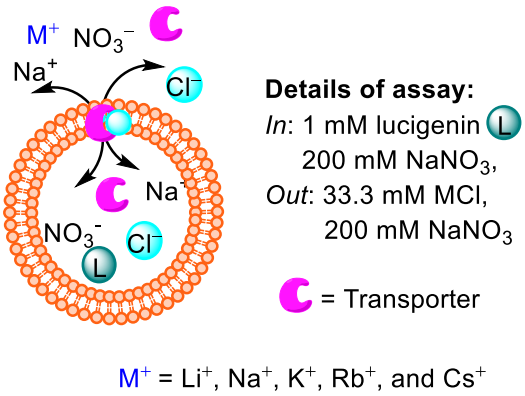


**Fig. S9** Schematic representation of fluorescent-based cation selectivity assay by the variation of extravesicular cations across EYPC-LUVs⊃lucigenin.

**Valinomycin coupled assay across EYPC-LUVs⊃lucigenin:** The vesicles were prepared by following the same protocol as stated above. In a clean and dry fluorescence cuvette, 1975 µL aqueous $KNO_3$ (200 mM) and 25 µL EYPC-LUVs⊃lucigenin vesicles were taken. The cuvette was placed in fluorescence instrument furnishes with slow stirring conditions ($t$ = 0). After 20 s, a KCl pulse (2 M, 33.3 µL) was given to create a chloride gradient across intra and extravesicular systems followed by the addition of valinomycin (0.2 µM in ACN) at 50 s. The time-dependent quenching of fluorescence intensity of lucigenin at $\lambda_{em}$ = 535 nm ($\lambda_{ex}$ = 455 nm) was monitored after the addition of transporter molecule at $t$ = 100 s. Finally, vesicles were lysed upon the addition of 10% Triton X-100 (20 µL) at $t$ = 300 s for the complete dissipation of the chloride gradient. The time-dependent data were normalized to percent change in fluorescence intensity using Equation S3.

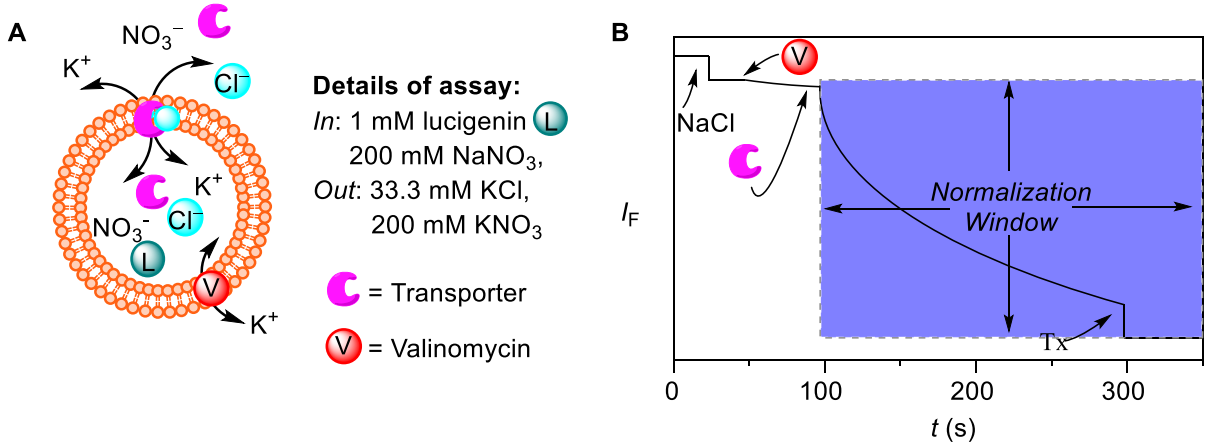


**Fig. S10** Schematic representation of valinomycin coupled assay using EYPC-LUVs⊃lucigenin (**A**), and illustration of ion transport kinetics showing normalization window (**B**).

**Ion transport activity studies across DPPC-LUVs⊃HPTS (Carrier vs channel mechanism):**

**Preparation of HEPES buffer and stock solutions:** The buffers and stock solutions were prepared in the same as for EYPC-LUVs⊃HPTS.

**Preparation of DPPC-LUVs⊃HPTS in NaCl:** 12.5 mg of 1,2-dipalmitoyl-*sn*-glycero-3-phosphocholine (DPPC) was dissolved in 0.5 mL of HPLC grade chloroform and a thin film of the lipid was prepared by slow evaporation of chloroform under nitrogen gas. It was then kept on a high vacuum for 5 h to remove all traces of chloroform. After that, the thin transparent film was hydrated with 0.5 mL HEPES buffer (10 mM HEPES, 100 mM NaCl, 1 mM HPTS) by giving vertex at 10 min intervals for 1 h. The resulting suspension was subjected to 15 cycles of freeze-thaw (liquid nitrogen, 55 °C) followed by extrusion through a 200 nm polycarbonate membrane 35 times, to access vesicles of average 200 nm diameter. The extravesicular HPTS dye was removed by the size exclusion chromatography using Sephadex-G50 (stationary phase) with HEPES buffer (10 mM HEPES, 100 mM NaCl, pH = 7.0) as the mobile phase. Finally, vesicles were diluted to 3 mL to get DPPC-LUVs⊃HPTS. *Final conditions*: ~5.5 mM DPPC, Inside: 1 mM HPTS, 10 mM HEPES, 100 mM NaCl, pH = 7.0, Outside: 10 mM HEPES, 100 mM NaCl, pH = 7.0.

**Ion transport assay across DPPC-LUVs⊃HPTS:** The DPPC assay was conducted on a HORIBA Jobin Yvon Fluoromax+ spectrofluorometers equipped with injector port, and a Quantum Northwest, Inc. (QNW) Luma 40 Peltier-based temperature-controlled cuvette holder, with temperature control achieved using a QNW TC-1 temperature controller. The experiments were conducted in the same way as in ion transport studies with EYPC-LUVs⊃HPTS. Temperatures of 25 °C and 45 °C for experiments were maintained using the temperature-controlled cuvette holder. The time-dependent data were normalized to percent change in fluorescence intensity using Equation S1.

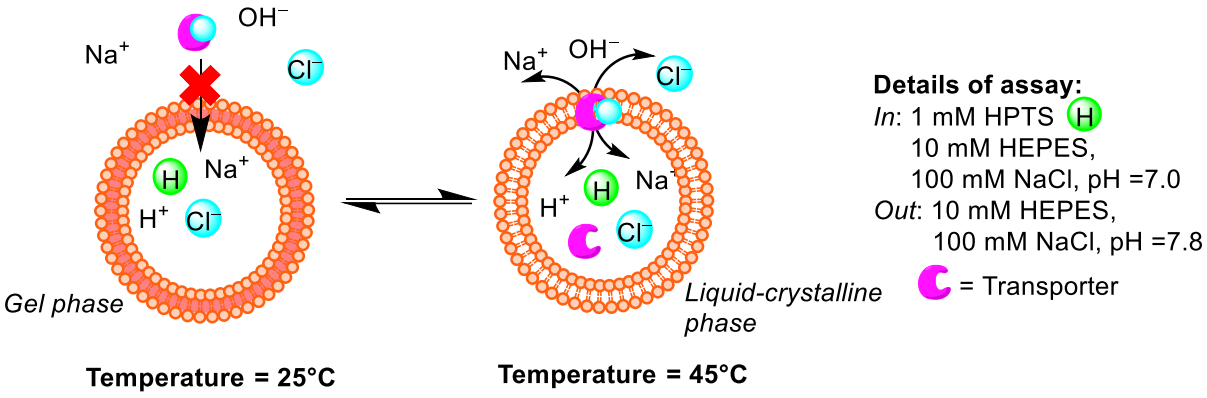


**Fig. S11** Schematic representation of DPPC assay.

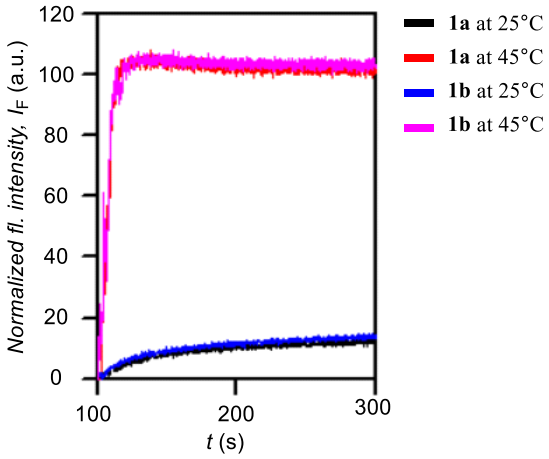


**Fig. S12** Assessment of compounds **1a** and **1b** (2.5 µM) across DPPC-LUVs⊃HPTS at 25 °C and 45 °C. Activity restoration at 45 °C confirms mobile carrier mechanism.

## V. $^1$H NMR Titration Studies

The $^1$H NMR titration study was conducted at ambient temperature on a Bruker Avance III HD 400 MHz spectrometer. The titration with $Cl^-$ ion was conducted by addition of aliquots of tetrabutylammonium chloride (TBACl) solution (0.2 M in 1:9 $CD_3COCD_3$ + $CD_3CN$) to a solution of the receptor in 1:9 $CD_3COCD_3$ + $CD_3CN$ (0.002 M). The spectra were calibrated using the residual signal from $CD_3CN$ (δH = 1.94 ppm) as internal reference. TBACl was dried under vacuum in a desiccator prior to use.

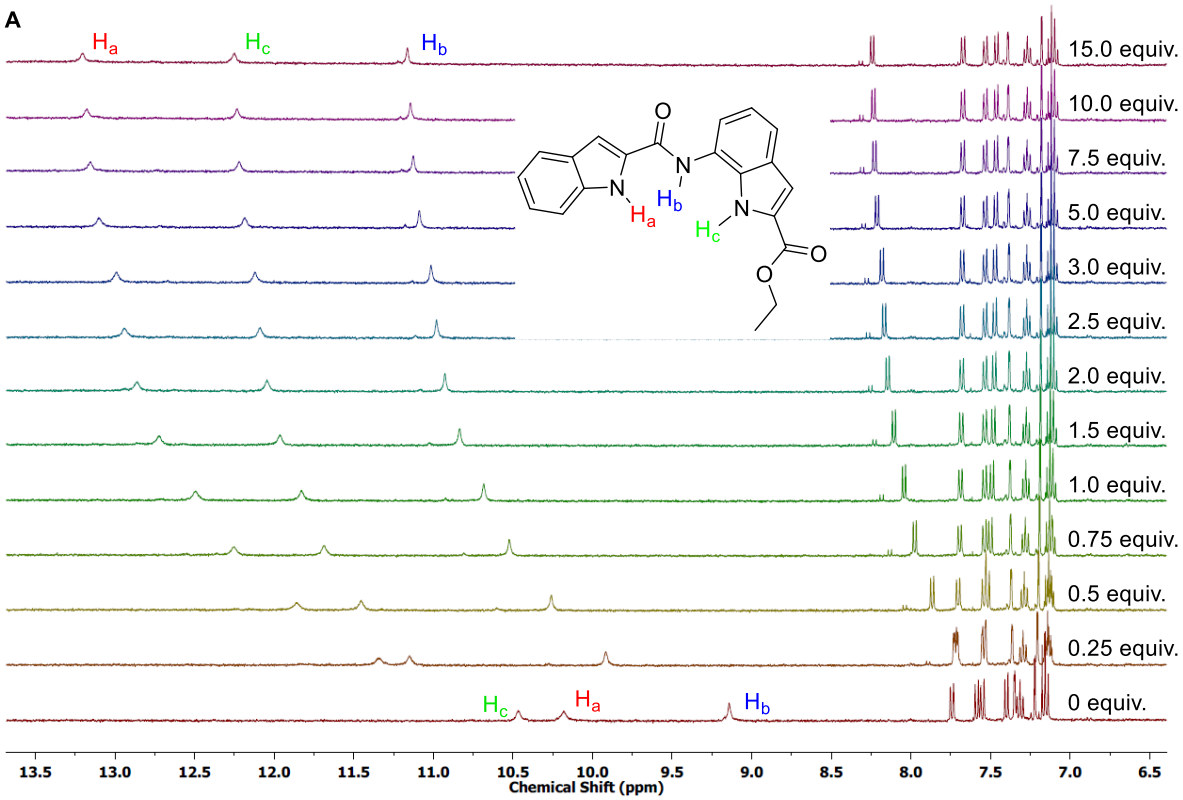


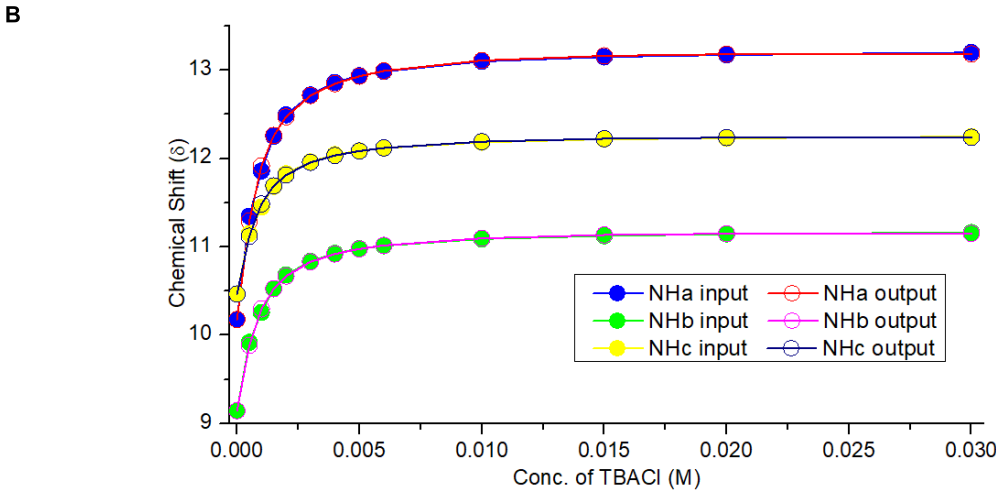


| Parameter (bounds) | Optimised | Error | Initial |
|---|---|---|---|
| $K_{11}$ ( 0 → 200 ) | 137.66 $M^{-1}$ | ± 8.8156 % | 150.00 $M^{-1}$ |
| $K_{21}$ ( 0 → 7000 ) | 5862.74 $M^{-1}$ | ± 6.7320 % | 5500.00 $M^{-1}$ |

**Fig. S13** (**A**) $^{1}$H NMR titration spectra of **1a** (2 mM) with stepwise addition of TBACl in 1:9 $CD_3COCD_3$ + $CD_3CN$. The number of TBACl equivalents added per reading is shown on the stacked spectra. (**B**) The plot of chemical shifts (δ) of protons $H_a$, $H_b$, and $H_c$ vs concentration of TBACl added, fitted to 2:1 binding model using BindFit v0.5.

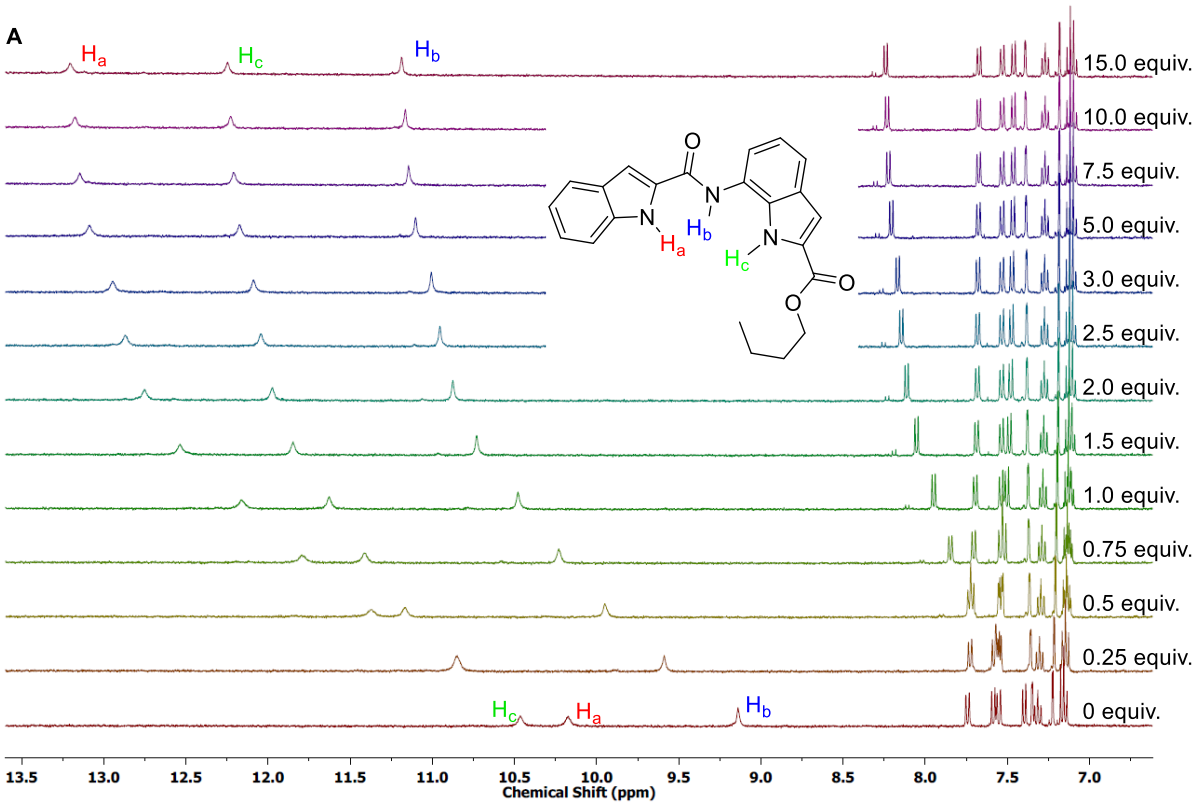


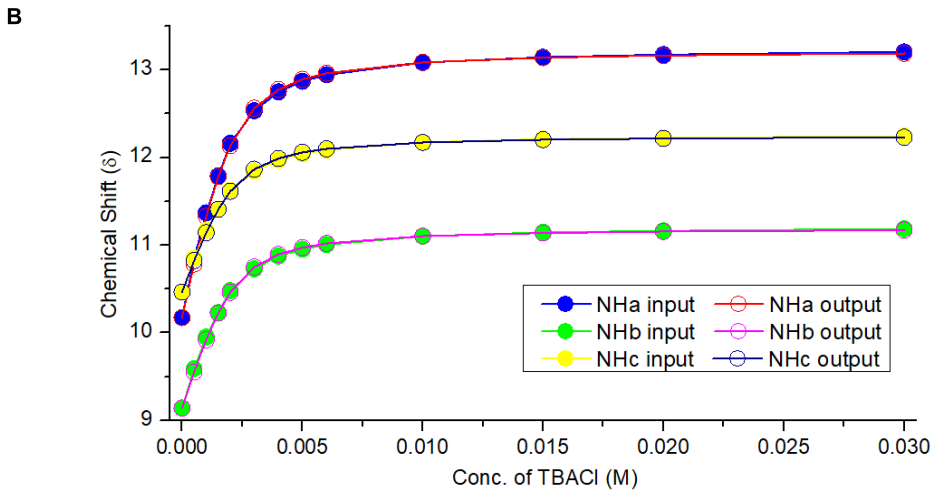


| Parameter (bounds) | Optimised | Error | Initial |
|---|---|---|---|
| K ( 0 → 5000 ) | 2489.49 $M^{-1}$ | ± 3.6658 % | 2500.00 $M^{-1}$ |

**Fig. S14** (**A**) $^{1}$H NMR titration spectra of **1b** (2 mM) with stepwise addition of TBACl in 1:9 $CD_3COCD_3$ + $CD_3CN$. The number of TBACl equivalents added per reading is shown on the stacked spectra. (**B**) The plot of chemical shifts (δ) of protons $H_a$, $H_b$, and $H_c$ vs concentration of TBACl added, fitted to 1:1 binding model using BindFit v0.5.

## VI. Single Crystal X-ray Diffraction Studies

**Single crystal data for 1d+DMSO (CCDC 2306377)**

The transporter **1d** was crystallized from slow evaporation of its saturated solution in DMSO in a glass vial to yield crystals as yellow rods. Single crystal X-ray diffraction data was collected on a Bruker D8 VENTURE single crystal X-ray diffractometer with Mo (Mo-Kα = 0.71073 Å) microfocus X-ray (IμS) source and PHOTON 100 CMOS detector. The data collection temperature was maintained at 296 K using a Cryostream cooler (Oxford Cryosystems).

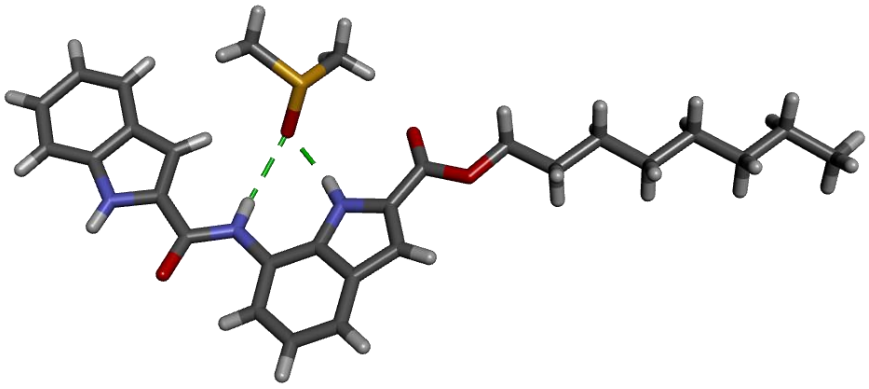

**Fig. S15** Co-crystal of **1d** with DMSO showing non-covalent binding of the solvent in the ion binding pocket of the transporter.

**Table S1:** Crystal data of **1d+DMSO**.

| | |
|---|---|
| Empirical formula | C28 H35 N3 O4 S |
| Formula weight | 509.65 |
| Temperature | 296(2) K |
| Wavelength | 0.71073 Å |
| Crystal system | Triclinic |
| Space group | P -1 |
| Unit cell dimensions | a = 7.914(6) Å α = 75.055(16)°.<br>B = 12.745(10) Å β = 78.771(16)°.<br>C = 13.674(11) Å γ = 84.956(16)°. |
| Volume | 1306.0(17) $Å^3$ |
| Z | 2 |
| Density (calculated) | 1.296 $Mg/m^3$ |
| Absorption coefficient | 0.163 $mm^{-1}$ |
| F(000) | 544 |
| Crystal size | 0.455 x 0.125 x 0.117 $mm^3$ |

| | |
|---|---|
| Theta range for data collection | 2.544 to 29.129° |
| Index ranges | -10<=h<=9, -17<=k<=17, -18<=l<=18 |
| Reflections collected | 6030 |
| Independent reflections | 5057 [R(int) = 0.1262] |
| Completeness to theta = 29.129° | 71.8 % |
| Absorption correction | Semi-empirical from equivalents |
| Max. and min. transmission | 0.5772 and 0.7462 |
| Refinement method | Full-matrix least-squares on $F^2$ |
| Data / restraints / parameters | 5057 / 0 / 328 |
| Goodness-of-fit on $F^2$ | 1.016 |
| Final R indices [I>2sigma(I)] | R1 = 0.1692, wR2 = 0.2231 |
| R indices (all data) | R1 = 0.3878, wR2 = 0.3070 |
| Extinction coefficient | n/a |
| Largest diff. peak and hole | 0.359 and -0.434 e.Å$^{-3}$ |

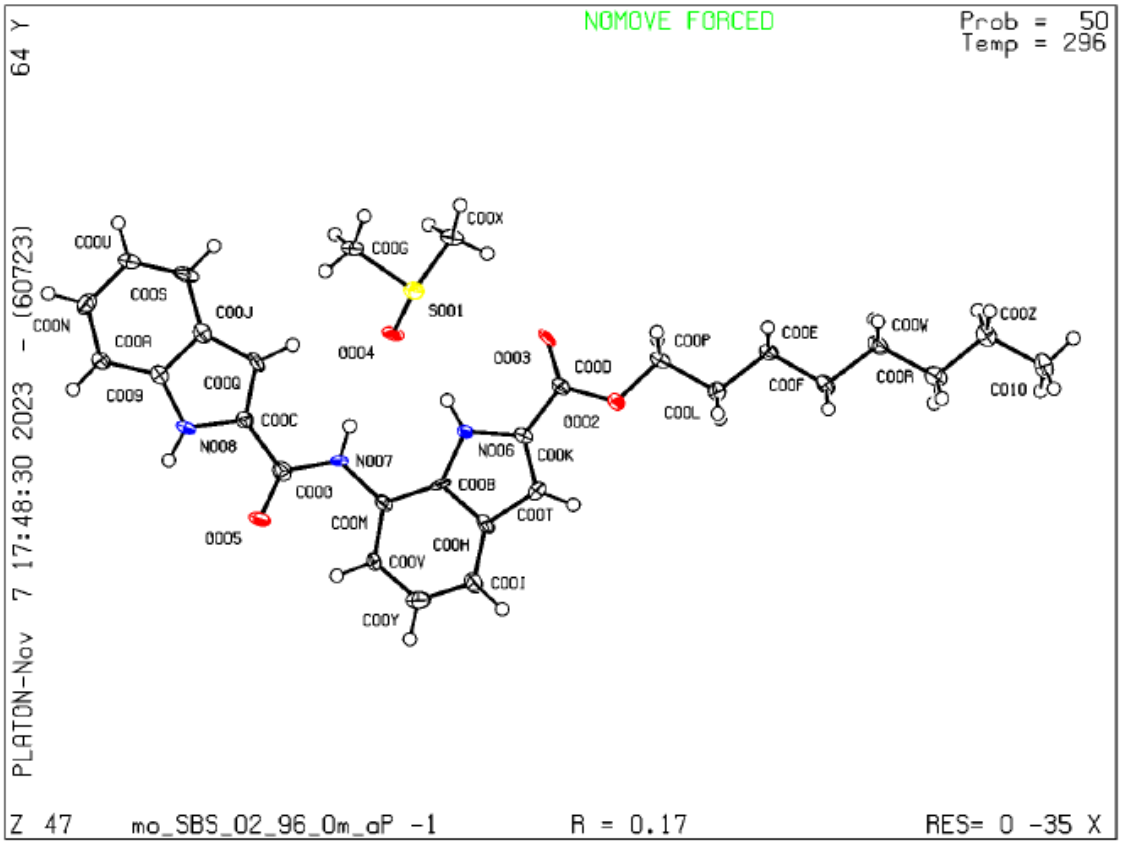


**Fig. S16** ORTEP diagram of **1d+DMSO**.

## VII. Theoretical Calculations

**Compound 1a:**

A list of possible geometries of the transporter **1a** was generated using the CONFLEX 8 conformation search software package[S1] using the MMFF94S (2010-12-04HG) force field with a search limit of 10 kcal/mol. A total of 26 predicted conformers were obtained, of which conformers with predicted Boltzmann population <5% were rejected. Geometry optimization of the remaining four conformations **CE1-CE4** were conducted on Gaussian 09 program suite[S2] using the B3LYP exchange-correlation functional[S3] and 6-31G (d,p) basis set.[S4] The conformations were observed to exhibit variation in their ethyl (ester) chains. The bis-indole core conformation remained constant, with adjacent NH bonds anti to each other. Hartree-Fock energies were observed to be very similar for the structures. The lowest energy structure, **CE1**, was selected for further calculations.

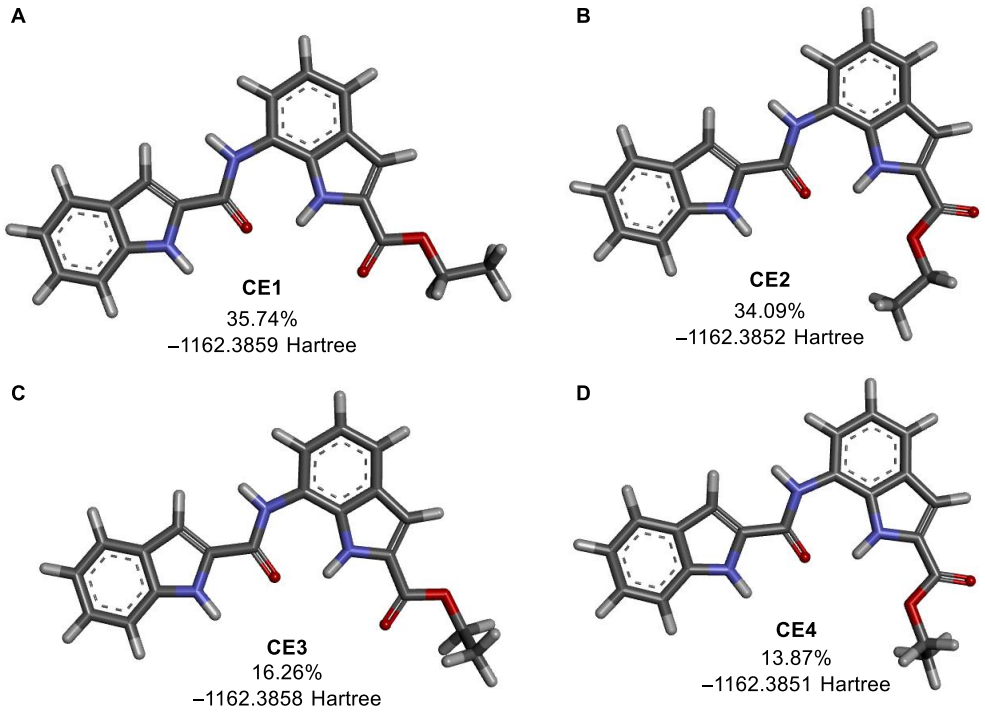


**Fig. S17** Geometry optimized structures of highest probability conformers of **1a** predicted using CONFLEX 8. The predicted Boltzmann populations (from CONFLEX 8 output) and calculated Hartree-Fock (HF) energies of the optimized structures are provided.

For **CE1**:

- HF energy = −1162.3859526 Hartree
- Zero-point energy = 0.3386918 Hartree

**Table S2.** Atomic coordinates of **CE1** after geometry optimization by Gaussian 09 using B3LYP/6-31G(d,p).

Charge = 0 Multiplicity = 1

| Atom # | Atom type | Coordinates (Angstroms) | | |
|---|---|---|---|---|
| | | X | Y | Z |
| 1 | O | 4.33805 | 5.70707 | 0 |
| 2 | O | 5.49217 | 4.89011 | 0 |
| 3 | O | 5.39242 | 3.50872 | 0 |
| 4 | O | 4.11273 | 2.91893 | 0 |
| 5 | O | 2.96178 | 3.76282 | 0 |
| 6 | O | 3.06346 | 5.16073 | 0 |
| 7 | O | 3.63749 | 1.57127 | 0 |
| 8 | O | 2.25603 | 1.62742 | 0 |
| 9 | N | 1.85904 | 2.94888 | 0 |
| 10 | O | 1.17757 | 0.61928 | 0 |
| 11 | O | 1.69325 | -3.06967 | 0 |
| 12 | O | 1.14177 | -4.3649 | 0 |
| 13 | O | -0.22762 | -4.55538 | 0 |
| 14 | O | -1.06101 | -3.4209 | 0 |
| 15 | O | -0.49629 | -2.10293 | 0 |
| 16 | O | 0.90602 | -1.91777 | 0 |
| 17 | O | -2.47728 | -3.25683 | 0 |
| 18 | O | -2.7239 | -1.89897 | 0 |
| 19 | N | -1.53176 | -1.2118 | 0 |
| 20 | O | -3.97773 | -1.13603 | 0 |
| 21 | N | 1.59803 | -0.6811 | 0 |
| 22 | O | 0 | 1.00056 | 0 |

| | | | | |
|---|---|---|---|---|
| 23 | O | -4.03236 | 0.08088 | 0 |
| 24 | O | -5.06097 | -1.94356 | 0 |
| 25 | C | -6.33942 | -1.27018 | 0 |
| 26 | C | -7.41653 | -2.33729 | 0 |
| 27 | H | 4.45343 | 6.78673 | 0 |
| 28 | H | 6.47125 | 5.35926 | 0 |
| 29 | H | 6.2837 | 2.8879 | 0 |
| 30 | H | 2.17892 | 5.79025 | 0 |
| 31 | H | 4.25429 | 0.68251 | 0 |
| 32 | H | 0.88332 | 3.20798 | 0 |
| 33 | H | 2.77567 | -2.96117 | 0 |
| 34 | H | 1.81367 | -5.21732 | 0 |
| 35 | H | -0.65543 | -5.55292 | 0 |
| 36 | H | -3.22724 | -4.03325 | 0 |
| 37 | H | -1.40198 | -0.2019 | 0 |
| 38 | H | 2.60173 | -0.79536 | 0 |
| 39 | H | -6.39949 | -0.62458 | 0.88205 |
| 40 | H | -6.39949 | -0.62458 | -0.88205 |
| 41 | H | -8.40455 | -1.86667 | 0 |
| 42 | H | -7.33809 | -2.97242 | -0.88691 |
| 43 | H | -7.33809 | -2.97242 | 0.88691 |

**Structure of [$(\mathbf{1a})_2$ + $Cl^-$] complex:**

Hill analysis of dose-dependent study of **1a** in HPTS assay gave a Hill coefficient value of ~2, indicating the formation of a [$(\mathbf{1a})_2$ + $Cl^-$] ion transport complex. The prediction of possible geometries of this complex using CONFLEX 8 conformation search software package[S1] using the MMFF94S (2010-12-04HG) force field with a search limit of 10 kcal/mol. A total of 10726 predicted conformers were obtained, of which conformers with predicted Boltzmann population <5% were rejected, which left 6 conformers. Geometry optimization of these conformations were conducted on Gaussian 09 program suite[S2] using the B3LYP exchange-correlation functional[S3] and 6-31G(d,p) basis set.[S4] The resultant conformations were

observed to be highly similar, with only slight conformational variations and had similar Hartree-Fock energies. The conformer with the lowest energy (**CEC**) was chosen for binding energy calculation. Geometry optimized conformer **CEC** exhibited interactions of chloride ion with all three NH groups in [(**1a**)$_2$ + Cl$^-$] complex. The two **1a** molecules were arranged in an orthogonal fashion to form a hydrophobic shell completely encapsulating the anion.

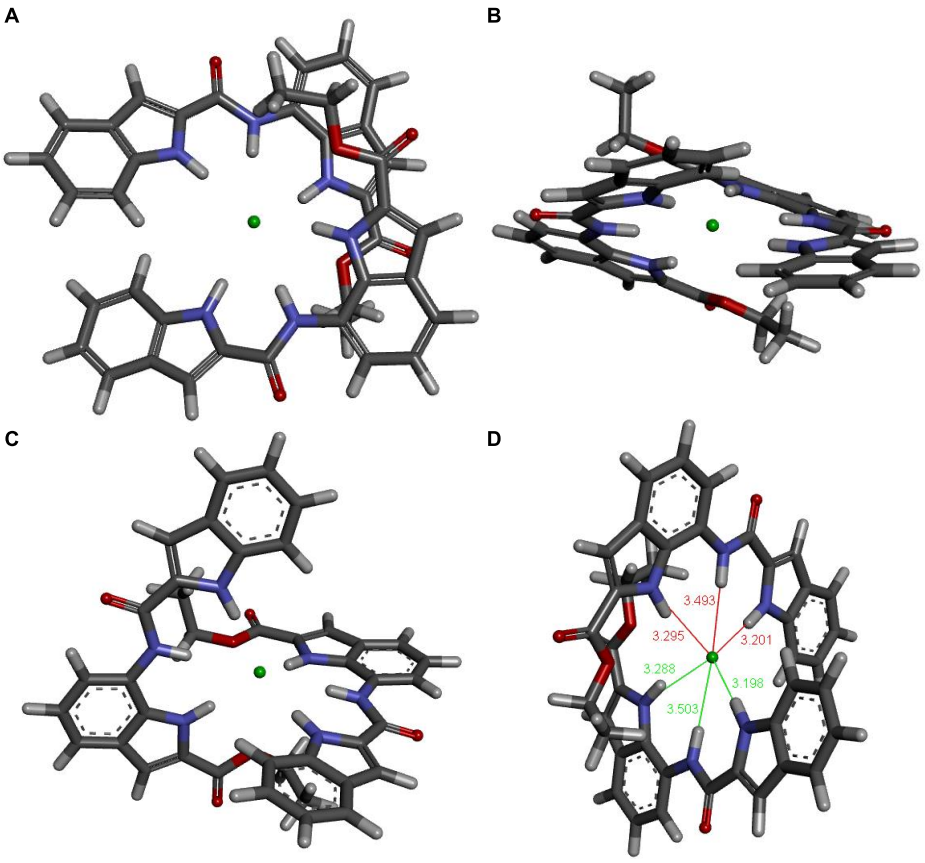


**Fig. S18** (**A**), (**B**) CONFLEX 8 predicted geometry of **CEC** conformer of [(**1a**)$_2$ + Cl$^-$] complex (predicted Boltzmann population- 9.38%). (**C**) Geometry optimized [(**1a**)$_2$ + Cl$^-$] complex (Gaussian 09, B3LYP/6-31G(d,p)) derived from **CEC** conformer. (**D**) N···Cl$^-$ H-bond distances in ion transport complex.

For [(**1a**)$_2$ + Cl$^-$]:

- HF energy = –2785.1237509 Hartree
- Zero-point energy = 0.6791279 Hartree
- BSSE = 0.019149779046 Hartree
- Binding energy = -0.078718321 Hartree = –49.39653358 kcal/mol

**Table S3.** Atomic coordinates of [(**1a**)$_2$ + $Cl^-$] after geometry optimization by Gaussian 09 using B3LYP/6-31G(d,p).

Charge = -1 Multiplicity = 1

| Atom # | Atom type | Coordinates (Angstroms) | | |
|---|---|---|---|---|
| | | X | Y | Z |
| 1 | C | -1.49231 | -4.46728 | -4.00289 |
| 2 | C | -2.78999 | -4.77363 | -4.47426 |
| 3 | C | -3.88658 | -4.0151 | -4.096 |
| 4 | C | -3.69494 | -2.92244 | -3.22682 |
| 5 | C | -2.37699 | -2.63345 | -2.76271 |
| 6 | C | -1.26689 | -3.40001 | -3.14558 |
| 7 | C | -4.55277 | -1.94677 | -2.64124 |
| 8 | C | -3.76777 | -1.11691 | -1.86366 |
| 9 | N | -2.44843 | -1.54041 | -1.93655 |
| 10 | C | -4.30647 | 0.02701 | -1.08765 |
| 11 | C | -4.96605 | 2.54485 | 0.43519 |
| 12 | C | -5.24054 | 3.65306 | 1.26437 |
| 13 | C | -4.29775 | 4.17029 | 2.13095 |
| 14 | C | -3.02882 | 3.56034 | 2.16828 |
| 15 | C | -2.74648 | 2.43772 | 1.33081 |
| 16 | C | -3.72359 | 1.90732 | 0.44793 |
| 17 | C | -1.84788 | 3.82136 | 2.91993 |
| 18 | C | -0.90765 | 2.88971 | 2.53828 |
| 19 | N | -1.45077 | 2.04517 | 1.58404 |
| 20 | C | 0.46592 | 2.77841 | 3.04209 |
| 21 | N | -3.40975 | 0.78631 | -0.35672 |
| 22 | O | -5.51661 | 0.2507 | -1.12087 |
| 23 | O | 0.94028 | 3.51355 | 3.89094 |
| 24 | O | 1.1362 | 1.76331 | 2.45017 |
| 25 | C | 2.5149 | 1.57469 | 2.849 |
| 26 | C | 3.44525 | 2.48357 | 2.06098 |

| | | | | |
|---|---|---|---|---|
| 27 | H | -0.65382 | -5.08171 | -4.31864 |
| 28 | H | -2.92398 | -5.61885 | -5.14385 |
| 29 | H | -4.88105 | -4.25608 | -4.46232 |
| 30 | H | -0.27186 | -3.16356 | -2.78191 |
| 31 | H | -5.62075 | -1.83878 | -2.75354 |
| 32 | H | -1.63616 | -1.10975 | -1.49107 |
| 33 | H | -5.73147 | 2.15855 | -0.2193 |
| 34 | H | -6.22911 | 4.10045 | 1.20799 |
| 35 | H | -4.51921 | 5.02107 | 2.7687 |
| 36 | H | -1.68793 | 4.59369 | 3.65741 |
| 37 | H | -0.91594 | 1.3281 | 1.09369 |
| 38 | H | -2.4256 | 0.54165 | -0.41638 |
| 39 | H | 2.59614 | 1.75921 | 3.92292 |
| 40 | H | 2.71309 | 0.52137 | 2.64343 |
| 41 | H | 4.48631 | 2.25956 | 2.3167 |
| 42 | H | 3.31779 | 2.33128 | 0.98597 |
| 43 | H | 3.24803 | 3.53223 | 2.29688 |
| 44 | C | 1.42429 | 4.28222 | -4.1487 |
| 45 | C | 2.71457 | 4.56882 | -4.65169 |
| 46 | C | 3.81612 | 3.82215 | -4.26429 |
| 47 | C | 3.63715 | 2.7618 | -3.3534 |
| 48 | C | 2.32648 | 2.49242 | -2.85798 |
| 49 | C | 1.21138 | 3.24683 | -3.25007 |
| 50 | C | 4.50313 | 1.80625 | -2.74668 |
| 51 | C | 3.72968 | 1.00644 | -1.92733 |
| 52 | N | 2.40985 | 1.43024 | -1.9934 |
| 53 | C | 4.27748 | -0.1092 | -1.11723 |
| 54 | C | 4.93918 | -2.59695 | 0.45726 |
| 55 | C | 5.22461 | -3.6704 | 1.32752 |
| 56 | C | 4.3066 | -4.12576 | 2.25372 |
| 57 | C | 3.05212 | -3.48797 | 2.31098 |

| | | | | |
|---|---|---|---|---|
| 58 | C | 2.75985 | -2.4001 | 1.43252 |
| 59 | C | 3.71116 | -1.93339 | 0.48849 |
| 60 | C | 1.89673 | -3.68615 | 3.11977 |
| 61 | C | 0.96245 | -2.7513 | 2.73142 |
| 62 | N | 1.48519 | -1.96393 | 1.71864 |
| 63 | C | -0.38687 | -2.58205 | 3.282 |
| 64 | V | 3.38735 | -0.84381 | -0.35433 |
| 65 | O | 5.48753 | -0.33278 | -1.15163 |
| 66 | O | -0.85258 | -3.27766 | 4.16805 |
| 67 | O | -1.04515 | -1.56061 | 2.68682 |
| 68 | C | -2.4059 | -1.32365 | 3.1196 |
| 69 | C | -3.38369 | -2.21011 | 2.36415 |
| 70 | H | 0.58165 | 4.88661 | -4.47263 |
| 71 | H | 2.83888 | 5.38923 | -5.35325 |
| 72 | H | 4.80485 | 4.04795 | -4.65503 |
| 73 | H | 0.22209 | 3.02549 | -2.86199 |
| 74 | H | 5.56912 | 1.69256 | -2.87175 |
| 75 | H | 1.6038 | 1.01337 | -1.52394 |
| 76 | H | 5.68632 | -2.25696 | -0.24275 |
| 77 | H | 6.20114 | -4.14126 | 1.25493 |
| 78 | H | 4.53698 | -4.94972 | 2.92277 |
| 79 | H | 1.75046 | -4.41803 | 3.90012 |
| 80 | H | 0.93906 | -1.27577 | 1.20056 |
| 81 | H | 2.40124 | -0.60763 | -0.41795 |
| 82 | H | -2.46486 | -1.49594 | 4.19694 |
| 83 | H | -2.57678 | -0.26678 | 2.90768 |
| 84 | H | -4.41054 | -1.95433 | 2.64611 |
| 85 | H | -3.28102 | -2.06828 | 1.28513 |
| 86 | H | -3.21109 | -3.26277 | 2.60188 |
| 87 | Cl | -0.00953 | -0.04582 | -0.50505 |

**Compound 1b:**

A list of possible geometries of transporter **1b** was generated using the CONFLEX 8 conformation search software package[S1] using the MMFF94S (2010-12-04HG) force field with a search limit of 10 kcal/mol. A total of 145 predicted conformers were obtained, of which conformers with predicted Boltzmann conformations <5% were rejected. Geometry optimization of the remaining four conformations **CB1-CB8** were conducted on Gaussian 09 program suite[S2] using the B3LYP exchange-correlation functional[S3] and 6-31G(d,p) basis set.[S4] The conformations were observed to exhibit variation in their ethyl (ester) chains. The bis-indole core conformation remained constant, with adjacent NH bonds anti to each other. Hartree-Fock energies were observed to be very similar for the structures. The lowest energy structure, **CB4**, was selected for further calculations.

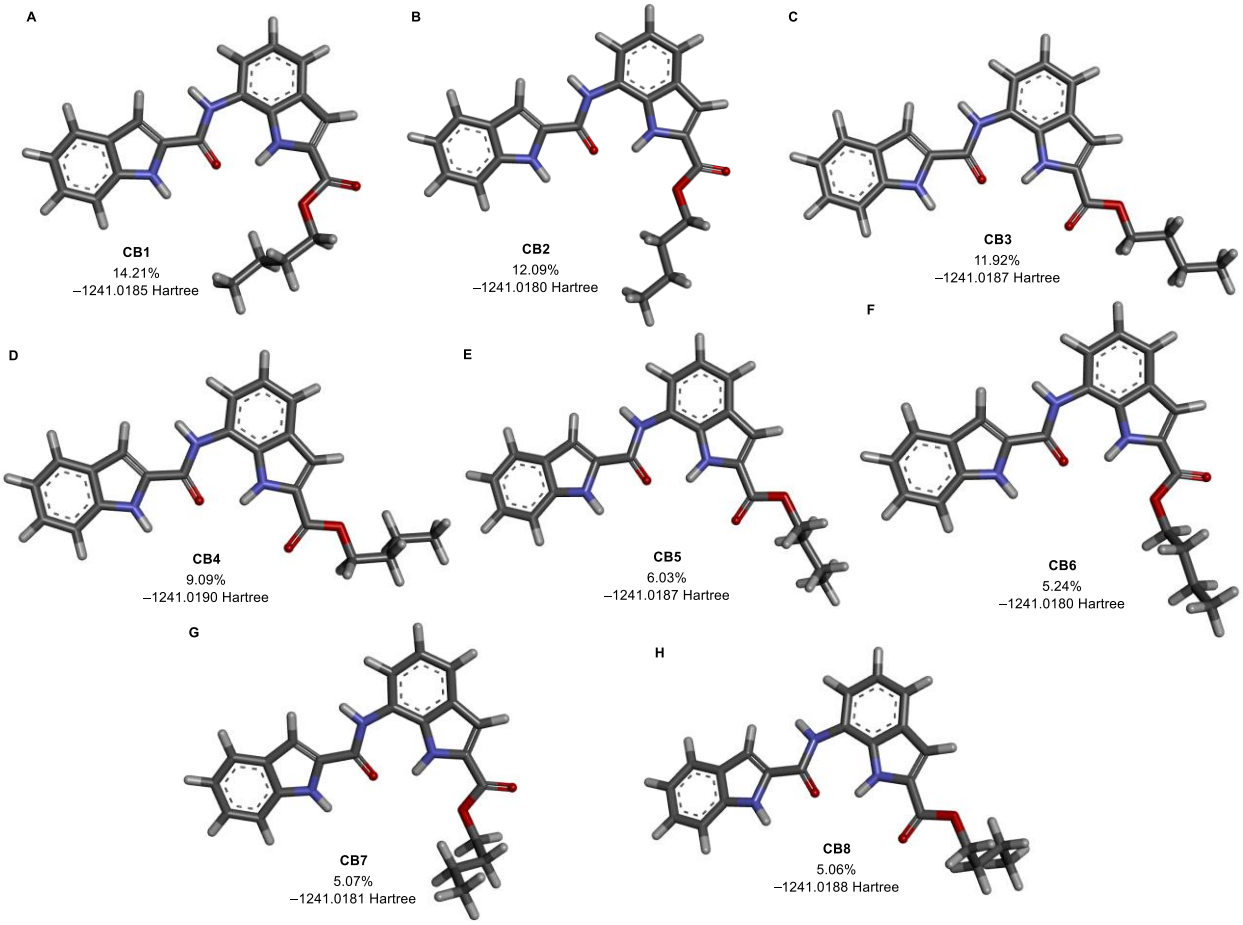


**Fig. S19** Geometry optimized structures of highest probability conformers of **1b** predicted using CONFLEX 8. The predicted Boltzmann populations (from CONFLEX 8 output) and calculated Hartree-Fock (HF) energies of the optimized structures are provided.

For **CB4**:

- HF energy = −1241.0190006 Hartree
- Zero-point energy = 0.3958468 Hartree

**Table S4.** Atomic coordinates of **CB4** after geometry optimization by Gaussian 09 using B3LYP/6-31G(d,p) basis set.

Charge = 0 Multiplicity = 1

| Atom # | Atom type | Coordinates (Angstroms) | | |
|---|---|---|---|---|
| | | X | Y | Z |
| 1 | C | 7.45429 | -2.34033 | 0.12599 |
| 2 | C | 7.97751 | -1.02914 | 0.2062 |
| 3 | C | 7.14317 | 0.07636 | 0.21044 |
| 4 | C | 5.75036 | -0.12237 | 0.13328 |
| 5 | C | 5.24432 | -1.45432 | 0.0533 |
| 6 | C | 6.08934 | -2.57268 | 0.04874 |
| 7 | C | 4.62001 | 0.75152 | 0.114 |
| 8 | C | 3.49254 | -0.04394 | 0.02603 |
| 9 | N | 3.87789 | -1.36855 | -0.01022 |
| 10 | C | 2.04114 | 0.2184 | -0.0324 |
| 11 | C | 0.47038 | 3.59546 | 0.03488 |
| 12 | C | -0.69528 | 4.38453 | 0.01554 |
| 13 | C | -1.9471 | 3.80288 | -0.06348 |
| 14 | C | -2.02987 | 2.39895 | -0.12444 |
| 15 | C | -0.84093 | 1.59807 | -0.10494 |
| 16 | C | 0.43561 | 2.20187 | -0.02372 |
| 17 | C | -3.1285 | 1.49422 | -0.20857 |
| 18 | C | -2.59821 | 0.22024 | -0.23682 |
| 19 | N | -1.22527 | 0.28899 | -0.17481 |
| 20 | C | -3.23574 | -1.09937 | -0.31772 |
| 21 | N | 1.68752 | 1.53821 | 0.00553 |
| 22 | O | 1.26077 | -0.73938 | -0.10907 |

| | | | | |
|---|---|---|---|---|
| 23 | O | -2.62025 | -2.15028 | -0.34122 |
| 24 | O | -4.58271 | -1.00801 | -0.36377 |
| 25 | C | -5.29374 | -2.26445 | -0.45018 |
| 26 | C | -6.78348 | -1.96273 | -0.42141 |
| 27 | C | -7.27167 | -1.34818 | 0.89634 |
| 28 | C | -8.77429 | -1.05466 | 0.89647 |
| 29 | H | 8.13771 | -3.18409 | 0.12497 |
| 30 | H | 9.05292 | -0.89228 | 0.26509 |
| 31 | H | 7.5525 | 1.08055 | 0.2721 |
| 32 | H | 5.69035 | -3.5805 | -0.01263 |
| 33 | H | 4.65426 | 1.83177 | 0.16036 |
| 34 | H | 3.20065 | -2.11455 | -0.07351 |
| 35 | H | 1.43695 | 4.09049 | 0.0985 |
| 36 | H | -0.59492 | 5.46417 | 0.06406 |
| 37 | H | -2.84751 | 4.40884 | -0.07826 |
| 38 | H | -4.17879 | 1.74067 | -0.24521 |
| 39 | H | -0.56749 | -0.48824 | -0.1788 |
| 40 | H | 2.46688 | 2.17788 | 0.06731 |
| 41 | H | -4.99905 | -2.77172 | -1.37451 |
| 42 | H | -4.98906 | -2.90108 | 0.38741 |
| 43 | H | -7.02745 | -1.29619 | -1.25861 |
| 44 | H | -7.3138 | -2.90592 | -0.6104 |
| 45 | H | -7.02951 | -2.03108 | 1.72203 |
| 46 | H | -6.7129 | -0.4252 | 1.08853 |
| 47 | H | -9.09433 | -0.61711 | 1.8474 |
| 48 | H | -9.04055 | -0.34987 | 0.10062 |
| 49 | H | -9.3594 | -1.96777 | 0.73737 |

**Structure of [1b + $Cl^-$] complex:**

Hill analysis of dose-dependent study of **1b** in HPTS assay gave a Hill coefficient value of ~1, indicating the formation of a [**1b** + $Cl^-$] ion transport complex. The prediction of possible

geometries of this complex using CONFLEX 8 conformation search software package[S1] using the MMFF94S (2010-12-04HG) force field with a search limit of 10 kcal/mol. A total of 101 predicted conformers were obtained, of which conformers with predicted Boltzmann population <5% were rejected, which left 7 conformers. Geometry optimization of these conformations were conducted on Gaussian 09 program suite[S2] using the B3LYP exchange-correlation functional[S3] and 6-31G(d,p) basis set.[S4] The resultant conformations were observed to be highly similar, with only slight conformational variations and had similar Hartree-Fock energies. The conformer with the lowest energy (**CBC**) was chosen for binding energy calculation. Geometry optimized conformer **CBC** exhibited interactions of chloride ion with all three NH groups in [**1b** + $Cl^-$] complex.

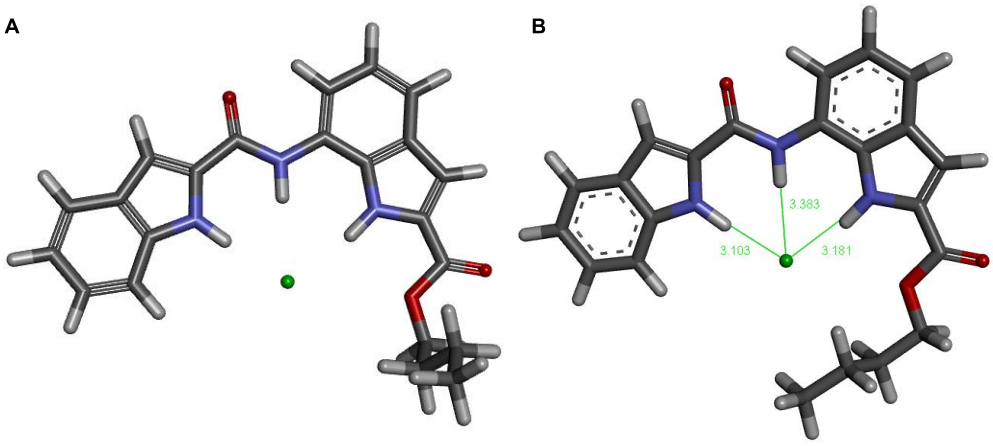


**Fig. S20** CONFLEX 8 predicted geometry of **CBC** conformer of [**1b** + $Cl^-$] complex (predicted Boltzmann population- 5.10%) (**A**). Geometry optimized [**1b** + $Cl^-$] complex (Gaussian 09, B3LYP/6-31G(d,p)) derived from **CBC** conformer showing N···$Cl^-$ H-bond distances (**B**).

For [**1b** + $Cl^-$]:

- HF energy = –1701.3436392 Hartree
- Zero-point energy = 0.3958335 Hartree
- BSSE = 0.010760023126 Hartree
- Binding energy = –0.061658577 Hartree = –38.69137357 kcal/mol

**Table S5.** Atomic coordinates of [**1b** + $Cl^-$] after geometry optimization by Gaussian 09 using B3LYP/6-31G(d,p).

Charge = −1 Multiplicity = 1

| Atom # | Atom type | Coordinates (Angstroms) | | |
|---|---|---|---|---|
| | | X | Y | Z |
| 1 | C | -5.73247 | -2.4522 | -0.28138 |
| 2 | C | -6.72764 | -1.46784 | -0.07693 |
| 3 | C | -6.39077 | -0.13307 | 0.08993 |
| 4 | C | -5.03234 | 0.24102 | 0.05455 |
| 5 | C | -4.04422 | -0.77058 | -0.15302 |
| 6 | C | -4.38555 | -2.12072 | -0.32256 |
| 7 | C | -4.32516 | 1.47078 | 0.18396 |
| 8 | C | -2.977 | 1.18521 | 0.05699 |
| 9 | N | -2.81303 | -0.17286 | -0.1464 |
| 10 | C | -1.90967 | 2.21575 | 0.13905 |
| 11 | C | 0.50555 | 4.00896 | 0.16757 |
| 12 | C | 1.68168 | 4.78828 | 0.22365 |
| 13 | C | 2.93974 | 4.22234 | 0.1705 |
| 14 | C | 3.02794 | 2.82055 | 0.05533 |
| 15 | C | 1.84006 | 2.02553 | -6.7E-4 |
| 16 | C | 0.54714 | 2.61672 | 0.05593 |
| 17 | C | 4.12695 | 1.92064 | -0.0227 |
| 18 | C | 3.60163 | 0.64805 | -0.11808 |
| 19 | N | 2.22049 | 0.70945 | -0.10091 |
| 20 | C | 4.35655 | -0.60438 | -0.2194 |
| 21 | N | -0.6019 | 1.79694 | 3.97E-4 |
| 22 | O | -2.23959 | 3.38942 | 0.3282 |
| 23 | O | 5.57309 | -0.68078 | -0.28186 |
| 24 | O | 3.53325 | -1.67452 | -0.23551 |
| 25 | C | 4.14314 | -2.96997 | -0.37743 |
| 26 | C | 3.03271 | -4.00753 | -0.306 |

| | | | | |
|---|---|---|---|---|
| 27 | C | 2.34435 | -4.08266 | 1.06197 |
| 28 | C | 1.19096 | -5.08832 | 1.08505 |
| 29 | H | -6.0303 | -3.48973 | -0.40891 |
| 30 | H | -7.77226 | -1.76765 | -0.05113 |
| 31 | H | -7.16215 | 0.61709 | 0.24643 |
| 32 | H | -3.61625 | -2.87046 | -0.47911 |
| 33 | H | -4.72294 | 2.46004 | 0.35154 |
| 34 | H | -1.91804 | -0.67371 | -0.28064 |
| 35 | H | -0.46036 | 4.48601 | 0.21872 |
| 36 | H | 1.57492 | 5.86648 | 0.31209 |
| 37 | H | 3.83912 | 4.83025 | 0.21614 |
| 38 | H | 5.18089 | 2.15615 | -0.00795 |
| 39 | H | 1.59623 | -0.10423 | -0.21124 |
| 40 | H | -0.43589 | 0.79988 | -0.16028 |
| 41 | H | 4.67497 | -3.00675 | -1.33518 |
| 42 | H | 4.88772 | -3.10377 | 0.41655 |
| 43 | H | 2.2857 | -3.76926 | -1.07183 |
| 44 | H | 3.46818 | -4.98395 | -0.56439 |
| 45 | H | 3.08811 | -4.34366 | 1.82971 |
| 46 | H | 1.95497 | -3.09037 | 1.30804 |
| 47 | H | 0.73694 | -5.14894 | 2.08013 |
| 48 | H | 0.40919 | -4.78197 | 0.38311 |
| 49 | H | 1.52622 | -6.09687 | 0.8094 |
| 50 | Cl | -0.0329 | -1.49363 | -0.53866 |

## VIII. Biological Studies

**Cell Culture**

Biological studies were carried out in the human breast cancer cells, namely, MCF-7 and the non-cancerous MEFs (mouse embryonic fibroblasts). These cells were grown in high glucose containing Dulbecco's Modified Eagle Medium (DMEM; Lonza) containing 2 mM of L-glutamine supplemented with 10% fetal bovine serum (FBS; Invitrogen), and 100 units/mL

penicillin and 100 μg/mL streptomycin (Invitrogen). Cells were maintained in tissue culture-treated T25 flasks at 37 °C in a humidified 5% $CO_2$ incubator (Thermo Scientific) until they achieved 80% confluence and were split in 1:3 ratios every alternate day.

**Assessment of Cellular Viability by MTT assay**

To check the anti-cancer activity of the bisindole compounds (**1a**-**1d**), cellular viability assay was performed using MTT (3-[4,5-dimethylthiazol-2-yl]-2,5 diphenyl tetrazolium bromide). Briefly, cells were seeded in a tissue culture-treated 96-well plate (Corning) at a density of 8 x $10^3$ cells/well/100 μL in DMEM and incubated at 37 °C in a humidified 5% $CO_2$ incubator for a period of 24 h. Post incubation, the cells were treated with increasing concentrations (range 1-20 μM) of the **1a**, **1b**, **1c**, and **1d** compounds for a period of 24 h. Subsequently, the media was removed, MTT solution (0.5 mg/mL MTT in PBS) was added and the plates were incubated in dark at 37 °C for an additional 4 h. The formazan crystals, thus formed, were dissolved using solubilization buffer (10% SDS/0.1N HCl in PBS) by incubating the plates overnight at room temperature. Absorbance was measured at 570 nm using a multi-mode plate reader (Hidex). All experiments were performed in triplicate (N = 3). Cellular viability was expressed as the percentage of viable cells for each treatment when compared with the untreated cells (control, set as 100%).

It was observed that amongst the four bisindole compounds tested, compound **1a** showed the maximum cytotoxicity in the cancerous MCF-7 cells (Fig. 4A). Interestingly, these compounds were relatively non-toxic up to 20 μM concentration in the non-cancerous MEFs (Fig. 4B). Since maximum cytotoxicity was observed for **1a** in MCF-7 cells, all further investigations were carried out using these cells.

**Chloride-based cell death studies**

**HBSS buffer composition**

Hank's balanced salt solution with chloride (HBSS with $Cl^-$) was prepared with the following components: 136.9 mM NaCl, 5.5 mM KCl, 0.34 mM $Na_2HPO_4$, 0.44 mM $KH_2PO_4$, 0.81 mM $MgSO_4$, 1.25 mM $CaCl_2$, 5.5 mM D-glucose, 4.2 mM $NaHCO_3$ and 10 mM HEPES (pH 7.4).

Likewise, chloride-free HBSS (HBSS without $Cl^-$) was prepared using the following constituents: 136.9 mM Na-gluconate, 5.5 mM K-gluconate, 0.34 mM $Na_2HPO_4$, 0.44 mM

$KH_2PO_4$, 0.81 mM $MgSO_4$, 1.25 mM Ca-gluconate, 5.5 mM D-glucose, 4.2 mM $NaHCO_3$ and 10 mM HEPES (pH 7.4).

To investigate whether chloride ion transport played a pivotal role in mediating cytotoxicity in MCF-7 cells, cellular viability was assessed in the presence/absence of chloride in the extracellular media with **1a**. Briefly, MCF-7 cells were seeded in 96-well tissue culture-treated plates (Corning) at a density of 8 x $10^3$ cells/well/100 µL in a complete DMEM medium and incubated at 37 °C in a humidified 5% $CO_2$ incubator for 24 h. Post incubation, the cellular media was replaced by 100 µL HBSS buffer (either with $Cl^-$ or without $Cl^-$) containing 10% fetal bovine serum, and 100 units/mL penicillin and 100 µg/mL streptomycin and cells were treated with increasing concentrations (range 1-20 µM) of **1a** compound for 24h. After incubation, MTT solution (5 mg MTT/mL of PBS) was added to each well and incubated for an additional 4 h. After 4 h, formazan crystals were dissolved using solubilization buffer (10% SDS/0.1N HCl in PBS) by incubating the plates overnight at room temperature. The absorbance was measured at 570 nm using a multi-mode plate reader (Hidex).

It was observed that compound **1a** mediated significantly higher cytotoxicity in the presence of HBSS buffer containing chloride ions when compared to HBSS buffer lacking chloride. These studies confirm that chloride ion transport plays an important role in inducing cytotoxicity in MCF-7 cells.

**Cell Cycle Analysis**

To gain further insights into the mechanism by which compound **1a** induces cytotoxicity in MCF-7 cells, cell cycle analysis was performed. Briefly, MCF-7 cells were dispersed in 35 mm tissue culture-treated plates (Corning) at the density of 8 x $10^3$ cells/well/100 µL in complete DMEM media and were incubated at 37 °C in a 5% CO2 incubator overnight for recovery. Post-recovery, the cells were treated with increasing concentration of **1a** (0-20 µM) for 24 h. After incubation, cells were harvested by trypsinization, washed with ice-cold 1X PBS and fixed with 70% methanol at -20 °C overnight. Subsequently, the cells were resuspended in PBS buffer containing 1 µL RNase A (stock 20 mg/mL; Himedia) and incubated for 20 min at room temperature. The cells were then stained with 50 µg/mL propidium iodide (Stock-1mg/mL; Himedia) for 30 min in dark at room temperature. The cells were analyzed by acquiring 10,000 events using a BD FACS Celesta™ flow cytometer (BD Biosciences, San Jose,

CA, USA) and analyzed using FloJo software (Ashland, OR). The representative overlay of histograms has been depicted in Fig. S19 and the percentage of cells in the different phases of the cell cycle has been quantitated in Fig. S19D.

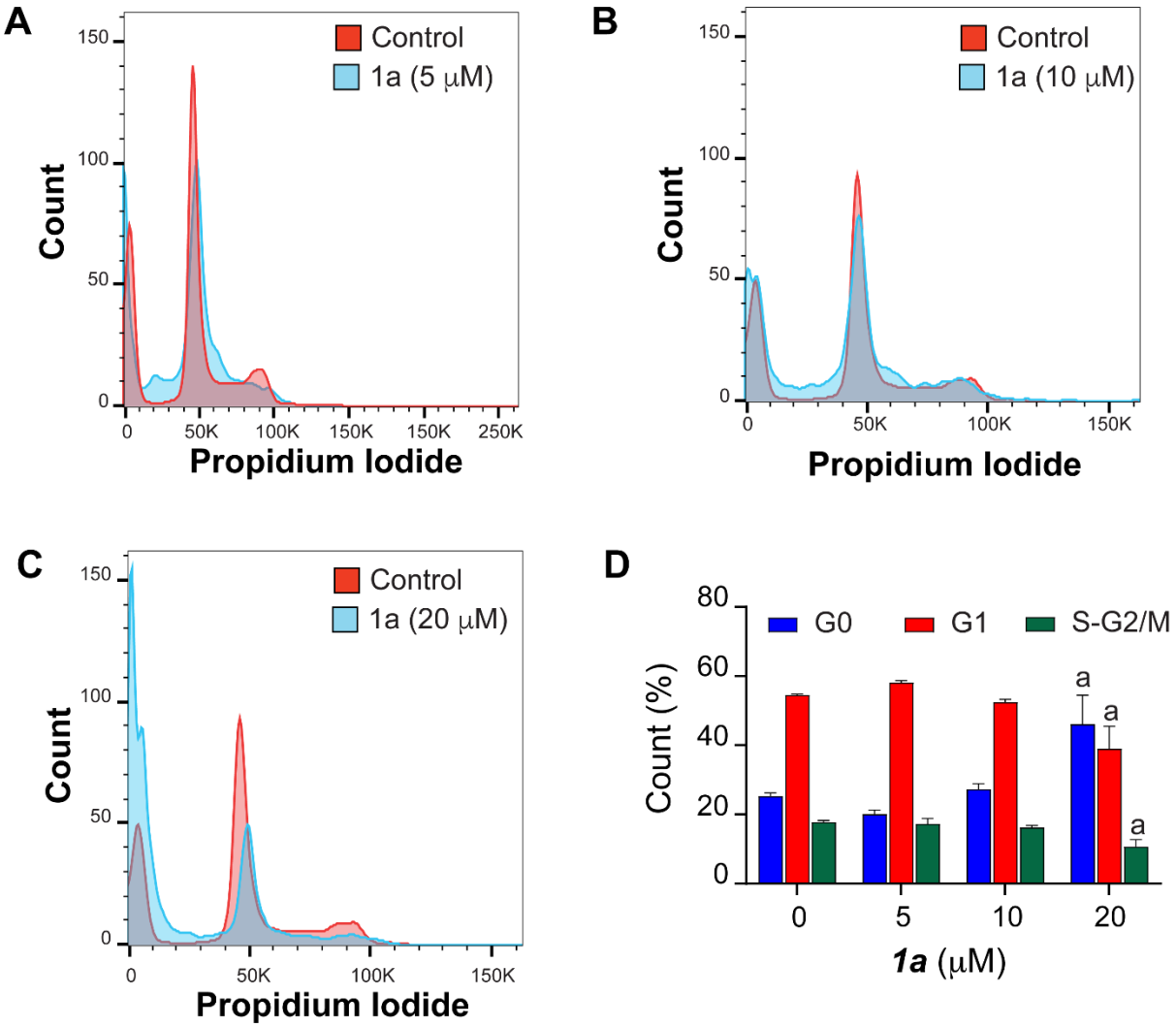


**Fig. S21** Representative cell cycle profile overlays of untreated MCF-7 cells with those treated for 24 hr. with A) 5 μM; B) 10 μM; and C) 20 μM concentration of **1a**. (D) Quantitation of cells (in %) in different phases of the cell cycle. a represents $p < 0.05$; b represents $p < 0.01$; c represents for $p < 0.001$; and d for $p < 0.0001$ when compared to untreated control using Tukey HSD tests.

**Measurement of Reactive oxygen species (ROS)**

To understand the cause of increased cytotoxicity, mitochondrial reactive oxygen species (ROS) levels were measured using MitoSox red dye. Briefly, MCF-7 cells were seeded in 96-well tissue culture-treated plates (Corning) at a density of 8 x $10^3$ cells/well/100 μL in complete DMEM medium and incubated at 37 °C in a humidified 5% $CO_2$ incubator for 24 h.

Post incubation, the cells were treated with increasing concentrations (0-20 µM) of **1a** for another 24h. After incubation, the cells were washed with ice-cold PBS and incubated with MitoSox red reagent (5 µM, Invitrogen) for ~20 minutes at 37 °C in dark. Following this, the cells were washed thrice with ice-cold 1X PBS, and the fluorescence intensities were read using a using a multi-mode plate reader (Hidex) ($\lambda_{ex}$- 510 nm/$\lambda_{em}$- 580 nm). All the experiments were performed in triplicate (N = 3). The readings obtained were then normalized with MTT values. In line with the observations made from the cellular viability data, increased mitochondrial ROS levels were observed in MCF-7 cells exposed to **1a** when compared to the untreated cells.

**Measurement of Mitochondrial membrane potential (MMP)**

Previous studies from our and other groups[S5] have shown that the loss of chloride ion homeostasis and the associated cytotoxicity occurs due to loss of mitochondrial membrane potential (MMP) - a measure of mitochondrial dysfunction in the cells. MMP can be measured in cells using JC-1, an MMP-sensitive dye that emits red fluorescence in healthy cells with healthy mitochondrial membranes due to the formation of J-aggregates. On the other hand, in cells with damaged mitochondria and depolarized mitochondrial membranes, green fluorescence is observed due to the presence of J-monomers. Therefore, to assess the MMP in cells exposed to **1a**, JC-1 staining was performed. Briefly, MCF-7 cells were seeded in 96-well tissue culture-treated plates (Corning) at a density of 8 x $10^3$ cells/well/100 µL in complete DMEM medium and incubated at 37 °C in a humidified 5% $CO_2$ incubator for 24 h. Post incubation, the cells were treated with increasing concentrations of **1a** (0- 20 µM) for 24 h. Following this, the cells were washed with ice-cold PBS and incubated with JC-1 reagent (2 µg/mL) for ~20 minutes at 37 °C in the dark. Subsequently, the cells were washed twice with ice-cold 1X PBS and the relative fluorescence intensities were read at 485/530 nm and 510/580 nm wavelengths for quantitation using a multi-mode plate reader (Hidex). All the experiments were performed in triplicate (N=3). The readings obtained were then normalized with MTT values. The ratios of red/green fluorescence intensities were quantified and plotted.

For qualitative analysis, fluorescence imaging was performed in red and green channels using EVOS FL Auto Imaging System (Life Technologies).

As can be seen from Fig. S20, control MCF-7 cells emit red fluorescence which significantly reduces when the cells are treated with increasing concentrations of **1a**. This is associated with a dose-dependent increase in the green fluorescence in the cells treated with **1a**, thereby indicating that these cells have damaged mitochondrial membranes and are thus experiencing a loss in the mitochondrial membrane potential – a trigger for apoptosis in these cells.

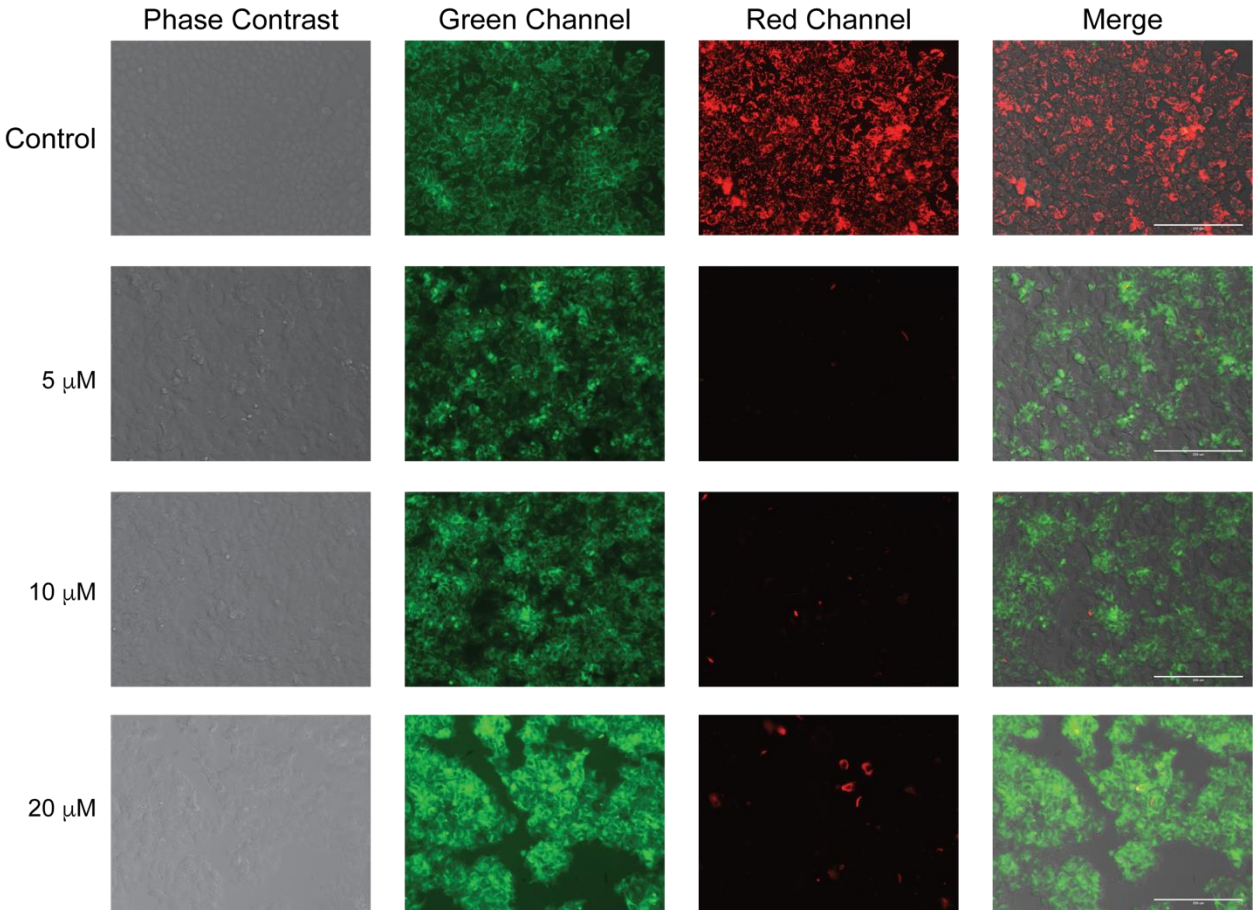


**Fig. S22** Representative merged images of JC-1 stained MCF-7 cells after treatment with different concentrations (0 (control), 5, 10 and 20 μM) of compound **1a** for 24 h.

**Acridine Orange (AO) Staining**

Since, compound **1a** was involved in perturbing chloride ion homeostasis, we attempted to measure the lysosomal pH using acridine orange dye. It is a membrane permeable pH-sensitive dye, which upon accumulation in acidified organelles including acidic lysosomes emits orange fluorescence and green in deacidified, inactive lysosomes. Briefly, MCF-7 cells were seeded in 24-well tissue culture-treated plates (Corning) at a density of 8 x $10^3$ cells/well/100 μL in complete DMEM medium and incubated at 37 °C in a humidified 5% $CO_2$

incubator for 24 h. Post incubation, the cells were treated with increasing concentrations of **1a** (0-20 µM) for 24 h. After incubation, the cells were washed with ice-cold 1X PBS and incubated with acridine orange reagent (5 µg/mL, Sigma) for ~20 minutes at 37 °C in the dark. The cells were washed thrice with ice-cold 1X PBS and fluorescence images were acquired in both red and green channels (Fig. S21) using EVOS FL Auto Imaging System (Life Technologies).

A significant reduction in the red fluorescence with a concomitant increase in green fluorescence was observed in MCF-7 cells treated with increasing concentrations of **1a**. These observations clearly point towards chloride transport in these cells which led to the deacidification of the lysosomes and induction of apoptosis in these cells.

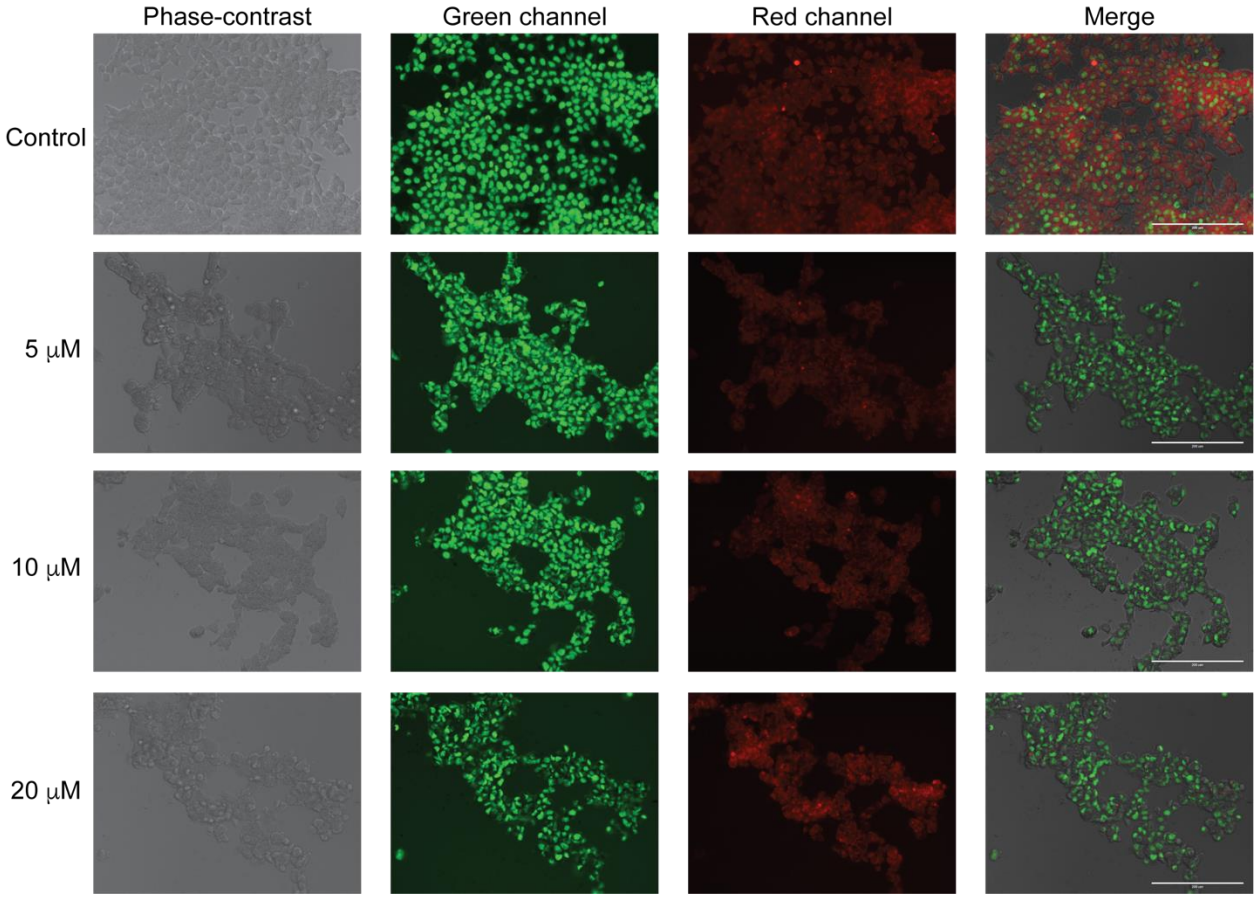


**Fig. S23** Live cell imaging of MCF-7 cells upon treatment with increasing concentrations of **1a** after staining with acridine orange dye.

**Statistical Analysis**

All cellular experiments were performed in triplicate, unless stated otherwise. Data has been represented as Mean ± SEM, where SEM represents standard error of mean and is expressed

as standard deviation divided by the square root of sample size. Statistical analysis was performed using one-way analysis of variance (ANOVA) followed by Tukey HSD post-hoc test. $p < 0.05$ was considered to be statistically different when comparing different groups.

## IX. NMR Spectra

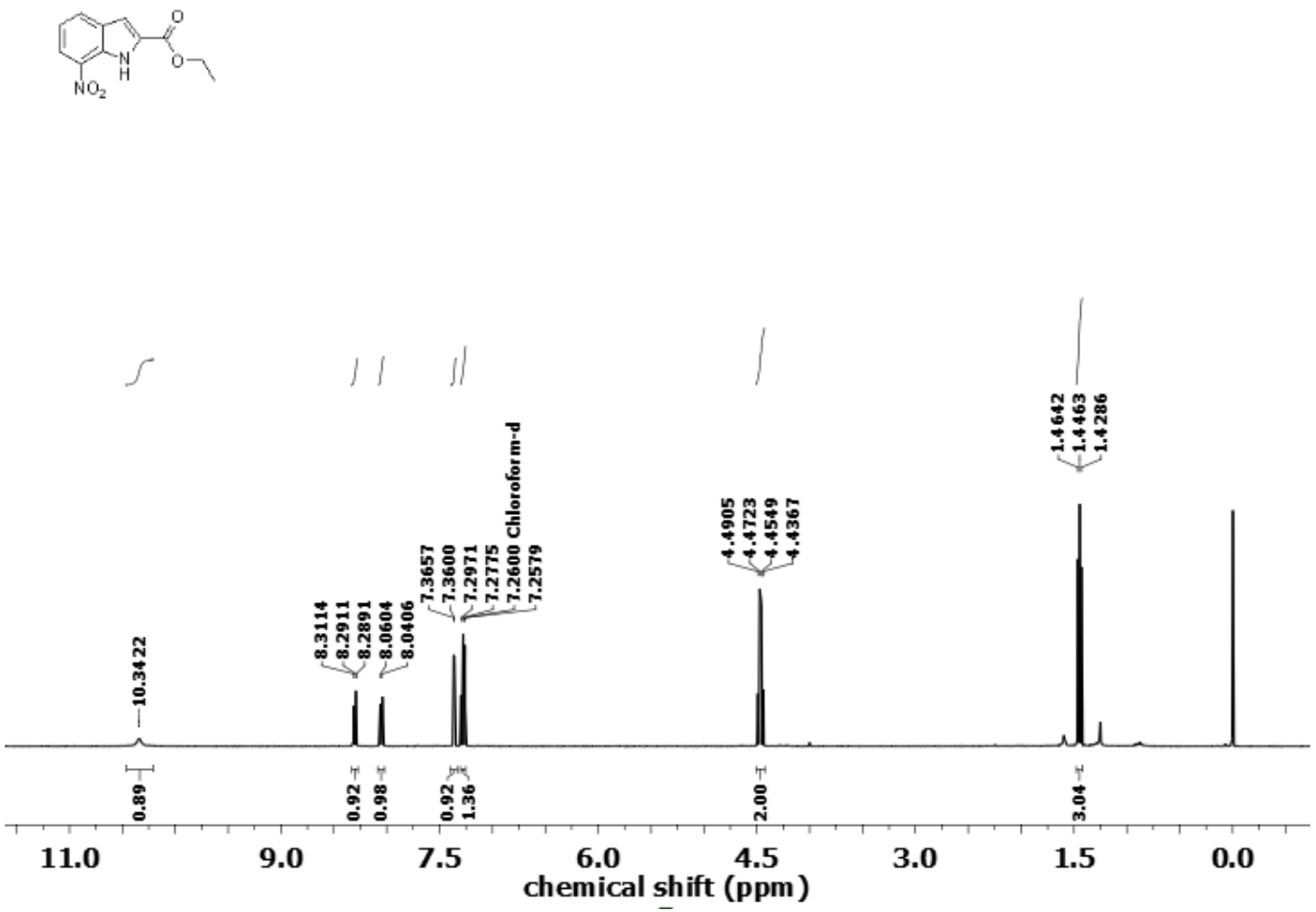


**Fig. S24** 400 MHz $^{1}$H NMR spectrum of compound **3a**.

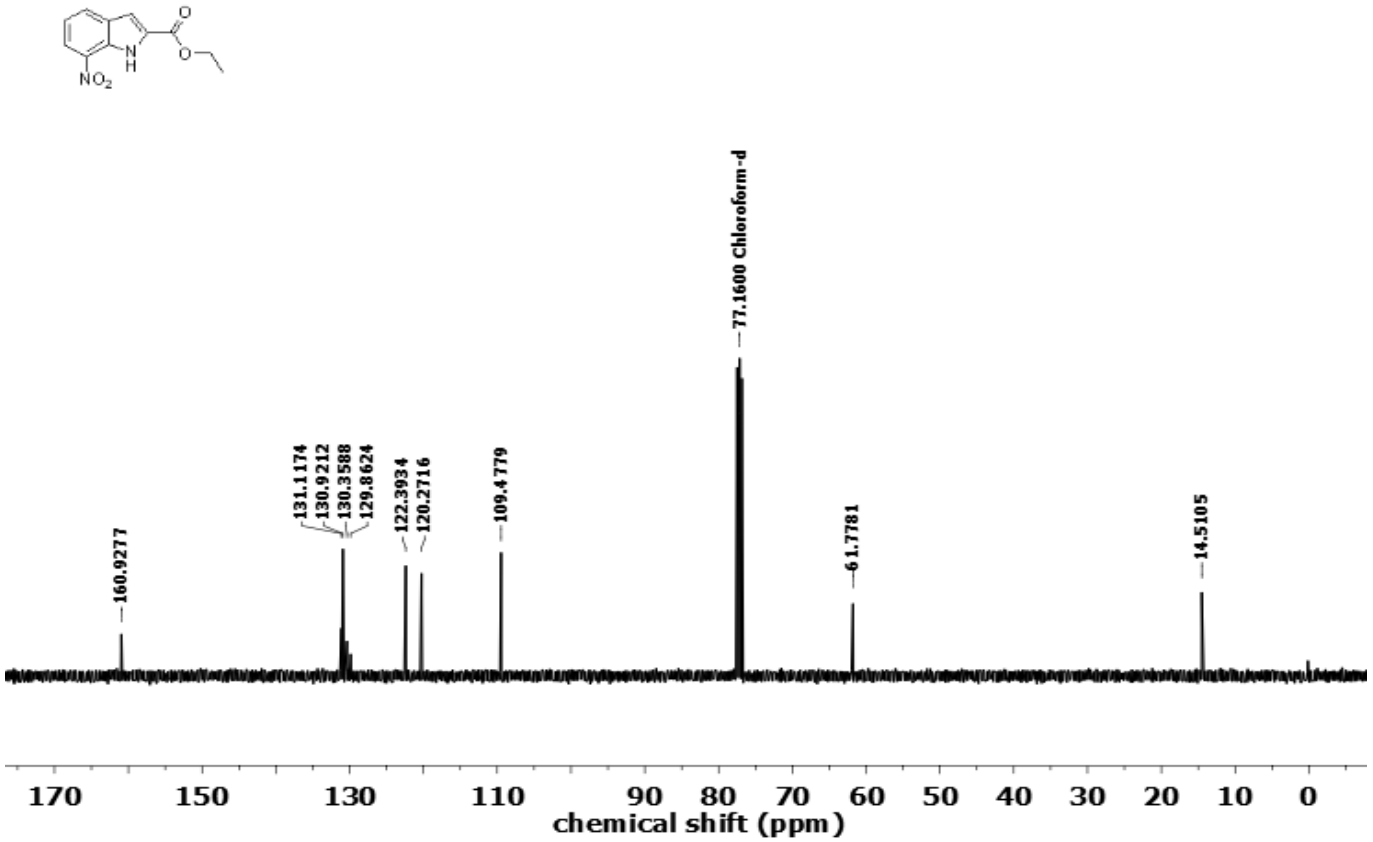


**Fig. S25** 101 MHz $^{13}C$ NMR spectrum of compound **3a**.

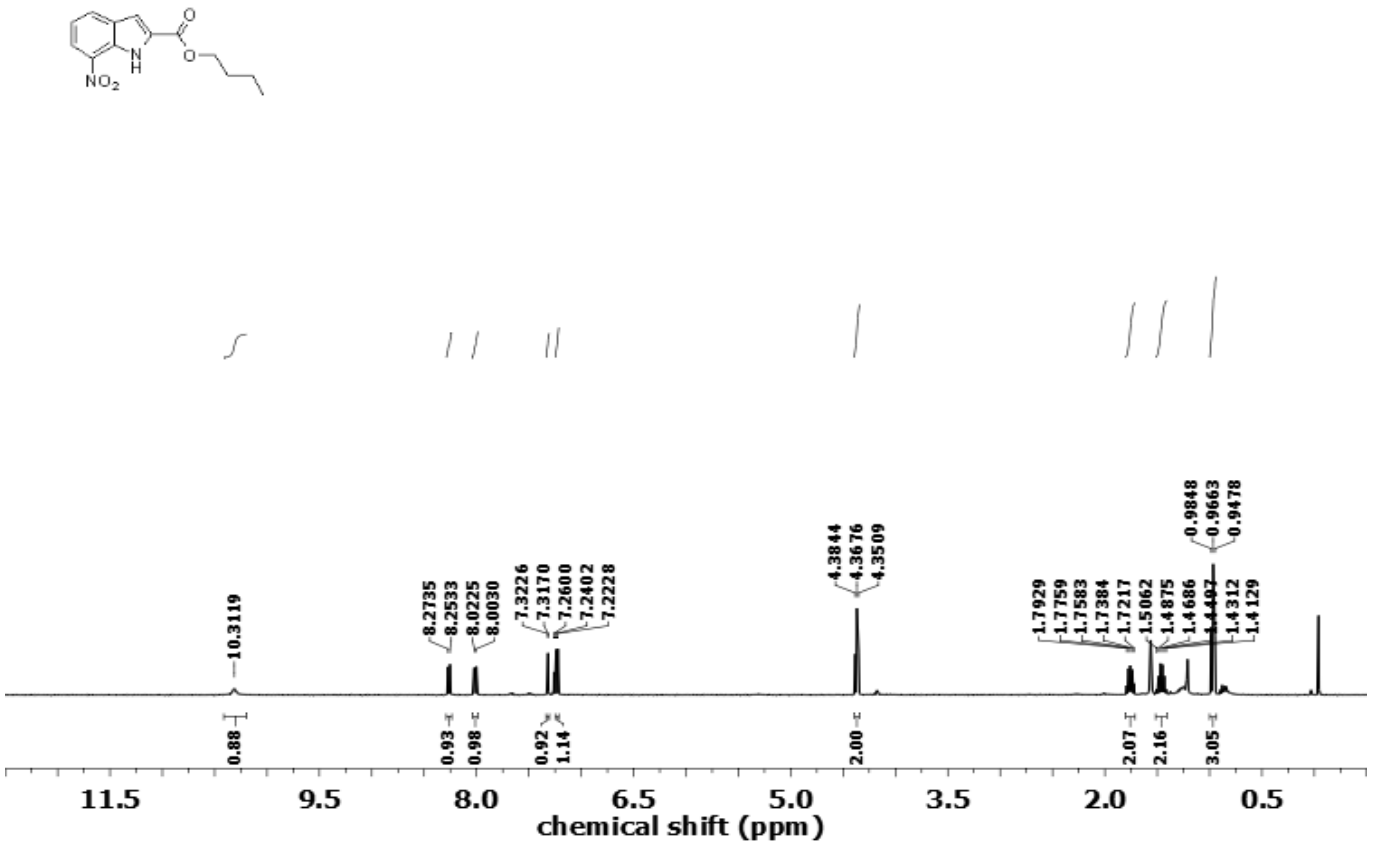


**Fig. S26** 400 MHz $^{1}$H NMR spectrum of compound **3b**.

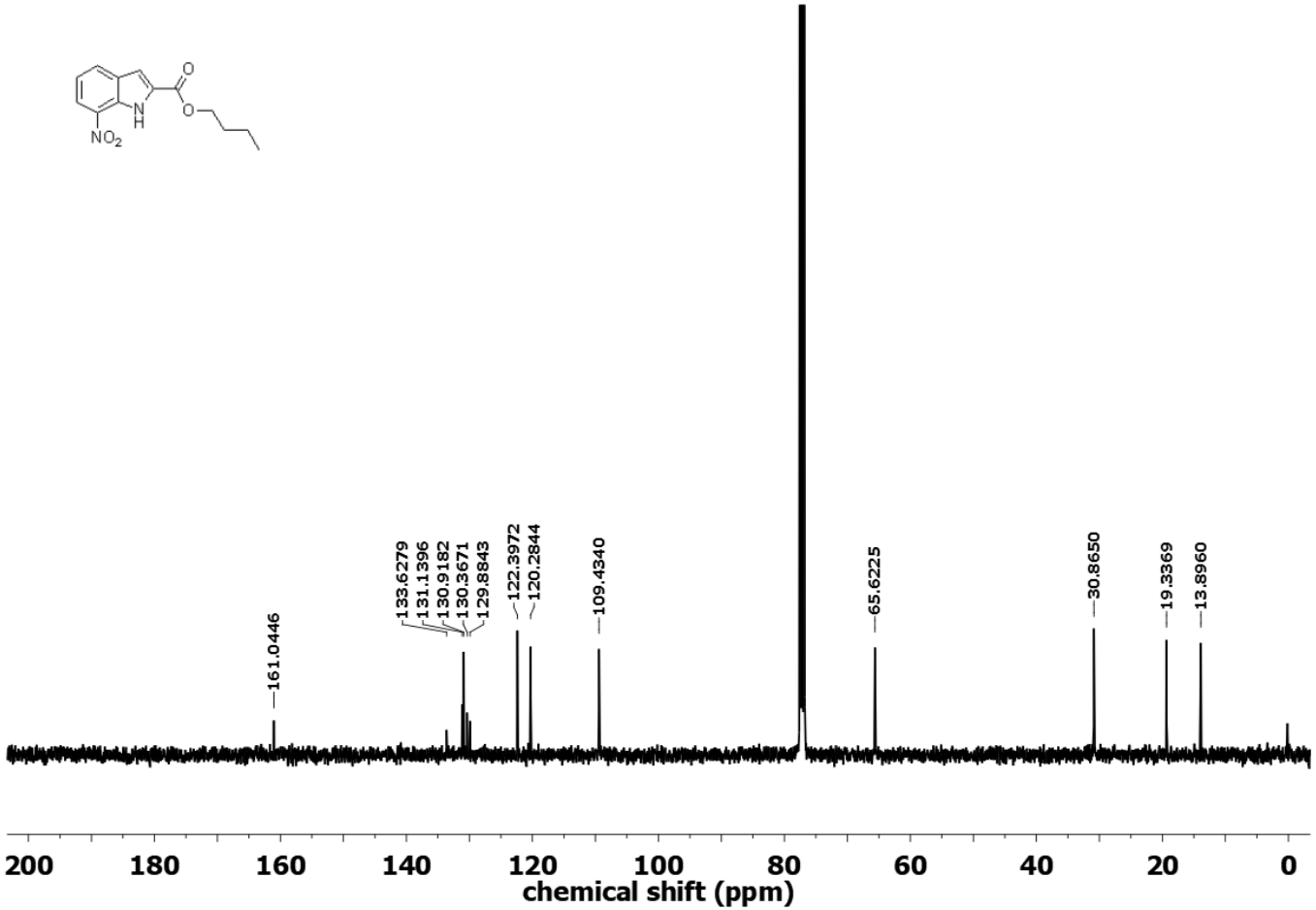


**Fig. S27** 101 MHz $^{13}C$ NMR spectrum of compound **3b**.

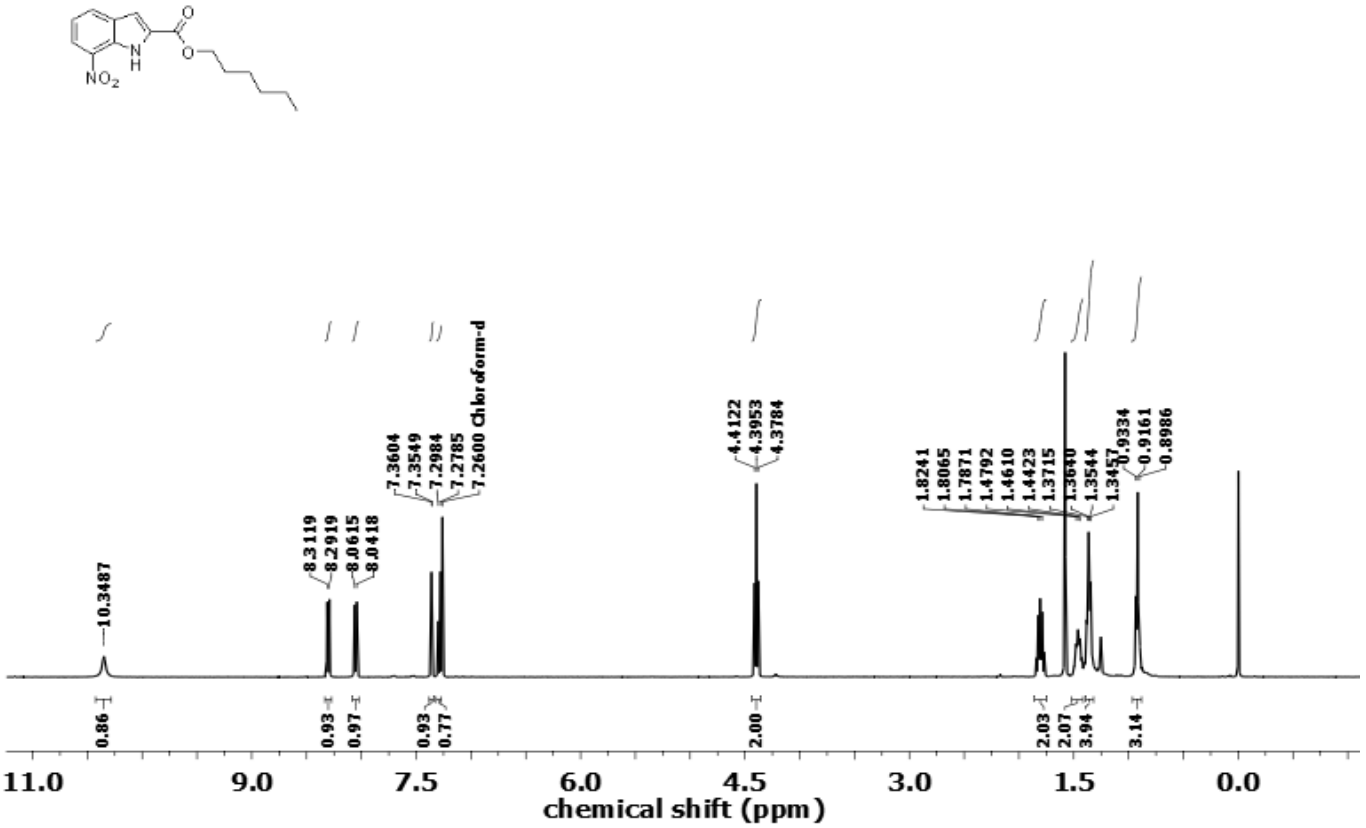


**Fig. S28** 400 MHz $^{1}$H NMR spectrum of compound **3c**.

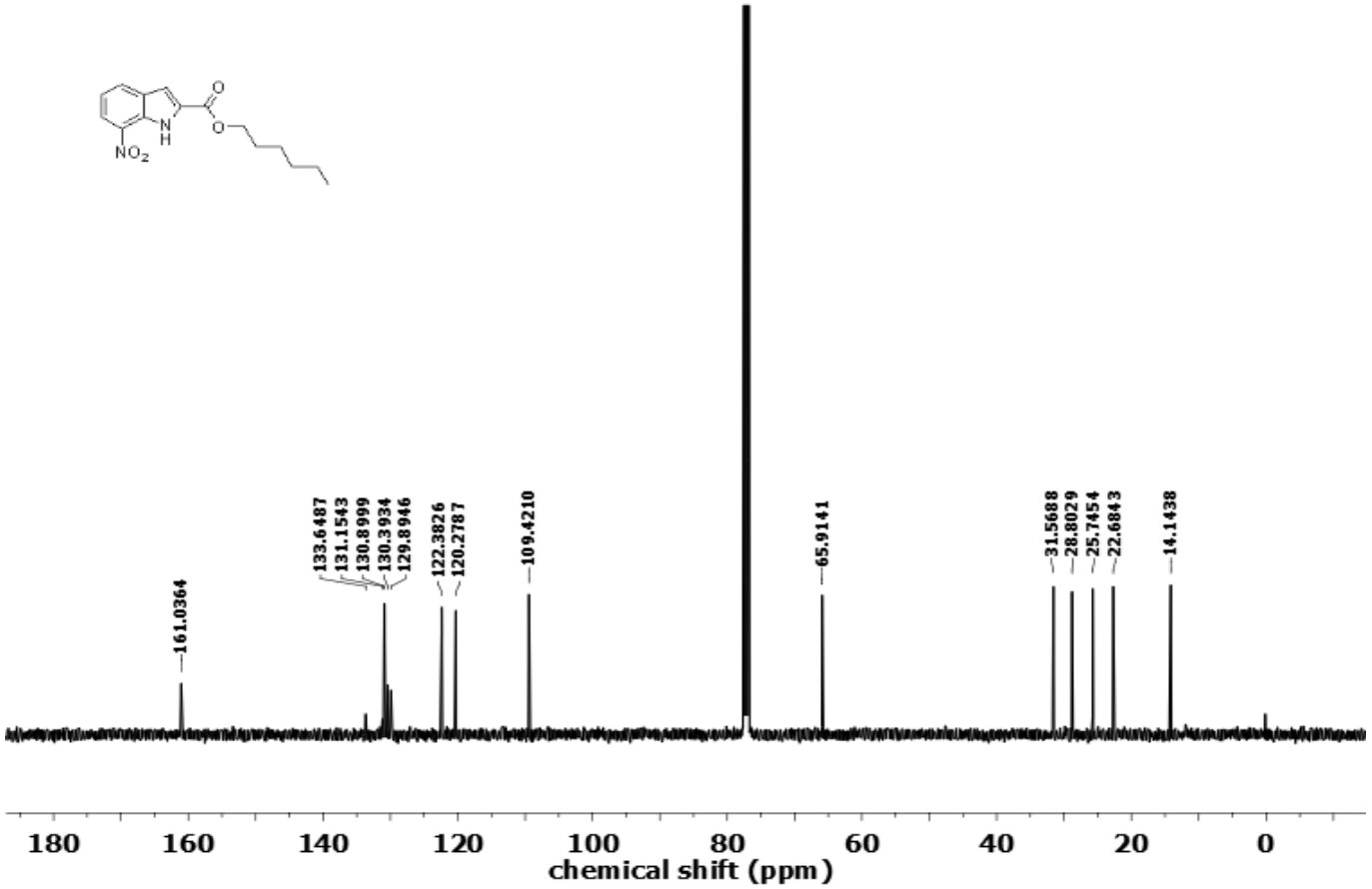


**Fig. S29** 101 MHz $^{13}C$ NMR spectrum of compound **3c**.

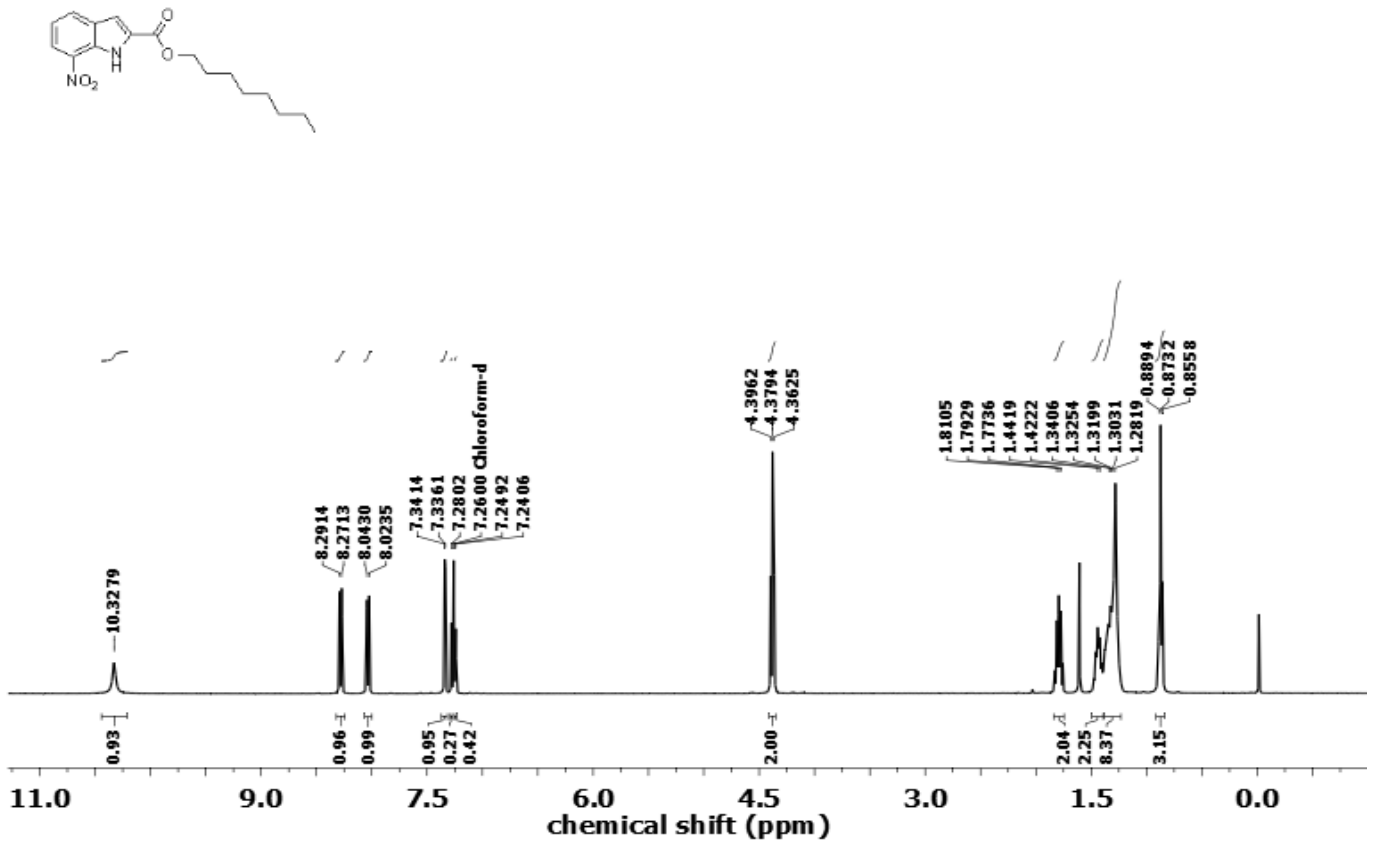


**Fig. S30** 400 MHz $^{1}$H NMR spectrum of compound **3d**.

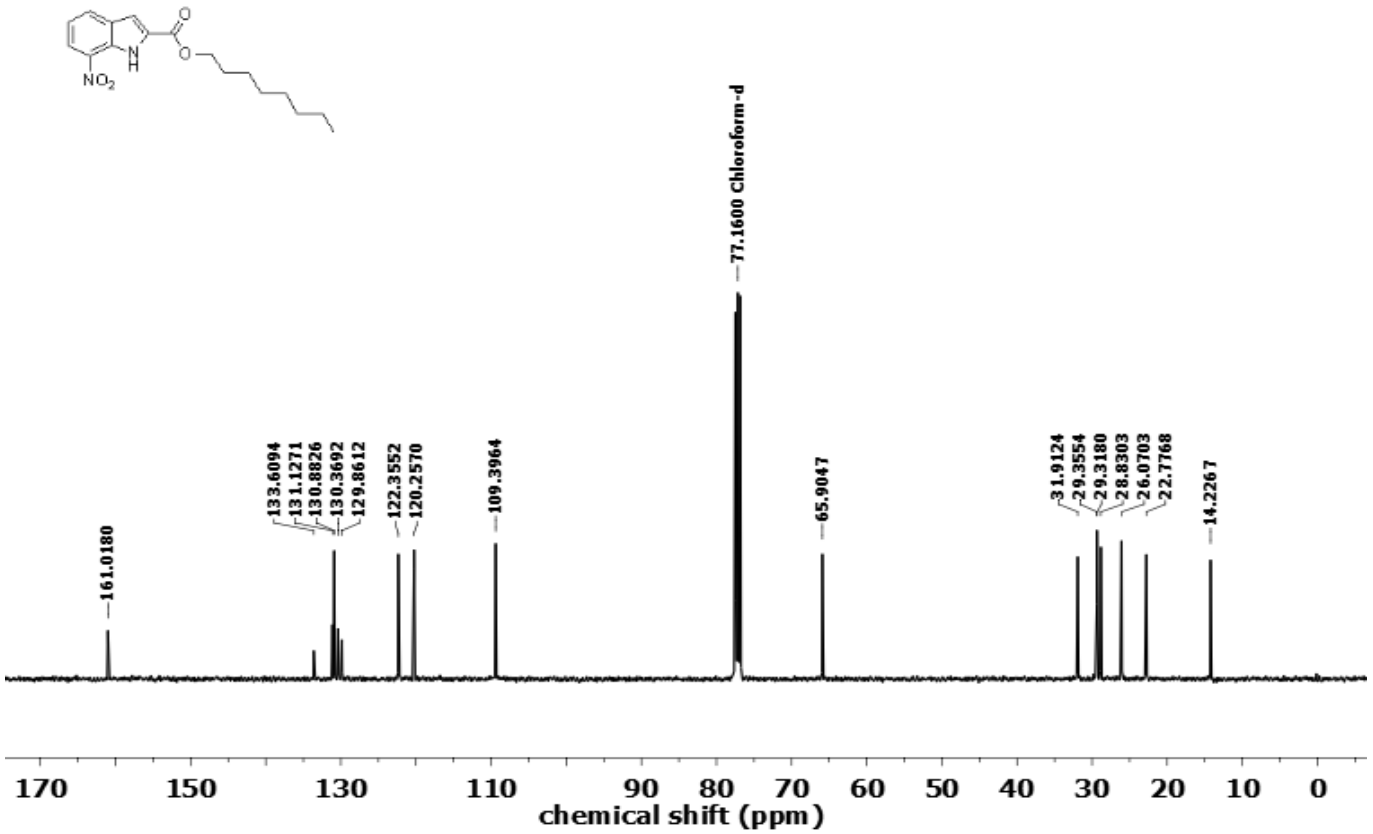


**Fig. S31** 101 MHz $^{13}C$ NMR spectrum of compound **3d**.

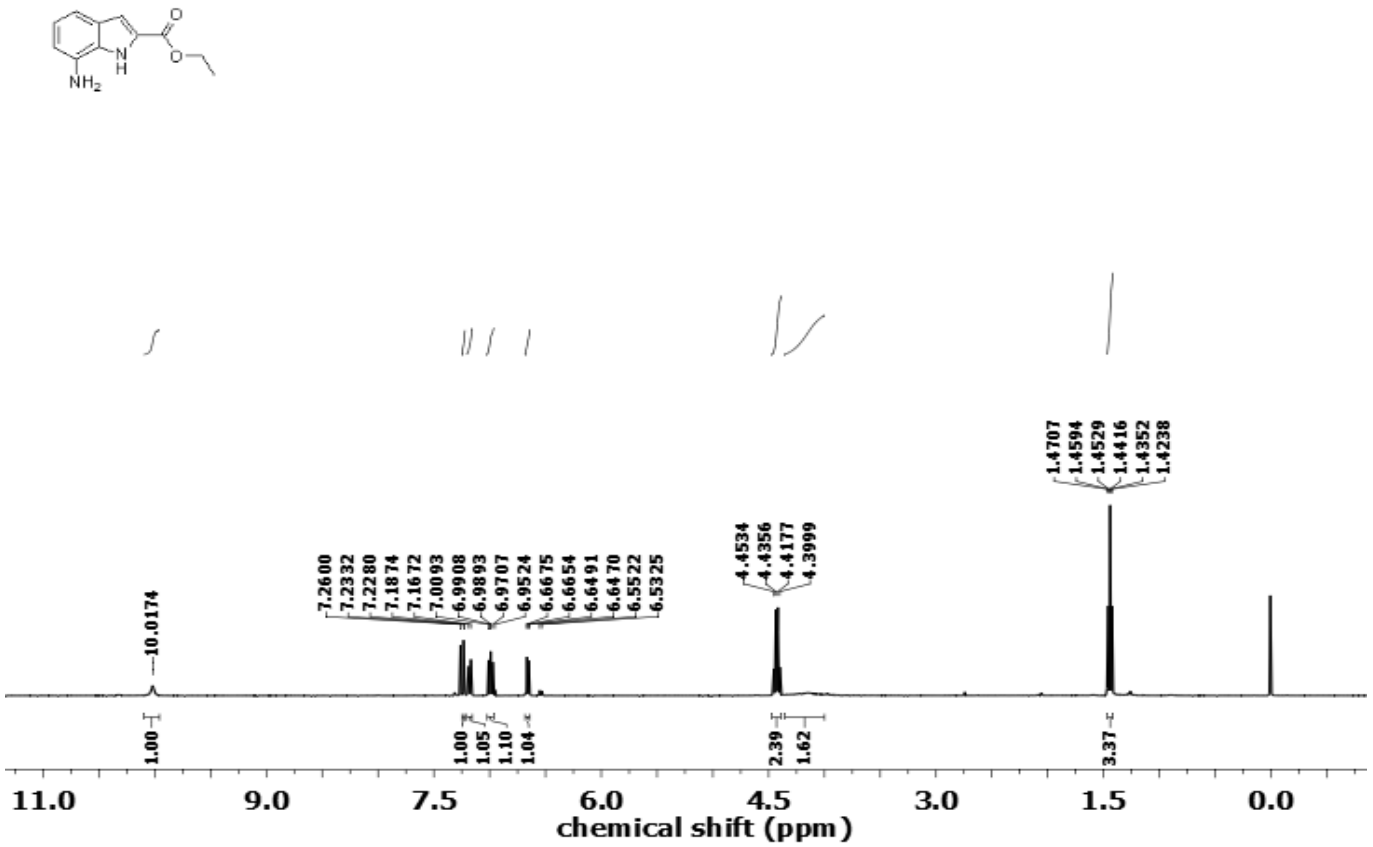


**Fig. S32** 400 MHz $^{1}$H NMR spectrum of compound **4a**.

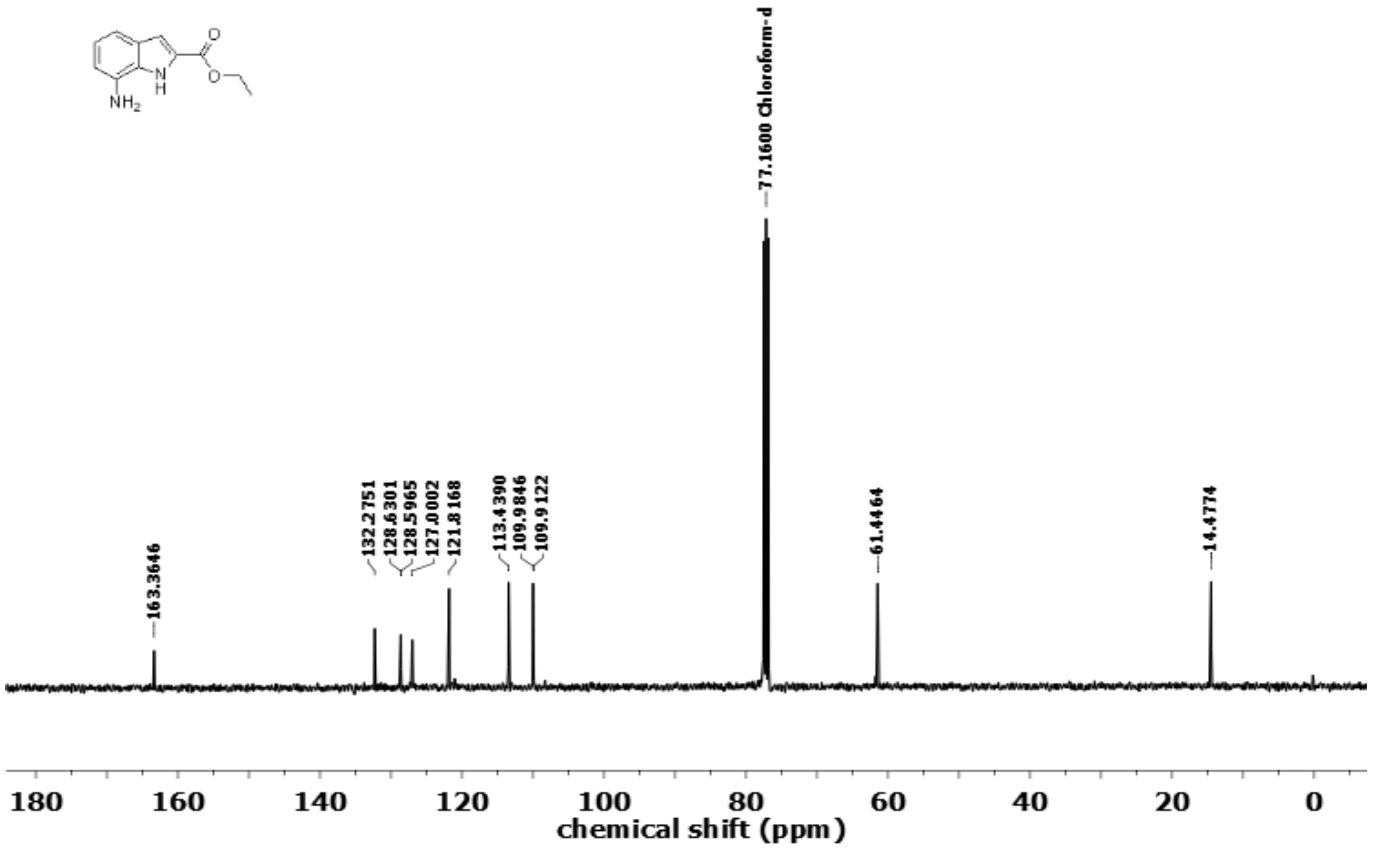


**Fig. S33** 101 MHz $^{13}C$ NMR spectrum of compound **4a**.

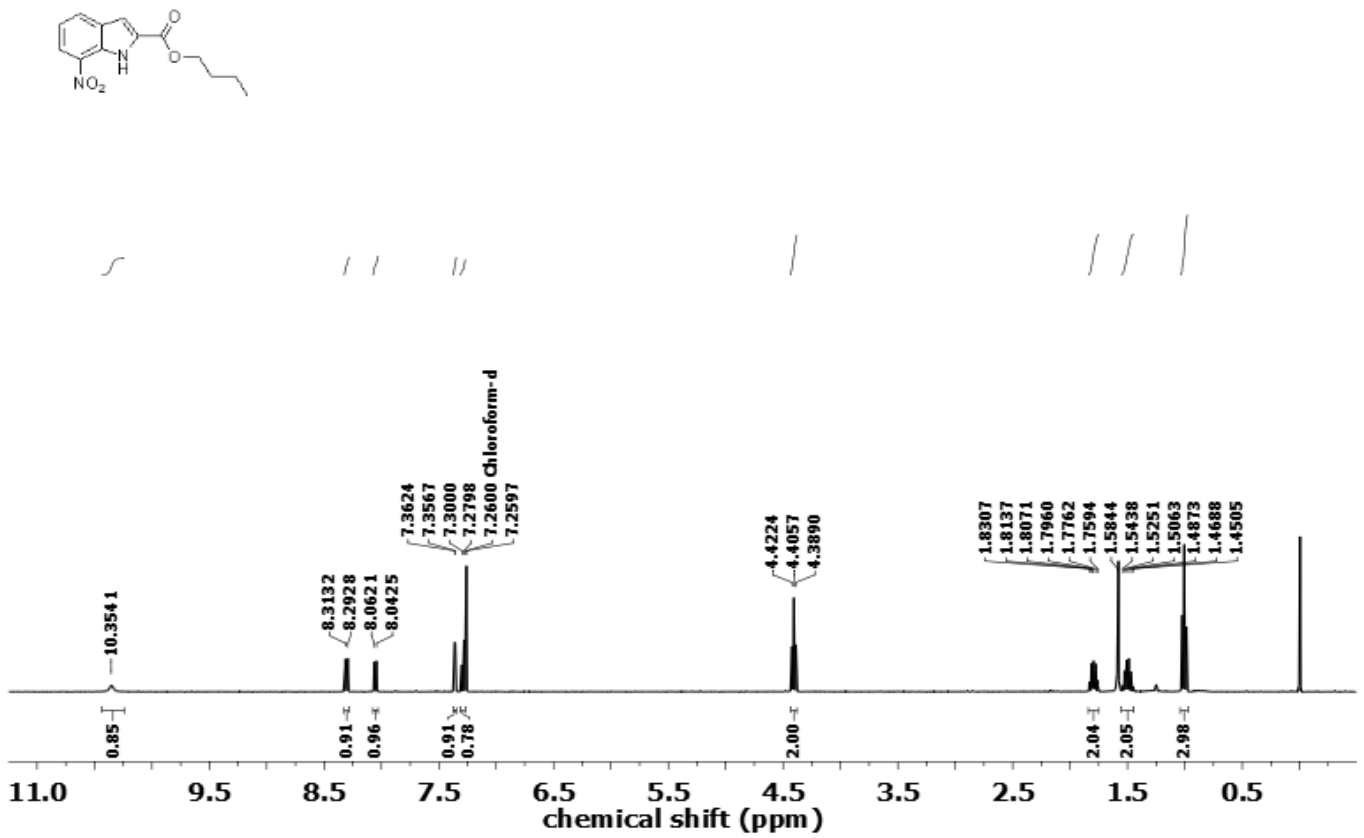


**Fig. S34** 400 MHz $^{1}$H NMR spectrum of compound **4b**.

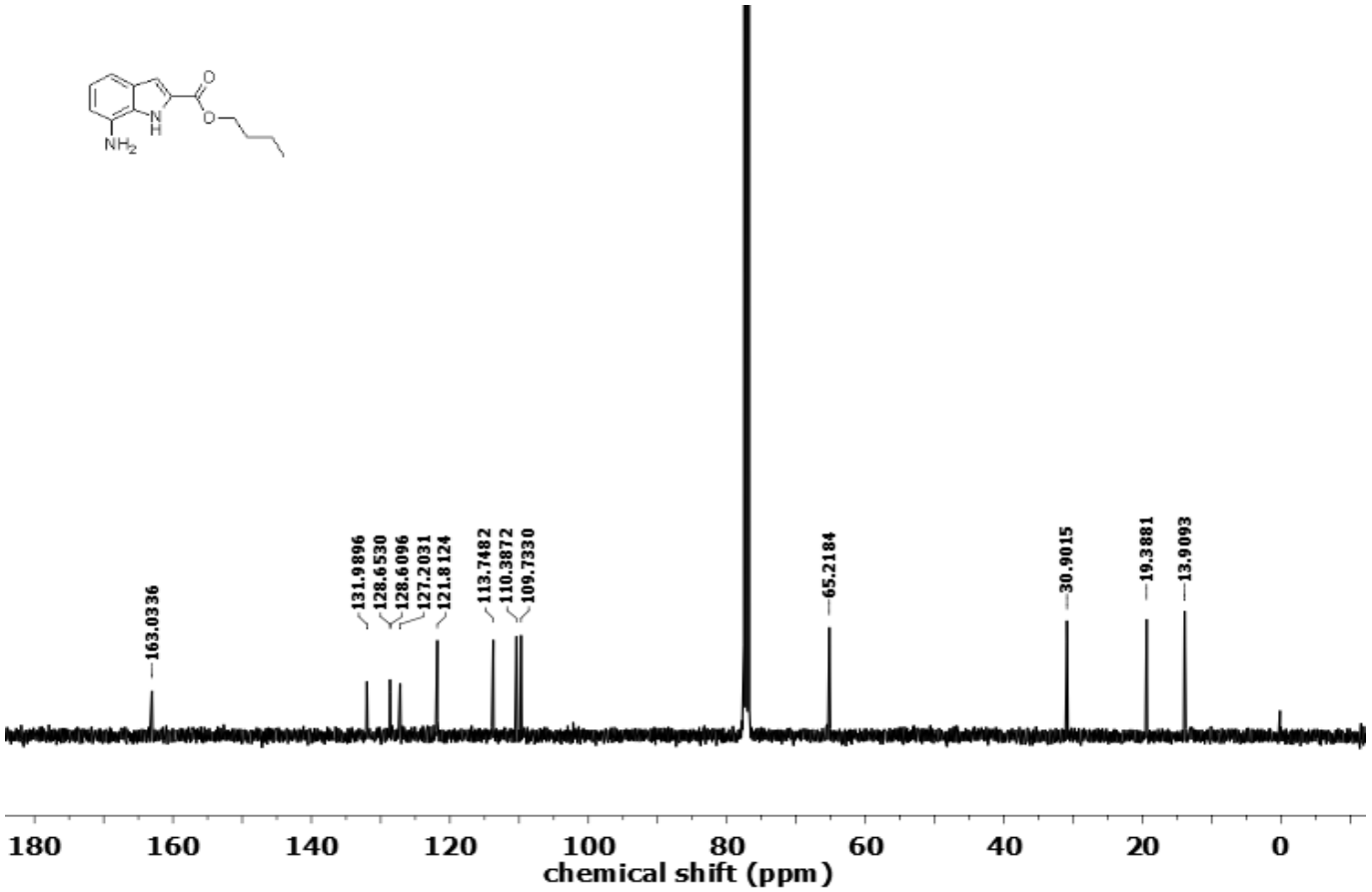


**Fig. S35** 101 MHz $^{13}C$ NMR spectrum of compound **4b**.

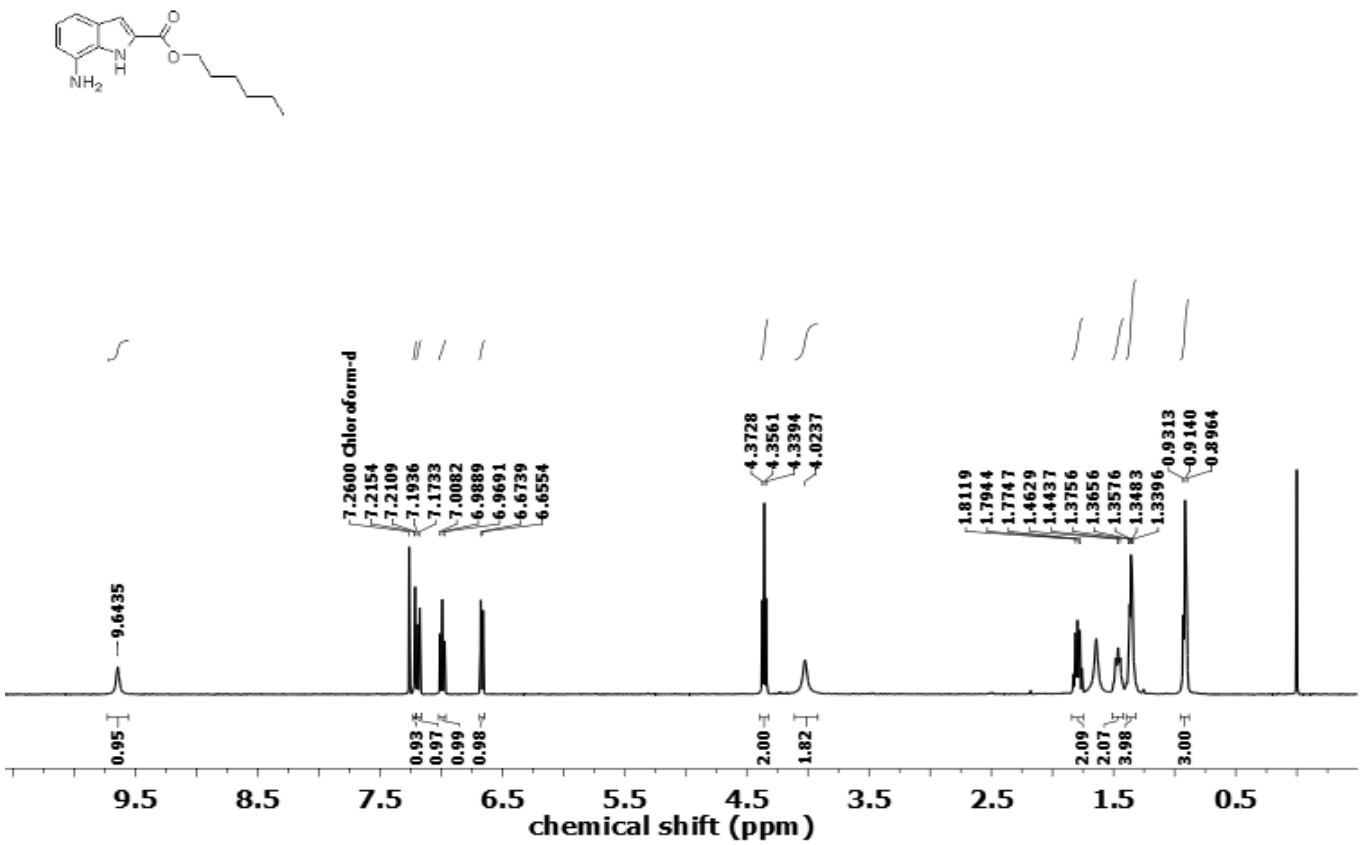


**Fig. S36** 400 MHz $^{1}$H NMR spectrum of compound **4c**.

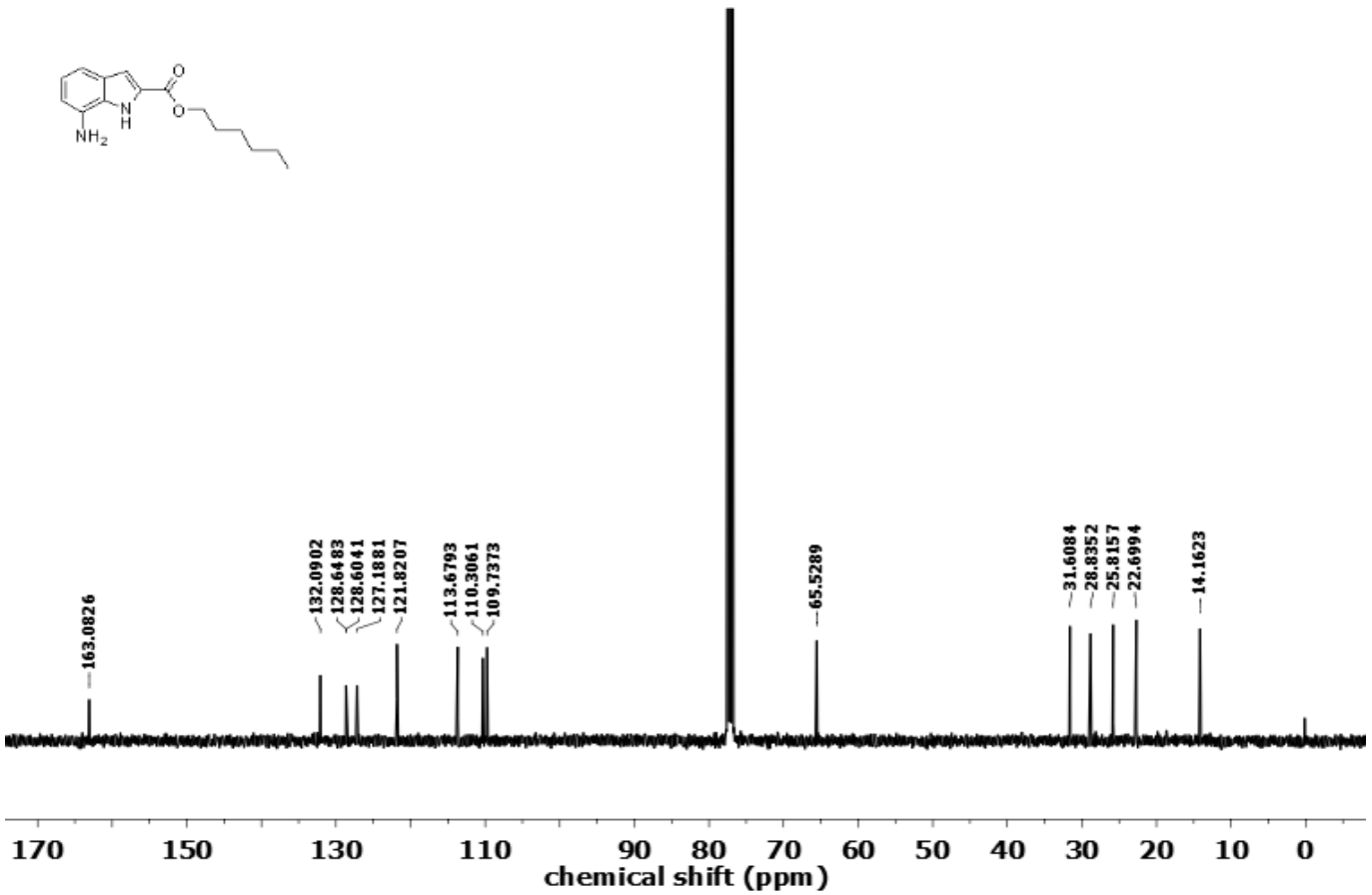


**Fig. S37** 101 MHz $^{13}C$ NMR spectrum of compound **4c**.

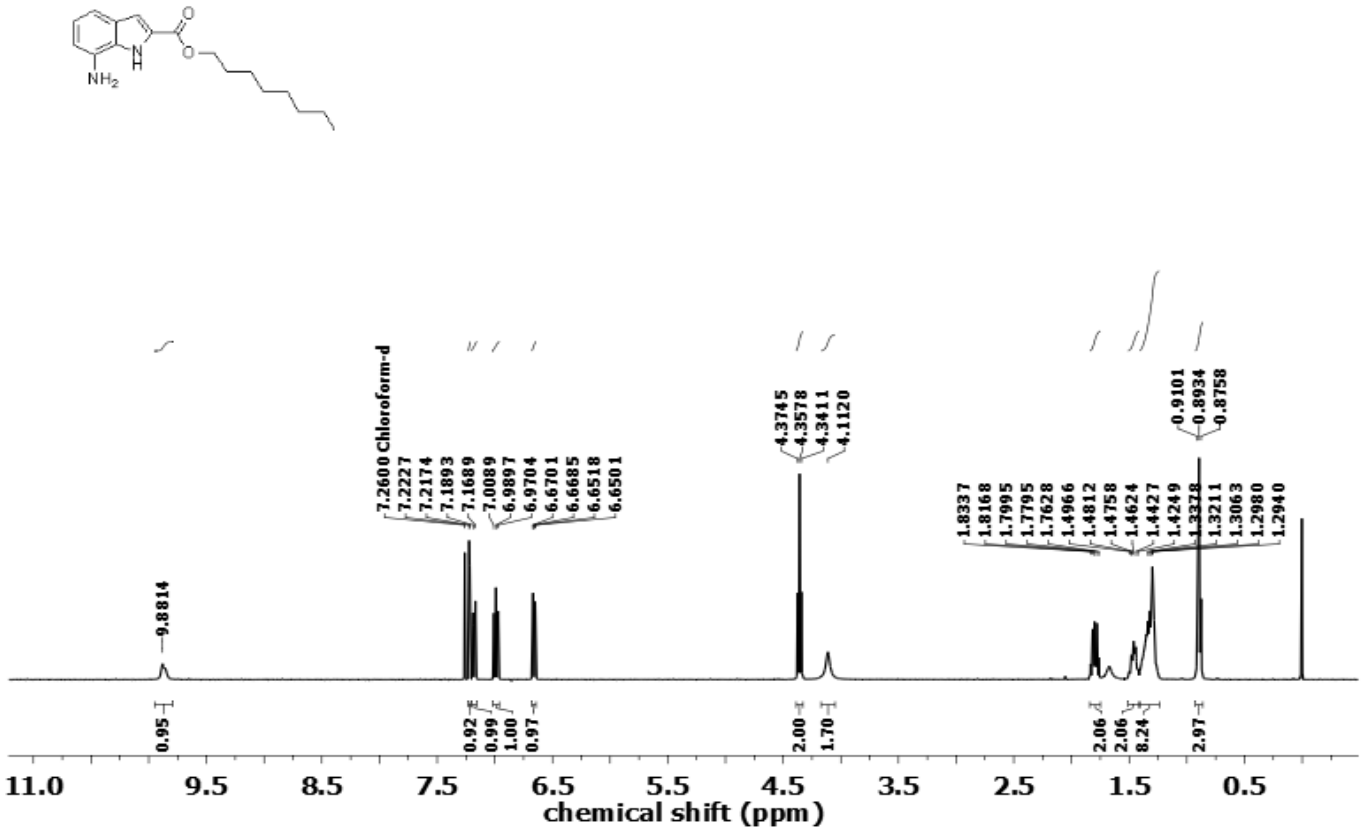


**Fig. S38** 400 MHz $^{1}$H NMR spectrum of compound **4d**.

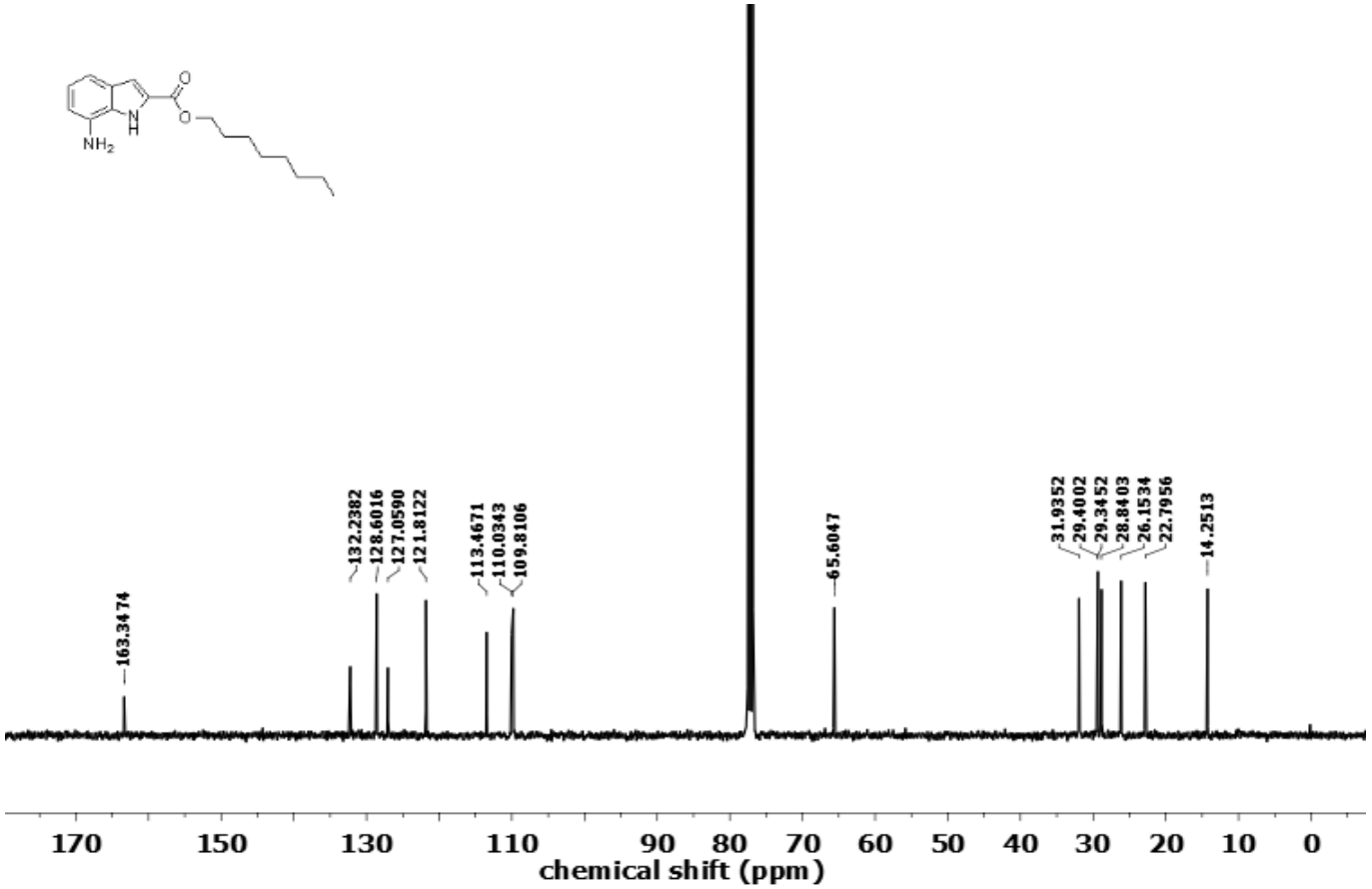


**Fig. S39** 101 MHz $^{13}C$ NMR spectrum of compound **4d**.

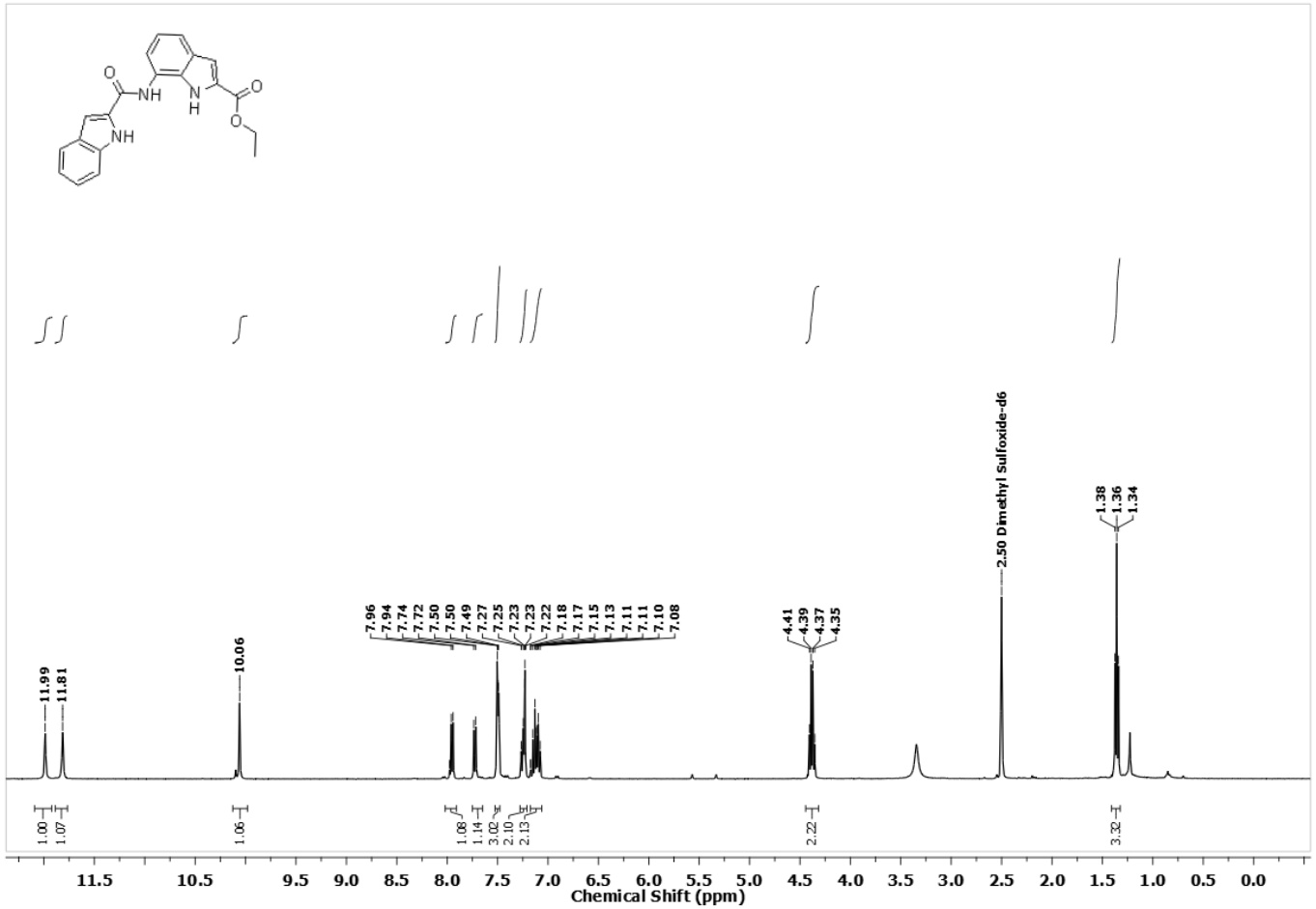


**Fig. S40** 400 MHz $^{1}$H NMR spectrum of compound **1a**.

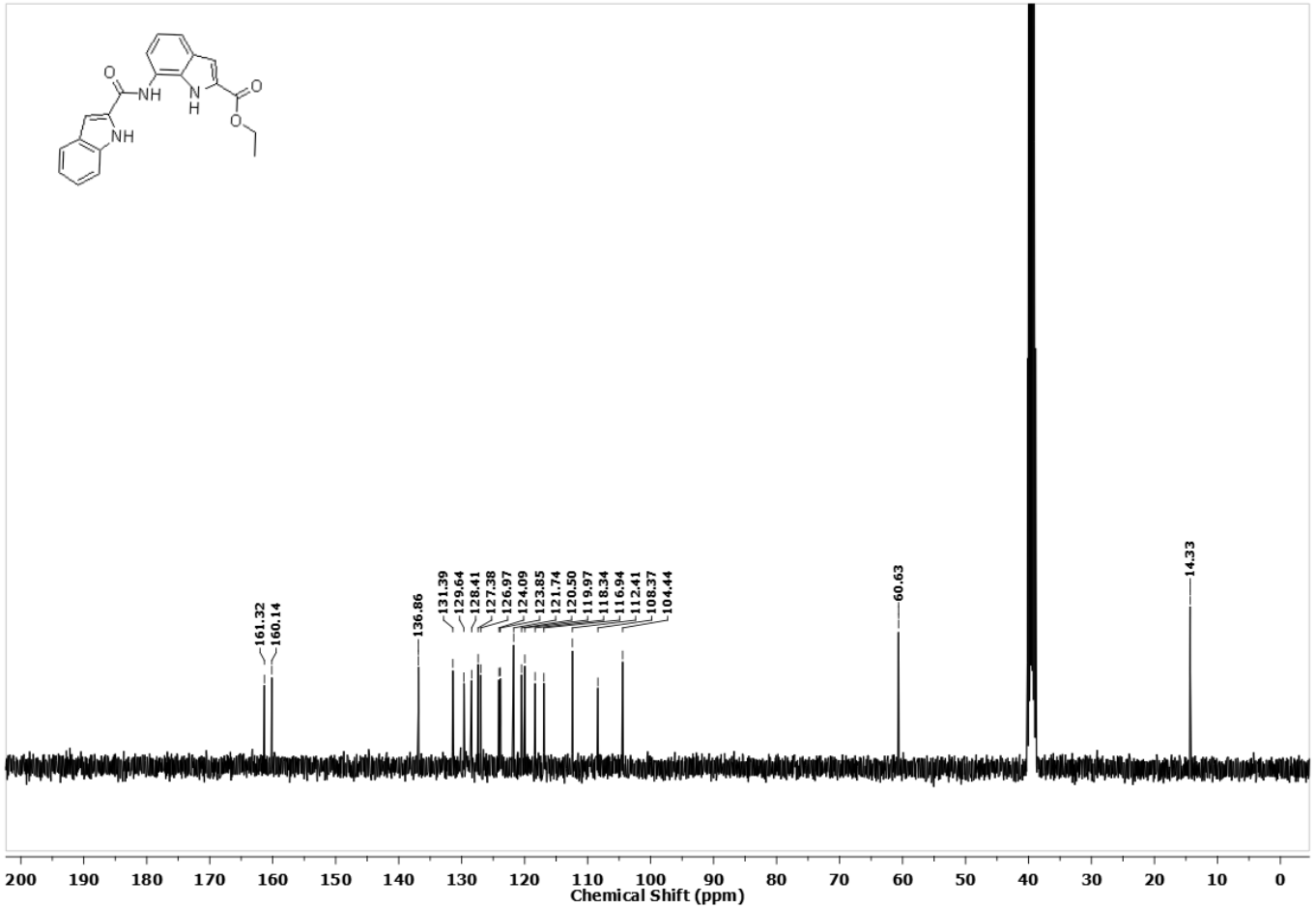


**Fig. S41** 101 MHz $^{13}C$ NMR spectrum of compound **1a**.

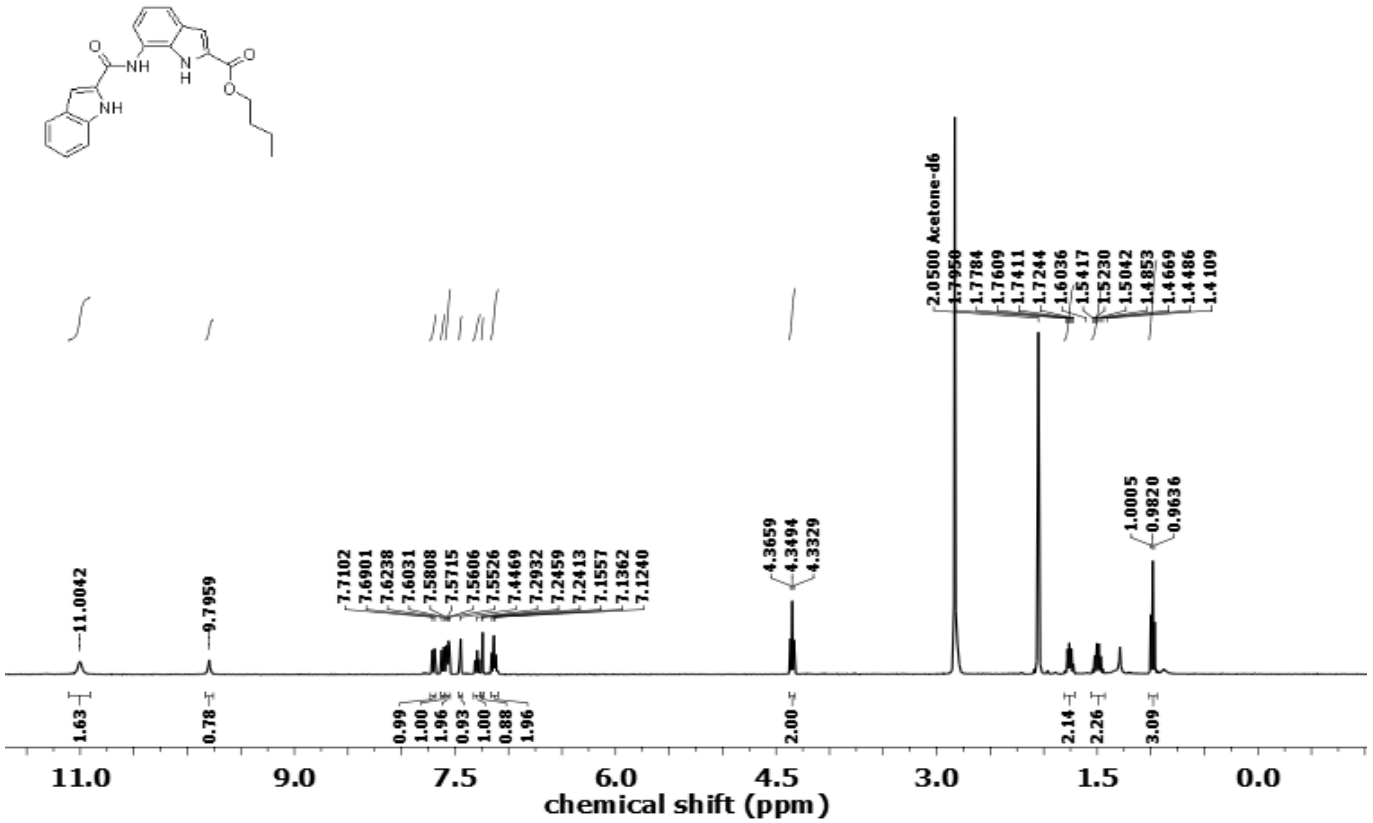


**Fig. S42** 400 MHz $^{1}$H NMR spectrum of compound **1b**.

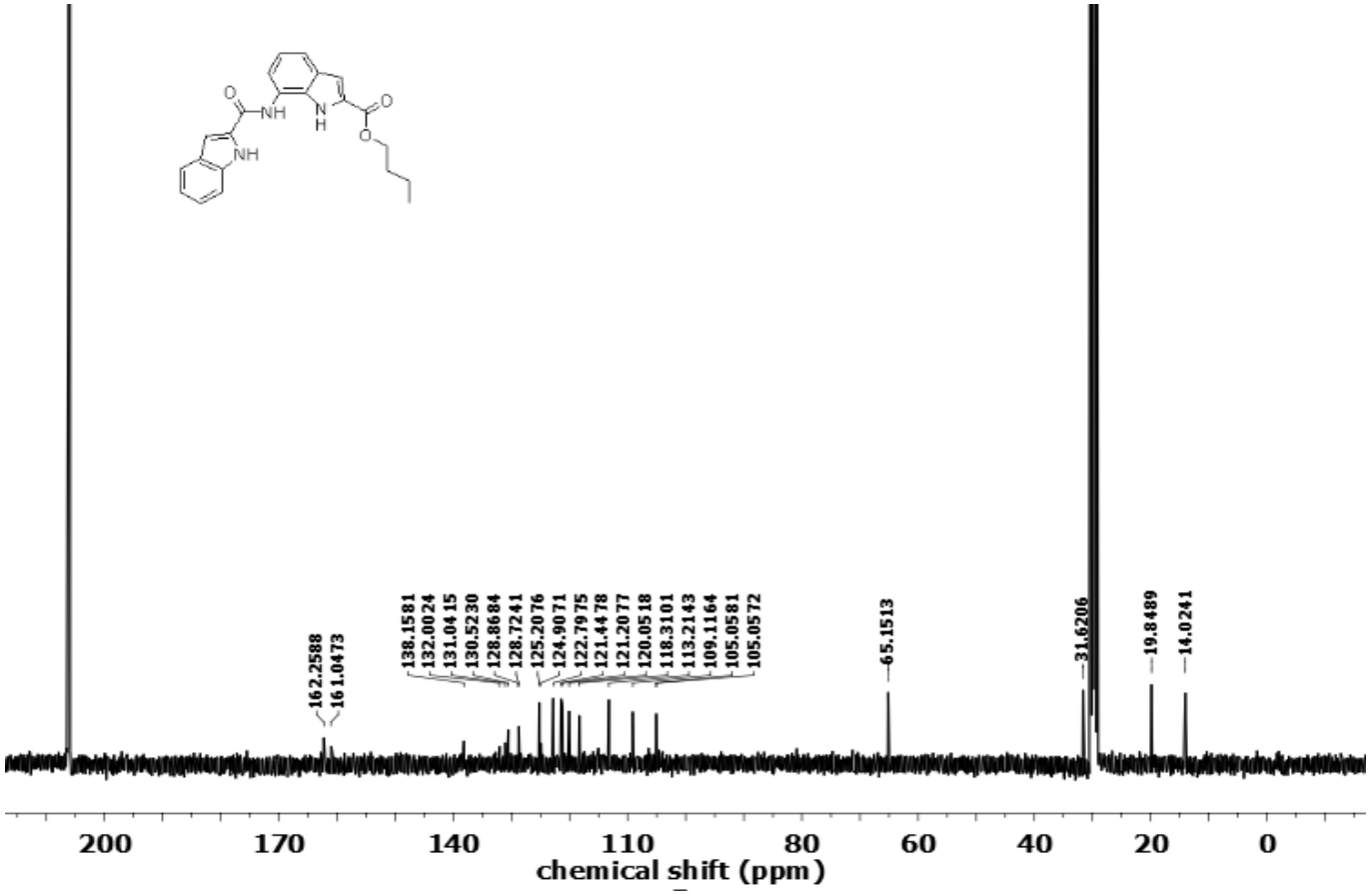


**Fig. S43** 101 MHz $^{13}C$ NMR spectrum of compound **1b**.

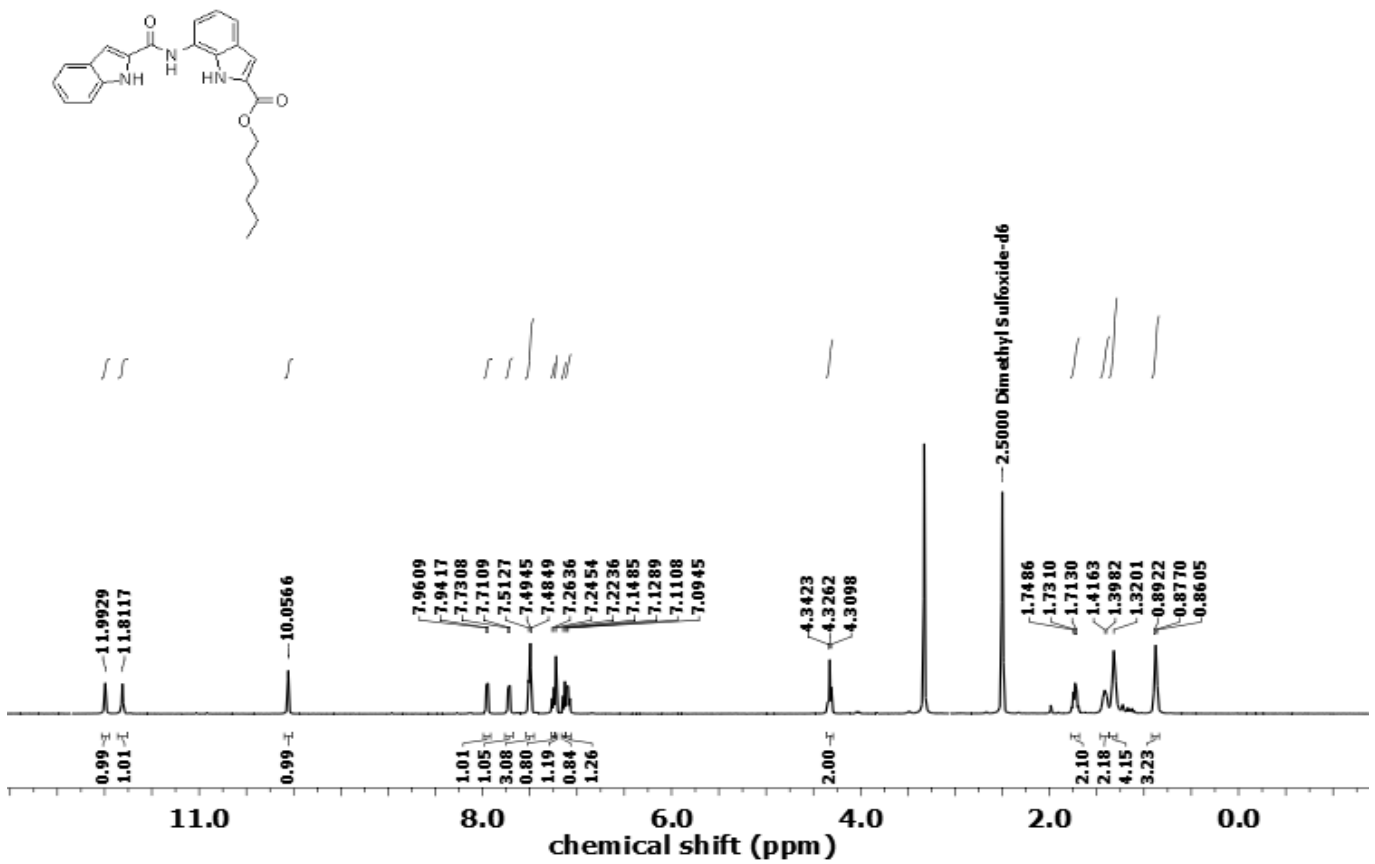


**Fig. S44** 400 MHz $^{1}$H NMR spectrum of compound **1c**.

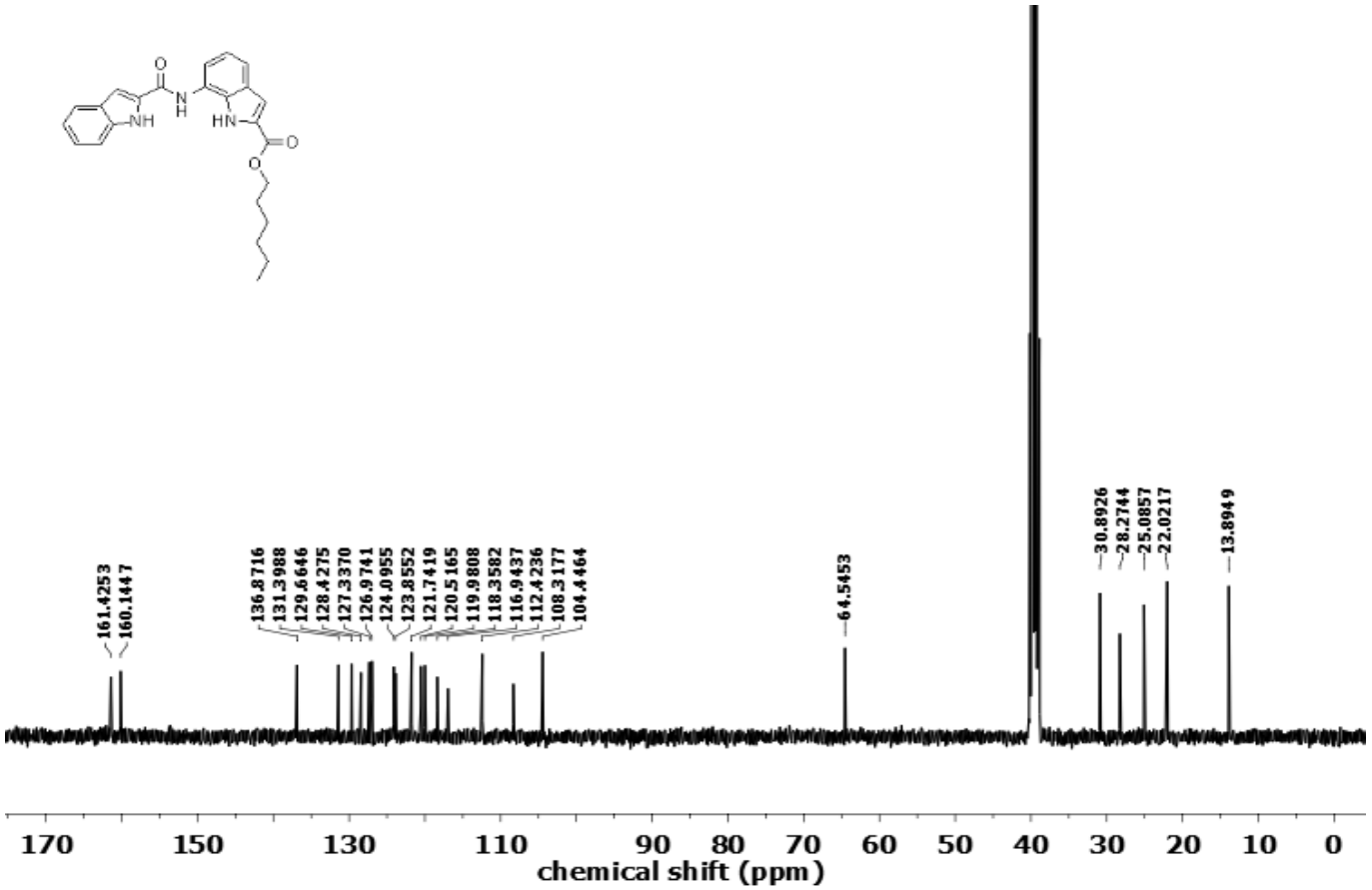


**Fig. S45** 101 MHz $^{13}C$ NMR spectrum of compound **1c**.

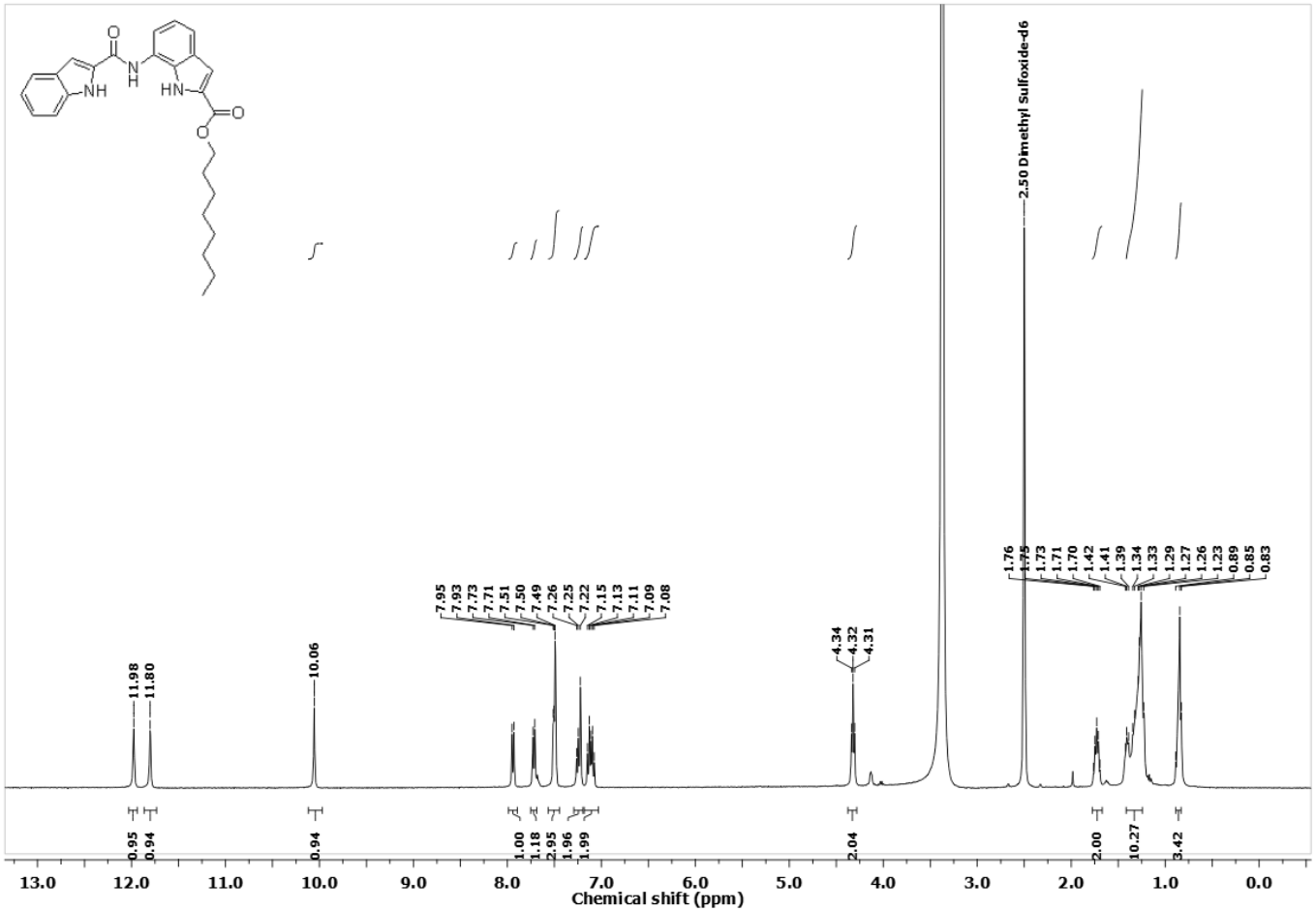


**Fig. S46** 400 MHz $^{1}$H NMR spectrum of compound **1d**.

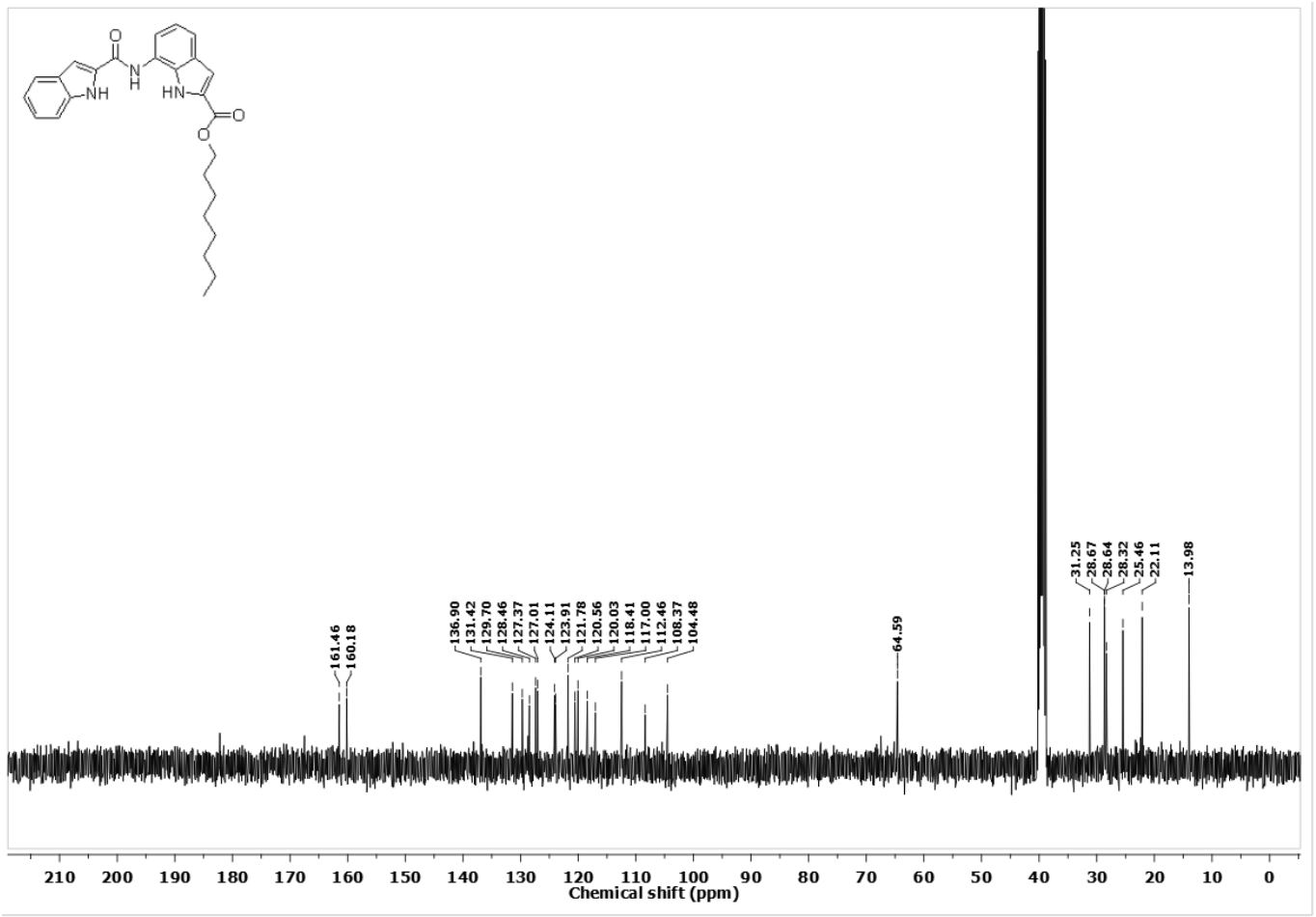


**Fig. S47** 101 MHz $^{13}C$ NMR spectrum of compound **1d**.

## X. References


S1. (a) *CONFLEX 8*, H. Goto, S. Obata, N. Nakayama and K. Ohta, CONFLEX Corporation, Tokyo, Japan, 2017; (b) H. Goto and E. Osawa, *J. Am. Chem. Soc.*, 1989, **111**, 8950-8951.

S2. *Gaussian 09*, Revision D.01, M. J. Frisch, G. W. Trucks, H. B. Schlegel, G. E. Scuseria, M. A. Robb, J. R. Cheeseman, G. Scalmani, V. Barone, B. Mennucci, G. A. Petersson, H. Nakatsuji, M. Caricato, X. Li, H. P. Hratchian, A. F. Izmaylov, J. Bloino, G. Zheng, J. L. Sonnenberg, M. Hada, M. Ehara, K. Toyota, R. Fukuda, J. Hasegawa, M. Ishida, T. Nakajima, Y. Honda, O. Kitao, H. Nakai, T. Vreven, J. J. A. Montgomery, J. E. Peralta, F. Ogliaro, M. Bearpark, J. J. Heyd, E. Brothers, K. N. Kudin, V. N. Staroverov, T. Keith, R. Kobayashi, J. Normand, K. Raghavachari, A. Rendell, J. C. Burant, S. S. Iyengar, J. Tomasi, M. Cossi, N. Rega, J. M. Millam, M. Klene, J. E. Knox, J. B. Cross, V. Bakken, C. Adamo, J. Jaramillo, R. Gomperts, R. E. Stratmann, O. Yazyev, A. J. Austin, R. Cammi, C. Pomelli, J. W. Ochterski, R. L. Martin, K. Morokuma, V. G. Zakrzewski, G. A. Voth, P. Salvador, J. J. Dannenberg, S. Dapprich, A. D. Daniels, O. Farkas, J. B. Foresman, J. V. Ortiz, J. Cioslowski and D. J. Fox, Gaussian, Inc., Wallingford CT, 2013.

S3. (a) A. D. Becke, *J. Chem. Phys.*, 1993, **98**, 5648-5652; (b) C. Lee, W. Yang and R. G. Parr, *Phys. Rev. B*, 1988, **37**, 785

S4. (a) P. C. Hariharan and J. A. Pople, *Theoret. Chim. Acta*, 1973, **28**, 213-222; (b) M. M. Francl, W. J. Pietro, W. J. Hehre, J. S. Binkley, M. S. Gordon, D. J. DeFrees and J. A. Pople, *J. Chem. Phys.*, 1982, **77**, 3654-3665.

S5. (a) T. Saha, M. S. Hossain, D. Saha, M. Lahiri and P. Talukdar, *J. Am. Chem. Soc.*, 2016, **138**, 7558-7567; (b) N. Busschaert, S.-H. Park, K.-H. Baek, Y. P. Choi, J. Park, E. N. W. Howe, J. R. Hiscock, L. E. Karagiannidis, I. Marques, V. Félix, W. Namkung, J. L. Sessler, P. A. Gale and I. Shin, *Nat. Chem.*, 2017, **9**, 667; (c) N. J. Roy, S. N. Save, V. K. Sharma, B. Abraham, A. Kuttanamkuzhi, S. Sharma, M. Lahiri and P. Talukdar, *Chem. Eur. J.*, 2023, **29**, e202301412.